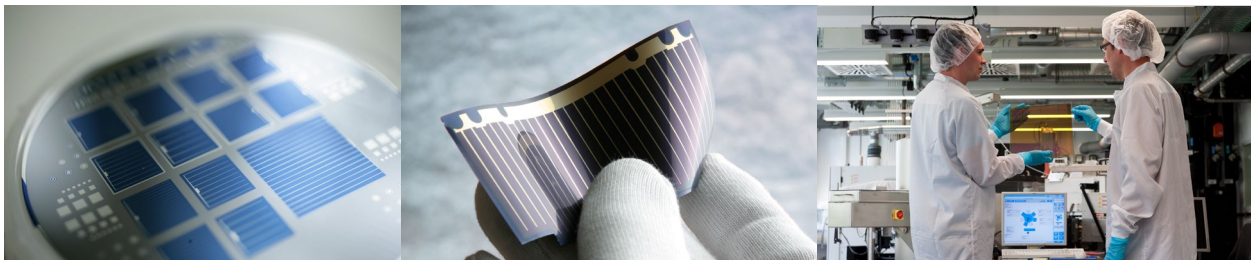


31TH EU PVSEC | HAMBURG, GERMANY 2015

POSTER PRESENTATIONS HZB

Posters presented by the Helmholtz-Zentrum Berlin at the 31th
EU PVSEC 2015.



SURFACE PHOTOVOLTAGE IN THIN FILMS OF $\text{Cu}_2\text{ZnSn}(\text{S}_x\text{Se}_{1-x})_4$ OBTAINED BY SPRAY PYROLYSIS

L.Bruc¹, Th. Ditrlich², L. Dermenji¹, G. Gurieva³, S. Vatavu^{2,4}, N. Curmei¹, M. Guc¹, D.A. Sherban¹, A.V. Simashkevich¹, S. Schorr^{3,5}, M.Ch. Lux-Steiner², M. Rusu^{2,4}, E. Arushanov¹

¹Institute of Applied Physics, str. Academiei 5, MD 2028, Chisinau, Republic of Moldova

²Institut für Heterogene Materialsysteme, Helmholtz-Zentrum Berlin für Materialien und Energie GmbH, Lise-Meitner Campus, Hahn-Meitner-Platz 1, 14109 Berlin, Germany

³Department Crystallography, Helmholtz-Zentrum Berlin für Materialien und Energie GmbH, Hahn-Meitner-Platz 1, D-14109 Berlin, Germany

⁴Moldova State University, 60 A. Mateevici str., MD-2009 Chisinau, Republic of Moldova

⁵Institute of Geological Sciences, Free University Berlin, Malteserstr. 74-100, 12249 Berlin, Germany



HZB Helmholtz
Zentrum Berlin

Approach

Spectral and time dependent surface photovoltage (SPV) measurements were performed on $\text{Cu}_2\text{ZnSn}(\text{S}_x\text{Se}_{1-x})_4$ (CZTSSe) thin films prepared on ITO/glass substrates by spray pyrolysis at ambient atmosphere from aqueous solutions and subsequent selenization of $\text{Cu}_2\text{ZnSnS}_4$ (CZTS) layers. The morphology, stoichiometry and phases of the crystalline thin films were studied by scanning electron microscopy (SEM), energy dispersive x-ray analysis (EDX) and x-ray diffraction (XRD), respectively.

Preparation:

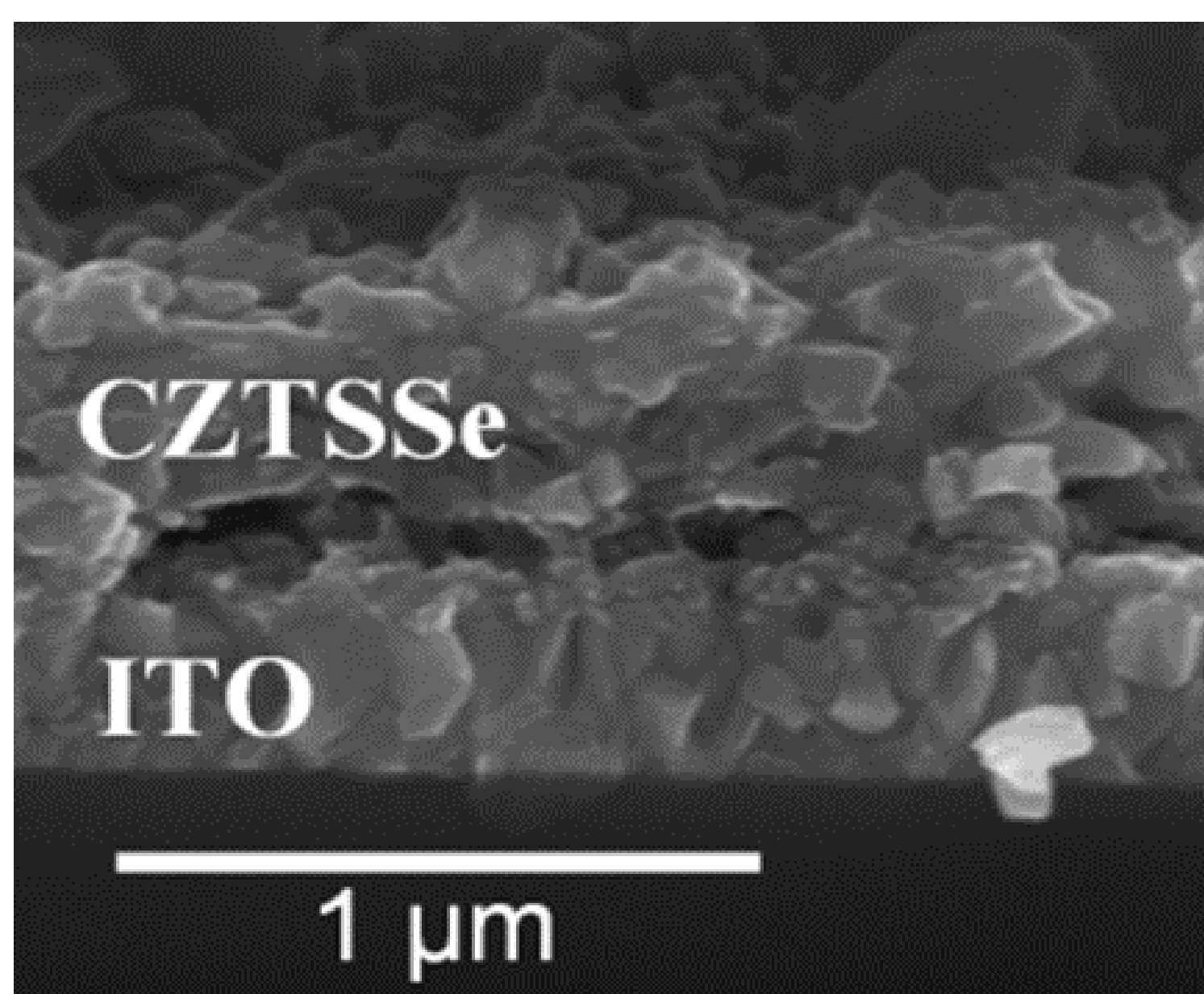
The CZTS thin films were prepared on ITO/glass substrates by spray pyrolysis at ambient atmosphere from aqueous solutions of metal salts (CuCl_2 , $\text{Zn}(\text{O}_2\text{CCH}_3)_2$, SnCl_4) and thiourea ($\text{SC}(\text{NH}_2)_2$) [1,2] at temperatures between 350 and 410 °C. At the next step the CZTS films were converted into CZTSSe films by subsequent selenization with elemental selenium in evacuated quartz ampoules at 525 °C for 30 min.

Experimental

Characterisation:

The morphology, stoichiometry and phases of the crystalline thin films were studied by scanning electron microscopy (SEM), energy dispersive x-ray analysis (EDX) and grazing incidence x-ray diffraction (GI-XRD), respectively. Time dependent and modulated spectral dependent surface photovoltage (SPV) measurements [3] were performed in the fixed capacitor arrangement with a mica spacer (thickness ~ 30 μm) between the sample and the reference ($\text{SnO}_2:\text{F}$ on a quartz cylinder) electrodes. Excitation was performed with a halogen lamp and a quartz prism monochromator (SPM) for spectral dependent measurements and with a tunable pulsed Nd:YAG laser for time dependent measurements. Measurements were performed in two regimes in-phase and phase-shifted by 90°. In-phase means that the signals follow the modulation period (fast processes), while phase-shifted by 90° means that the signals are strongly retarded in relation to the modulation period (slow processes); the modulation frequency was 5 Hz.

Physical properties



Morphology by SEM:

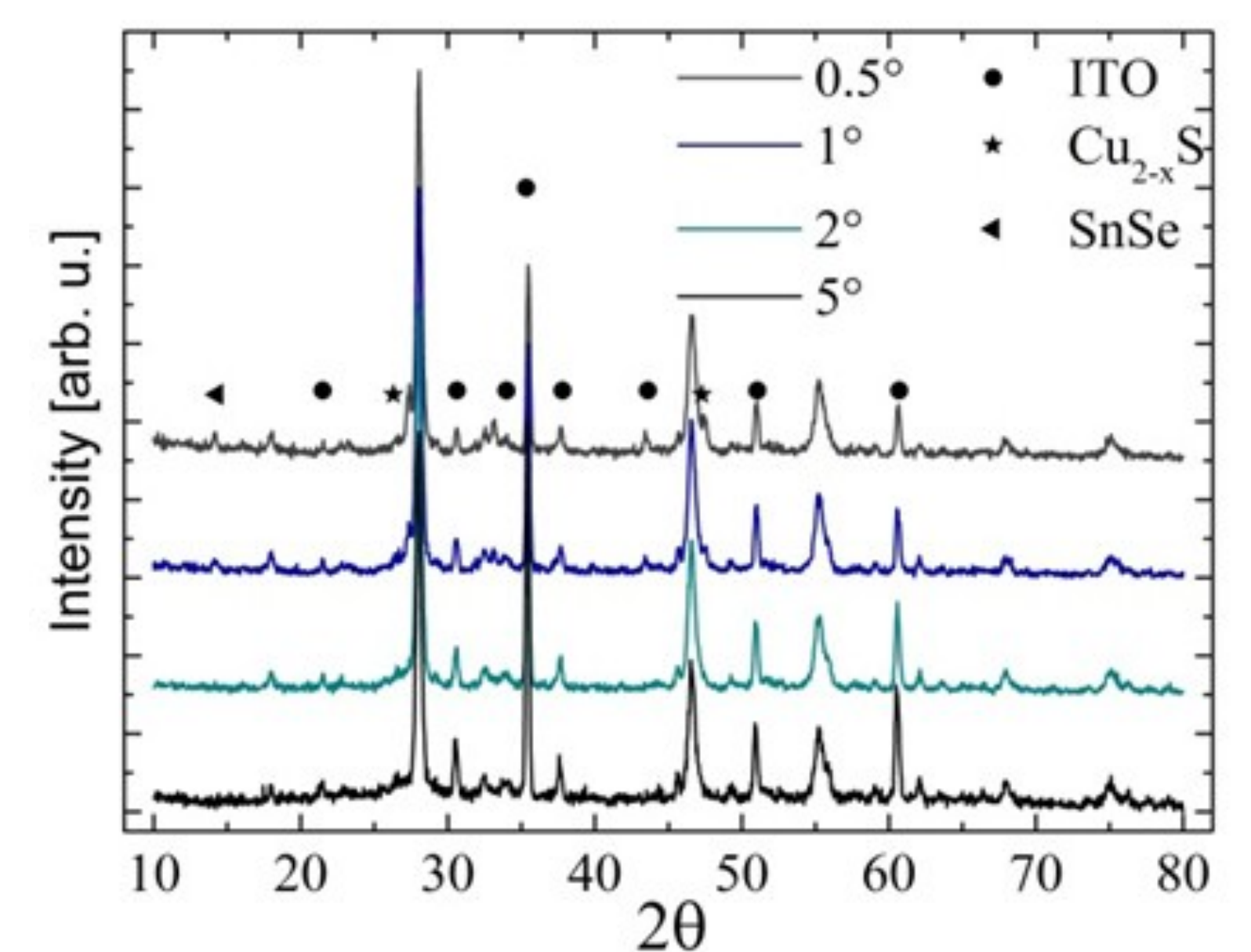
- Film thickness of about 0.5 μm
- Maximum crystallites size of ~200 nm

Structure by XRD:

- Most of the XRD peaks assigned to kesterite type CZTSSe phases (space group $I\bar{4}$).
- Lattice constants of the main kesterite type phase calculated by using Le Bail refinement: $a = 5.502 \text{ \AA}$, $c = 10.971 \text{ \AA}$
- The Cu_{2-x}S secondary phase is present through the whole thin film
- SnSe secondary phase is present at the top of the absorber layer

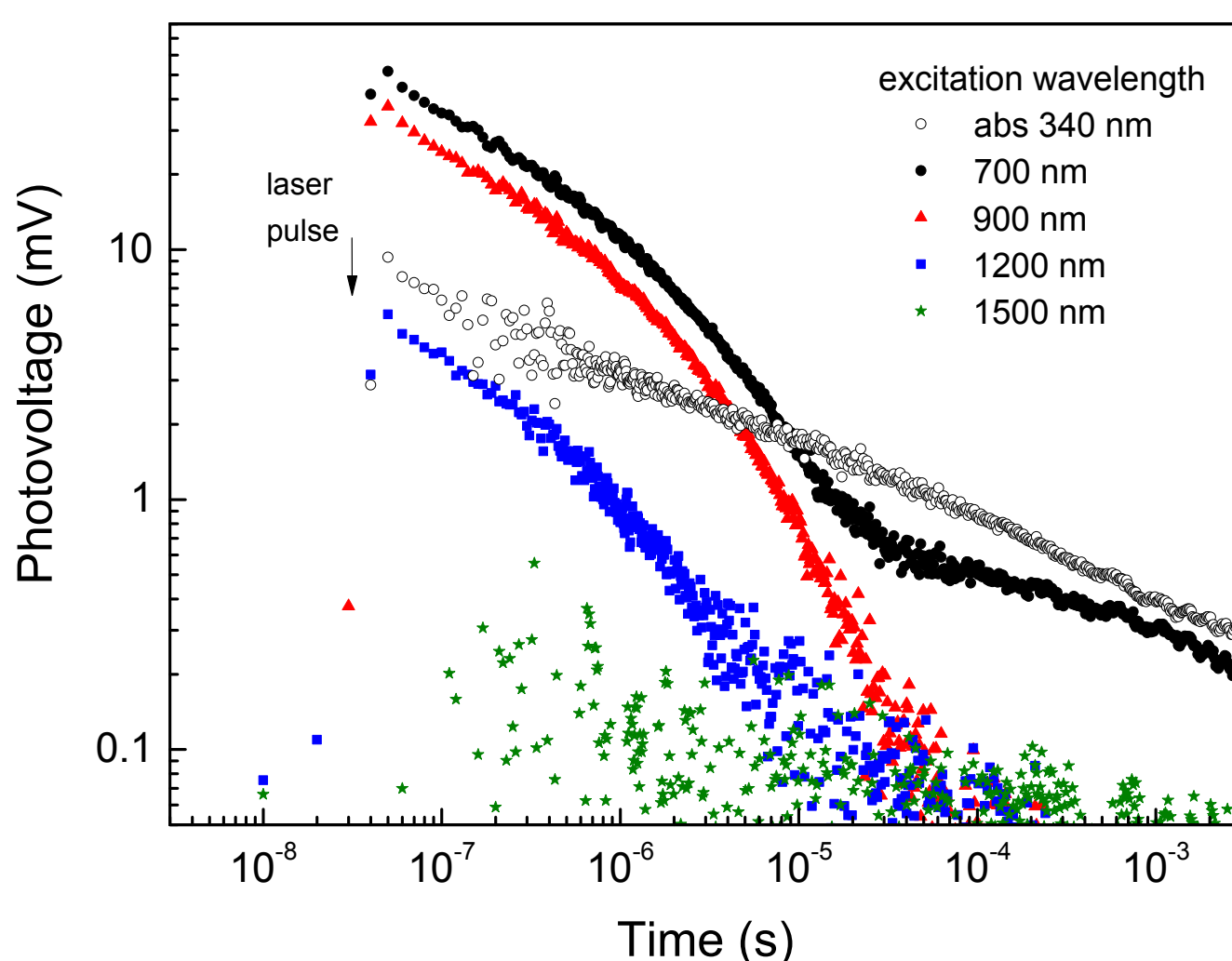
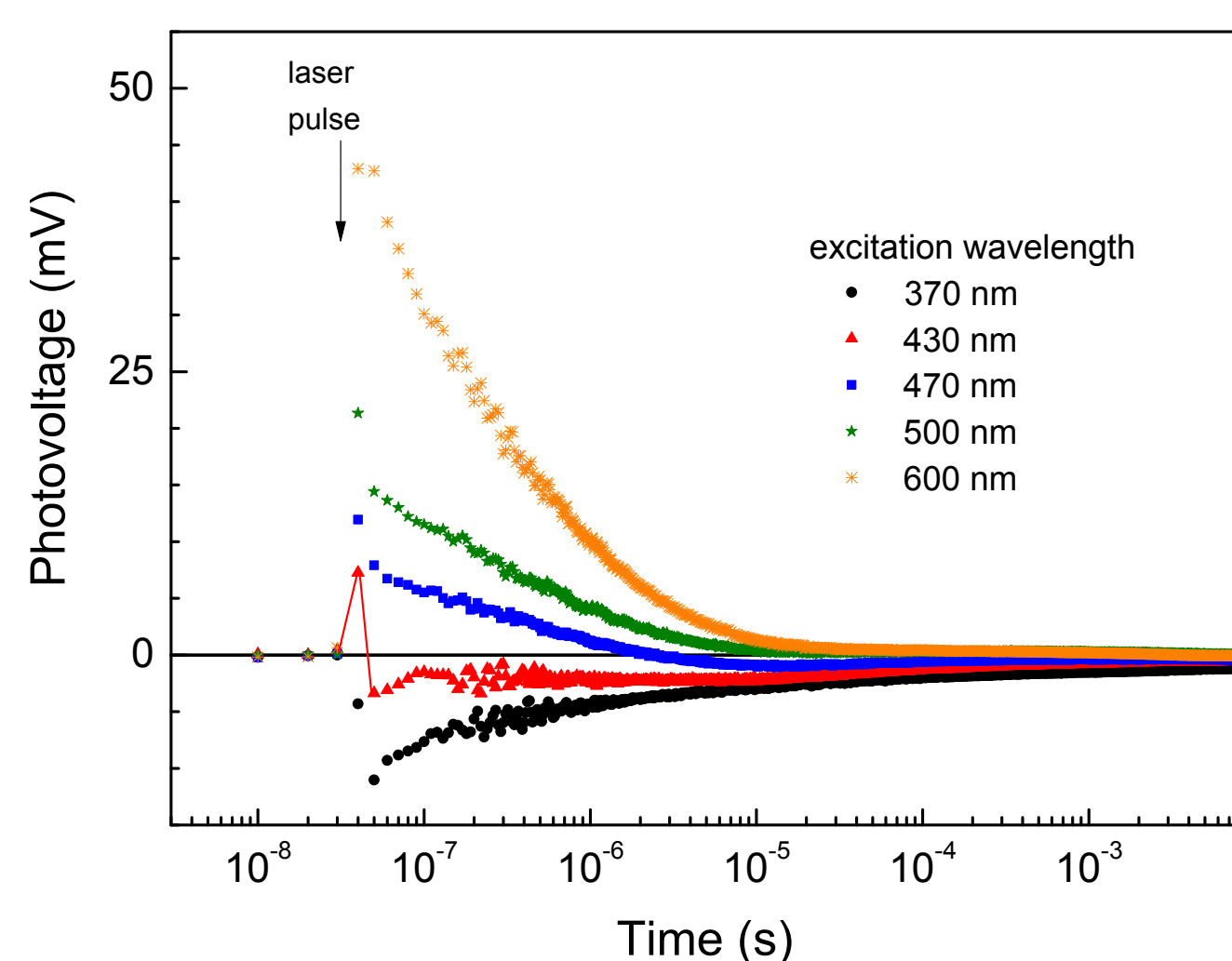
Composition by EDX:

- Cu:Zn:Sn:S:Se = 24.4 : 19.8 : 10.6 : 33.2 : 12.0 (all values in at.%)
- $\text{Cu}/(\text{Zn}+\text{Sn}) = 0.80$; $(\text{S}+\text{Se})/\text{Metals} = 0.82$; $\text{Se}/(\text{S}+\text{Se}) = 0.27$

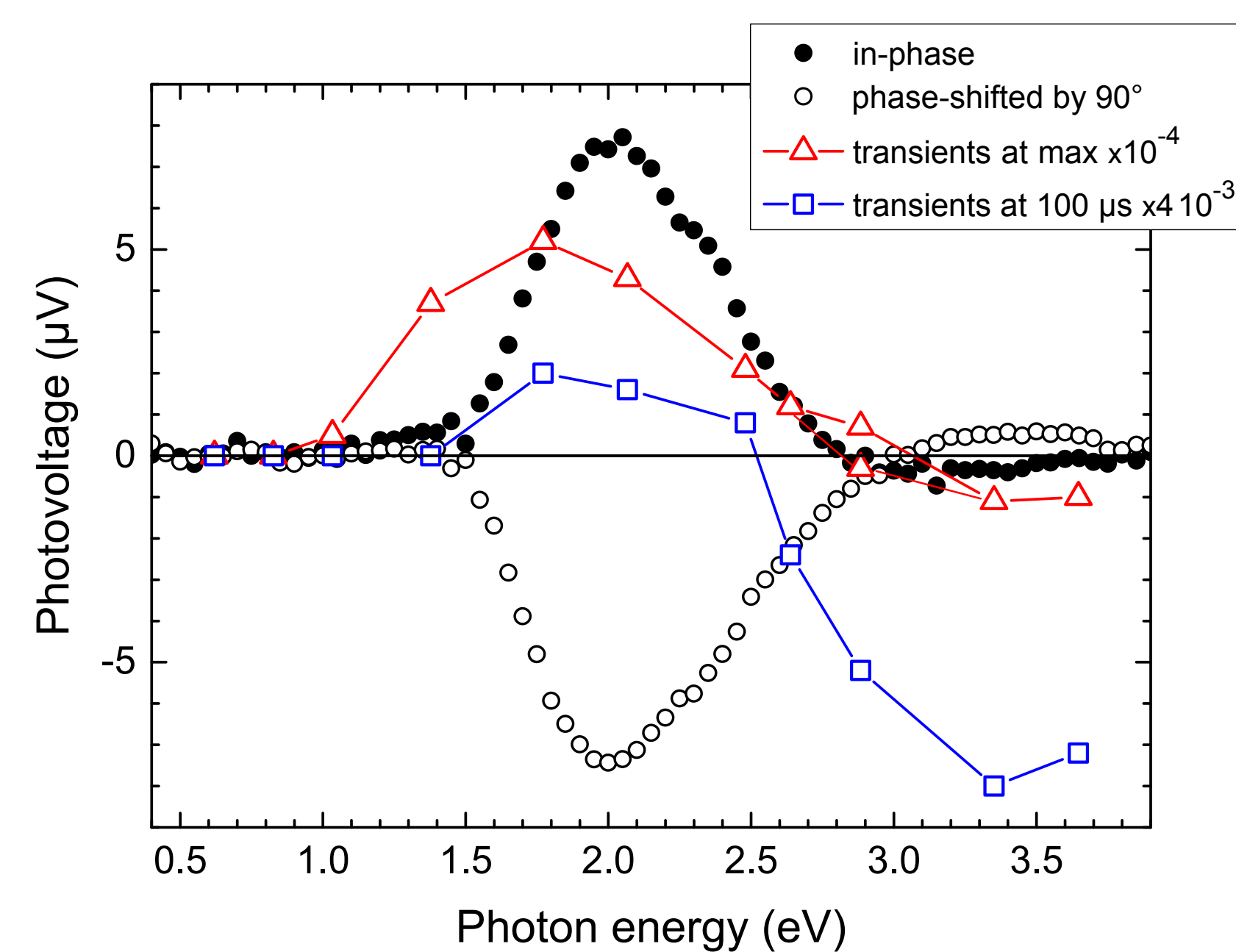


Electronic properties

SPV transients

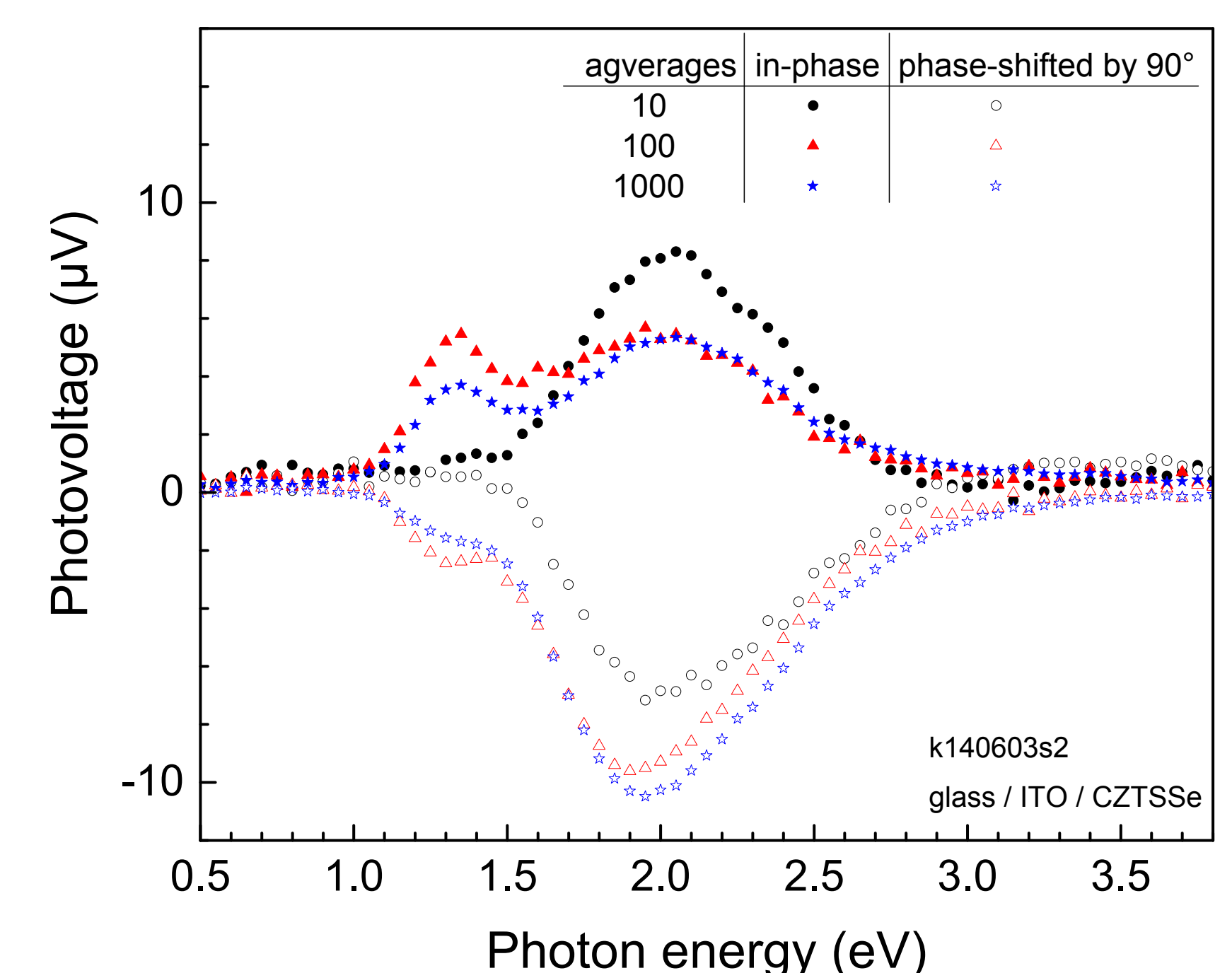
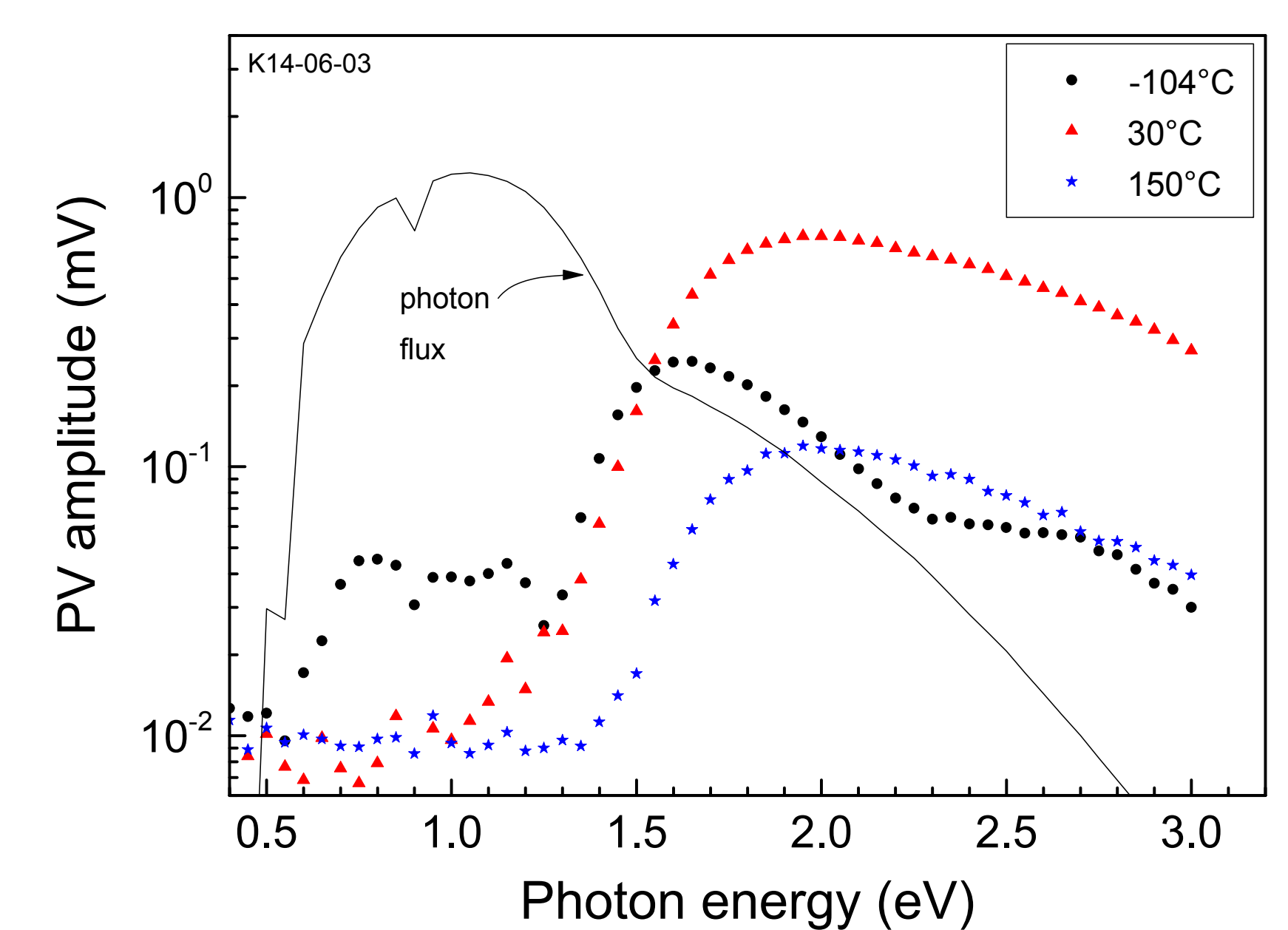


- Depth-dependent charge generation and separation processes
- Excitations $\leq 370 \text{ nm}$: electrons separate towards the surface
- Excitation range 370-1500 nm: holes separate towards the surface
- Two decay regions of the SPV signals point to two different competitive recombination processes



- Modulated SPV spectra set on at about 1.5 eV \Rightarrow The absorber band gap $E_g = 1.5 \text{ eV}$
- A shoulder in the spectrum of the modulated in-phase SPV signals around 2.4 eV is a signature for the onset of the process leading to charge separation with the opposite sign.
- SPV signals derived from the maximum of transients appear at photon energies *below* the $E_{g-\text{CZTSSe}}$ and are temperature dependent
- SPV signals derived from transients at 100 μs appear only at photon energies *larger* than $E_{g-\text{CZTSSe}}$
- Temperature dependent measurements demonstrate the presence of a broad spectrum of electronic states which can be excited from the near IR to the range of the $E_{g-\text{CZTSSe}}$
- Comparison between slow and fast scans gives the evidence for persistent processes in modulated charge separation

SPV spectra



Conclusions

- The CZTSSe thin-films prepared by selenization of the spray pyrolysis deposited CZTS layers show mostly kesterite type CZTSSe phases
- The as-prepared CZTSSe layers are Cu-poor and contain Cu_{2-x}S and SnSe secondary phases
- The onset energy of 1.5 eV observed in the SPV spectra corresponds to the band gap of the CZTSSe with about 25 % of Se content
- The transition at 1.0 eV can be attributed to the SnSe secondary phase with an indirect band gap of 0.90 eV

References:

- [1] L.I. Bruc, M. Guc, M. Rusu, D.A. Sherban, A.V. Simashkevich, S. Schorr, V. Izquierdo-Roca, A. Pérez-Rodríguez, E.K. Arushanov, Proceedings of 27th EU PVSEC (2012) 2763.
- [2] G. Gurieva, M. Guc, L.I. Bruc, V. Izquierdo-Roca, A. Pérez Rodríguez, S. Schorr, E. Arushanov, Physica Status Solidi C 10 (2013) 1082.
- [3] L. Kronik, Y. Shapira, Surface Science Reports 37 (1999) 1.

ACKNOWLEDGMENTS

This work was supported by projects STCU No. 5985, IRSES PVICOEST – 269167, FRCFB 13.820.05.11/BF and by the institutional project CSSDT No. 15.817.02.04A.

Dr. Leonid Bruc
leonid.bruc@phys.asm.md
www.phys.asm.md

Dr. Marin Rusu
rusu@helmholtz-berlin.de
www.helmholtz-berlin.de

Raman spectroscopy study for In situ monitoring of $\text{Cu}_2\text{ZnSnS}_4$ synthesis and identification of secondary phases

Stephan van Duren¹, Yi Ren², Jonathan Scragg², Justus Just¹, Thomas Unold¹

¹Helmholtz-Zentrum Berlin, Hahn-Meitner-Platz 1, 14109 Berlin, Germany

²Ångström Solar Center, Solid State Electronics, Uppsala University, Box 534, SE-751 21 Uppsala, Sweden

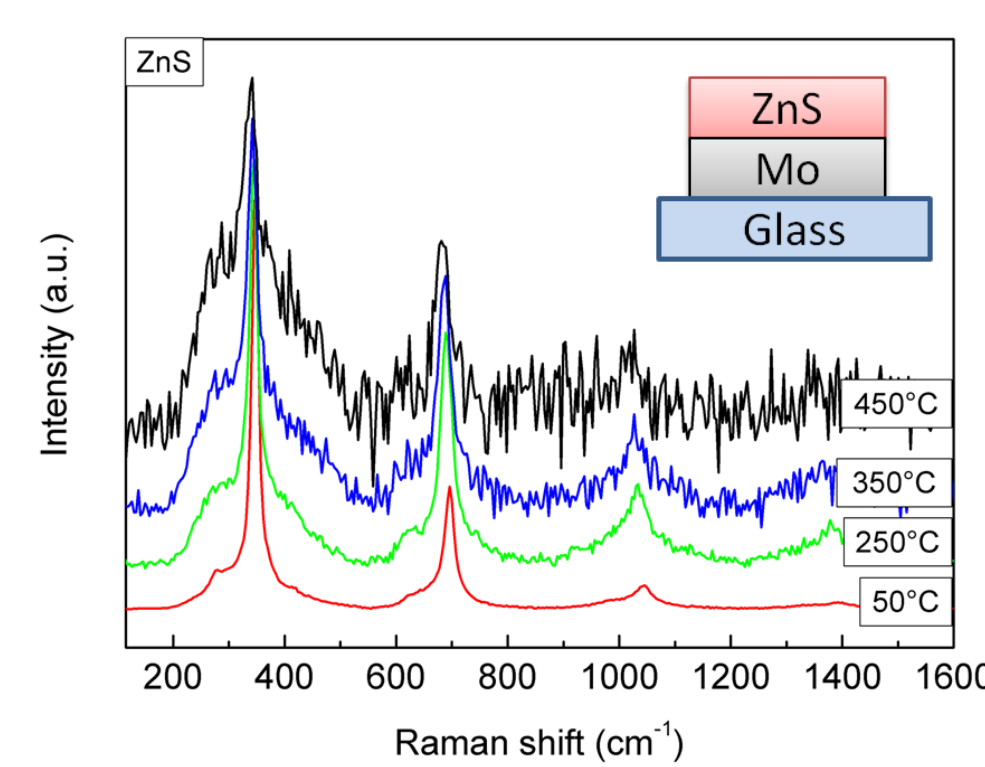
Motivation

- Kesterite ($\text{Cu}_2\text{ZnSnS}_4$) is an interesting material for solar cells; it has a high absorption coefficient, suitable bandgap and earth abundant constituents.
- As a complex quaternary compound it has a small single phase region and outside this region secondary phases are formed.
- Optimization of process parameters and process monitoring is required to identify point of formation of CZTS and reduce its decomposition and formation and loss of volatile secondary phases such as Sn_xS_y and ZnS.
- Raman spectroscopy has proven to be a valuable technique for phase identification of secondary phases and other compound semiconductors.
- Most CZTS fabrication processes involve an annealing step. A temperature dependent insitu Raman spectroscopy study is performed to mimic real annealing conditions.

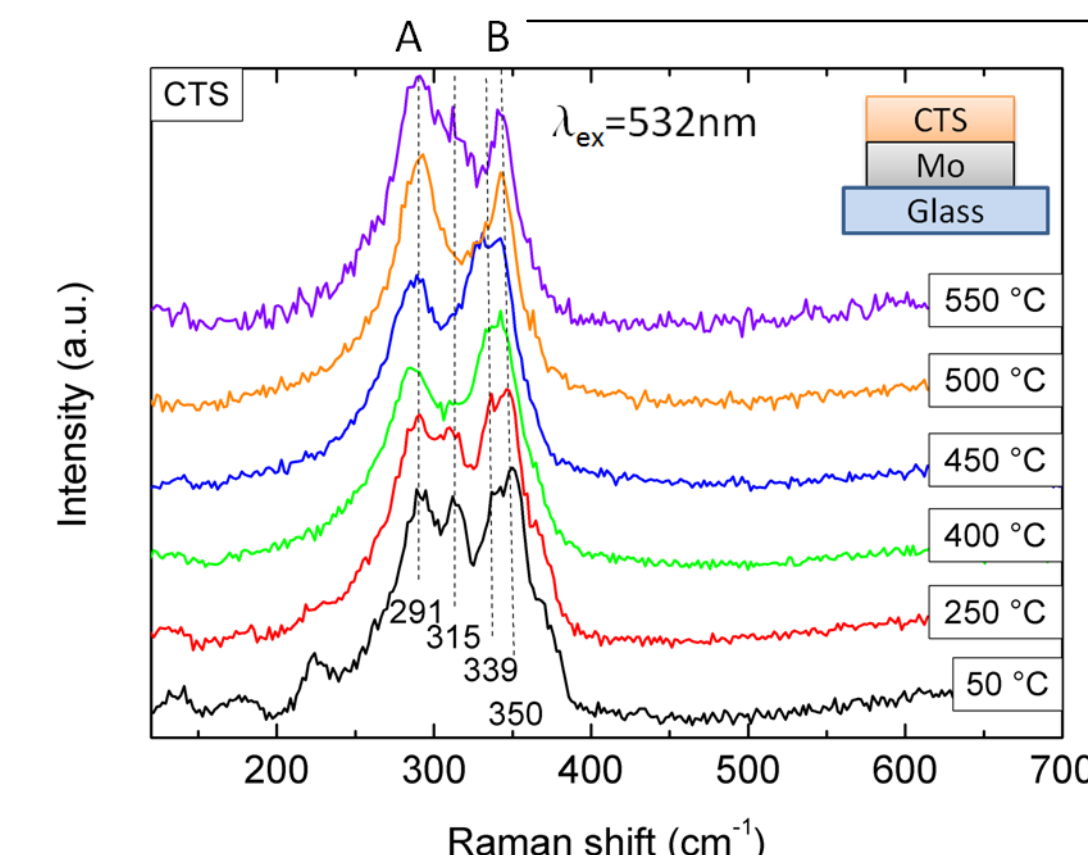
Results - In situ monitoring of secondary phases and CZTS synthesis

Monitoring of secondary phases

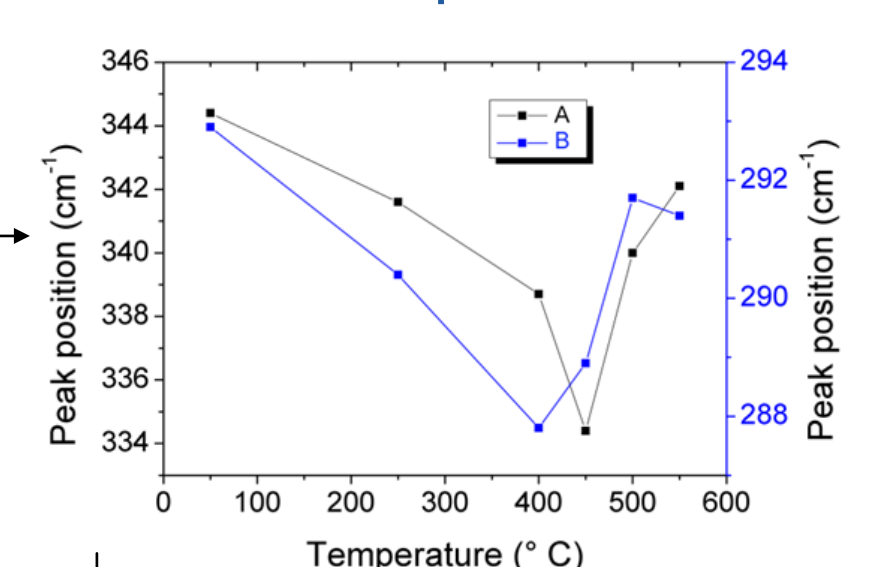
- Main mode of ZnS at 349 cm^{-1} can be observed up to 450°C



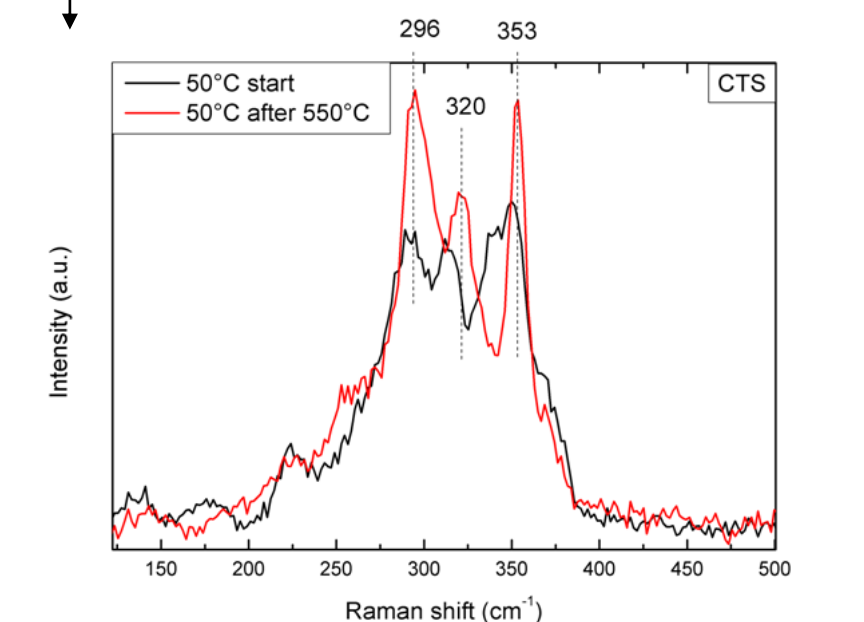
Identification of Cu_2SnS_3 is possible up to 550°C



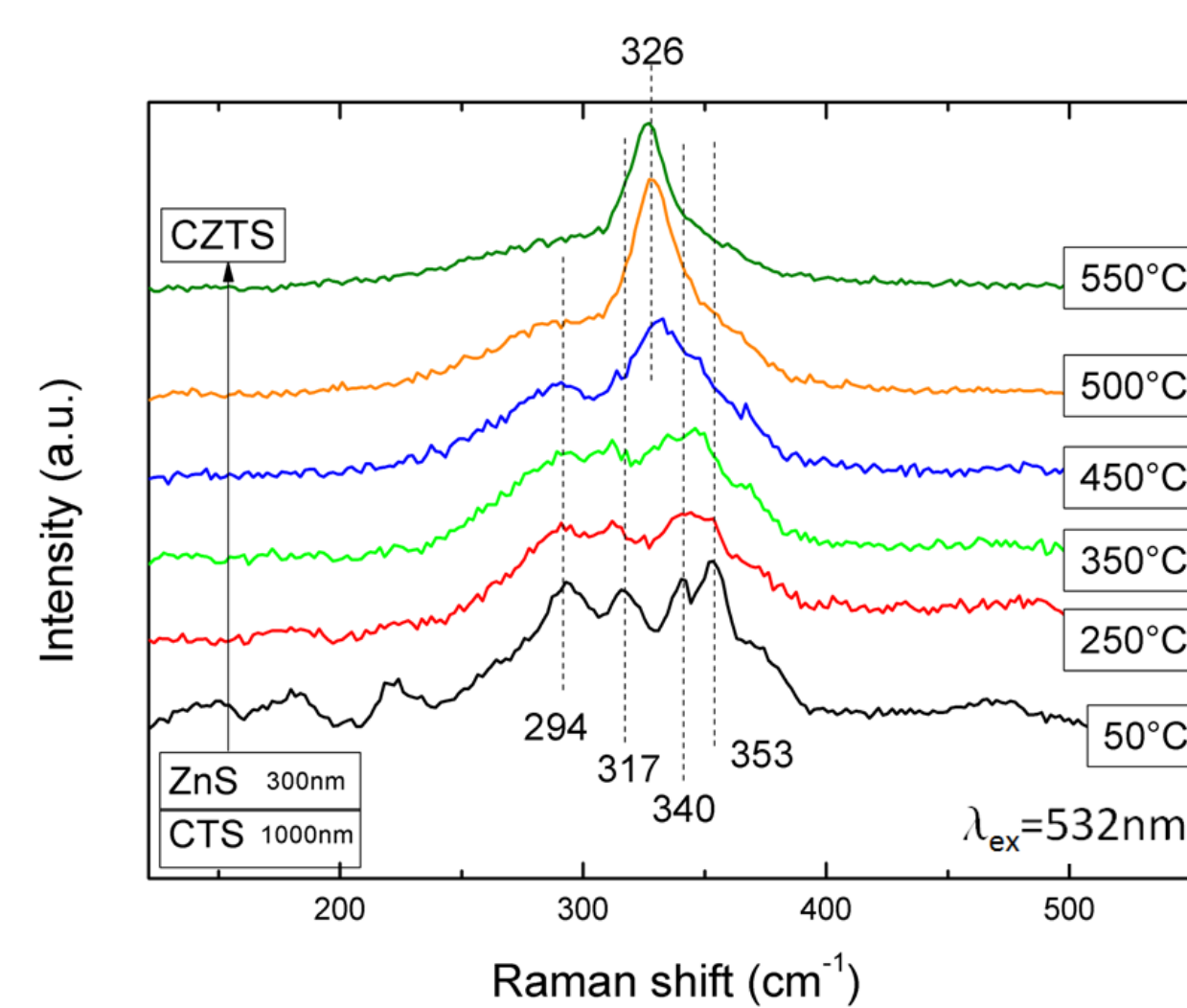
Red shift up to $400/450^\circ$



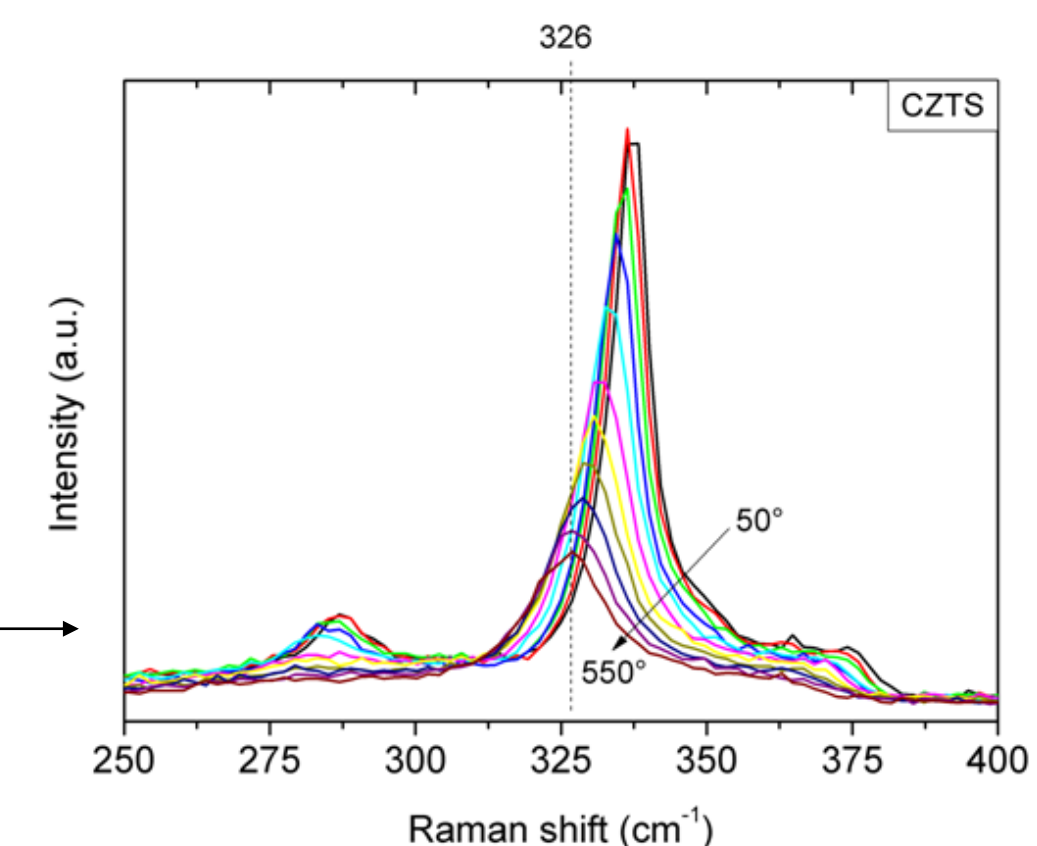
Recrystallization of film



Monitoring of CZTS synthesis from ZnS/CTS stack

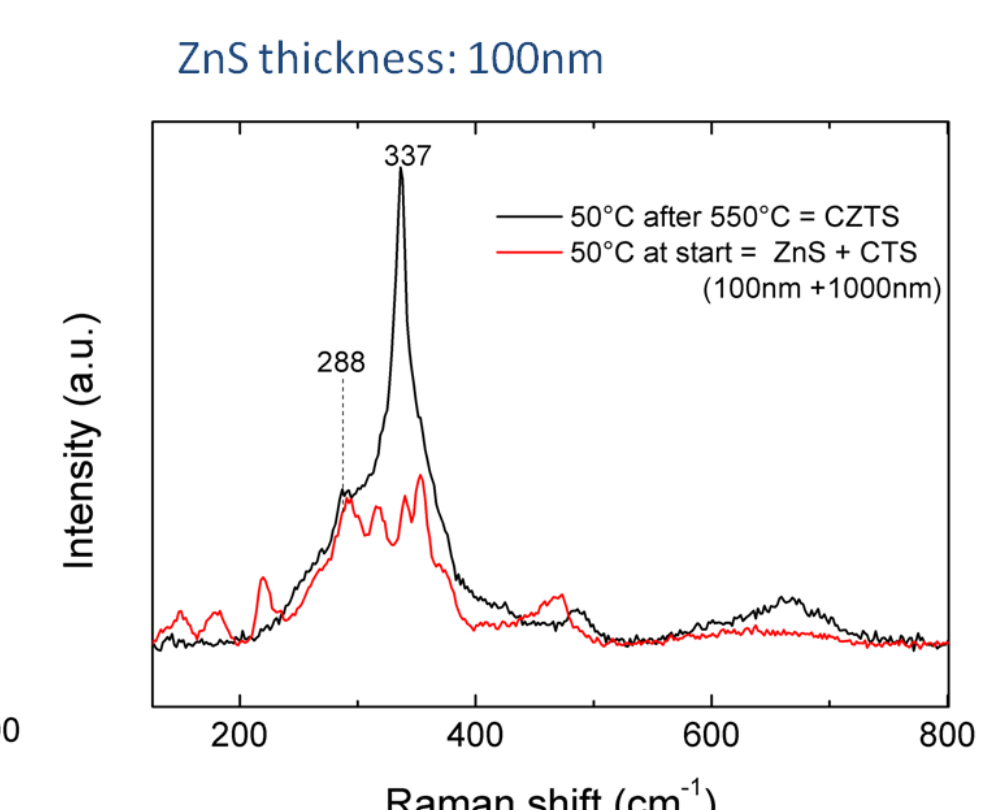
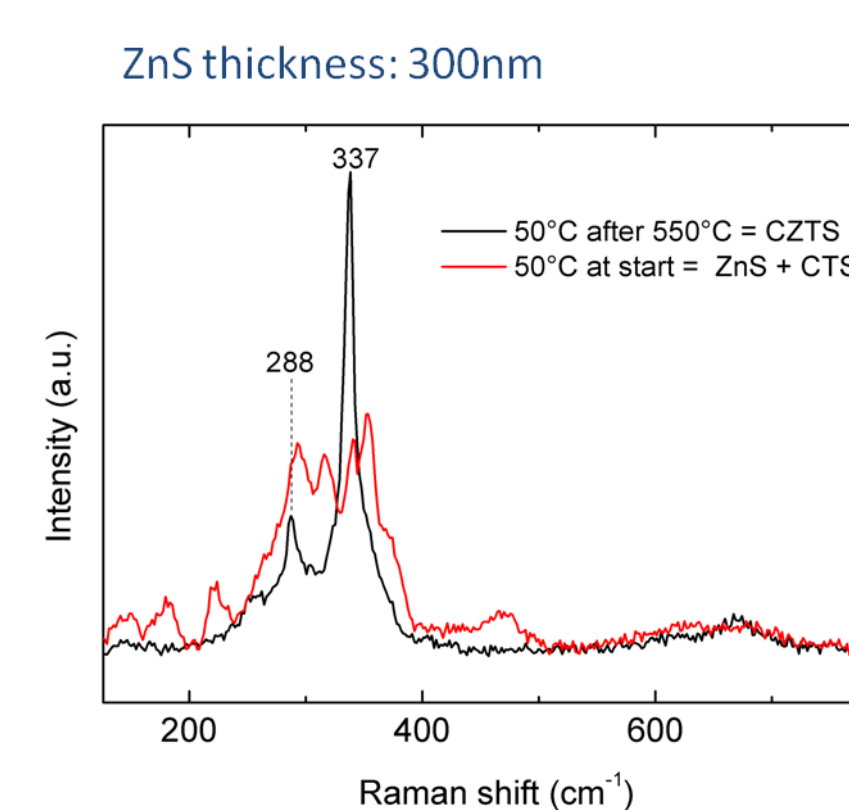


- Amorphous phase from 250°C
- Transformation ZnS/CTS to CZTS observed at 450°C
- Main A-mode CZTS can be observed at 550°C at 326 cm^{-1}
- This corresponds to CZTS reference measurement



Comparison different ZnS thickness: Stack before and after annealing

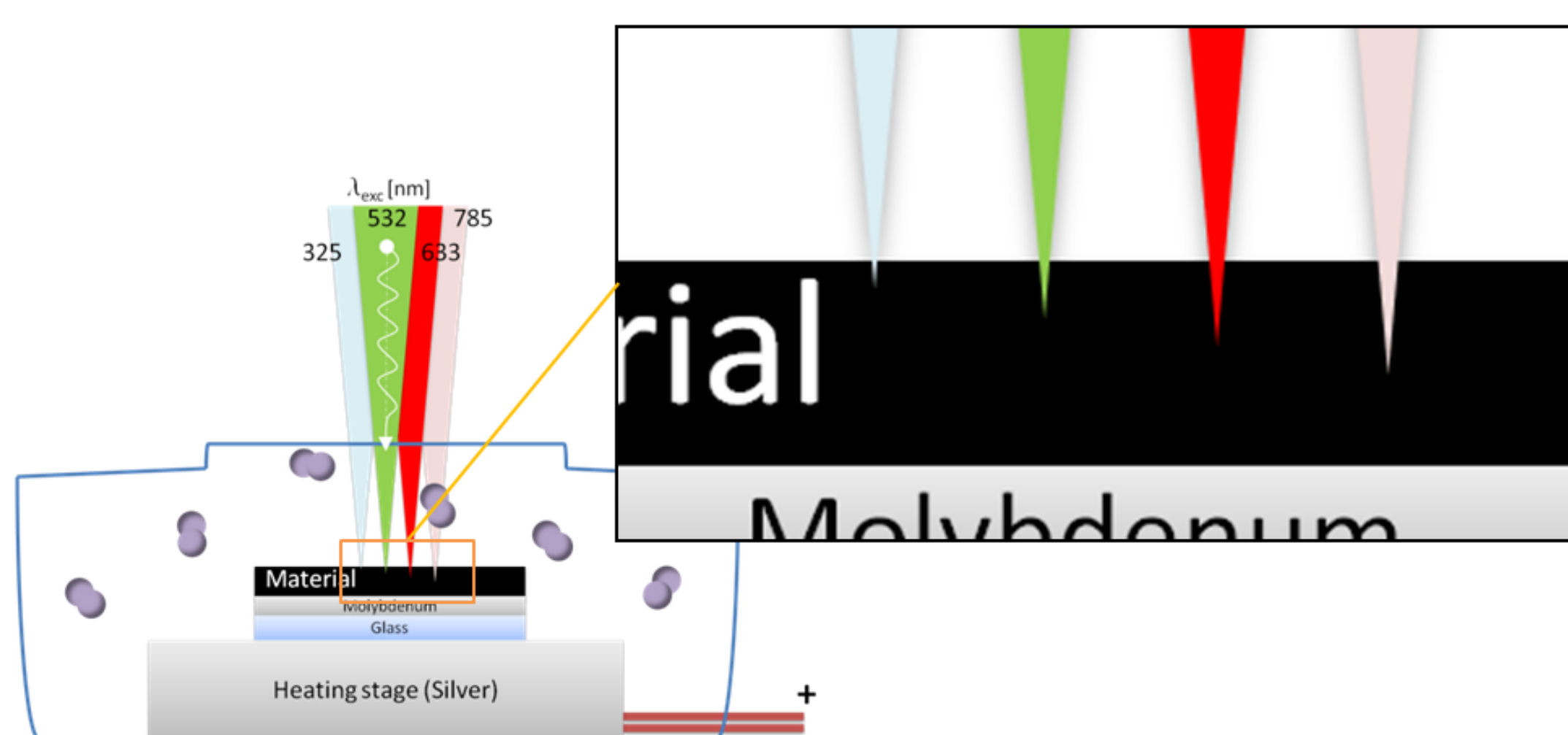
- **300nm:** Clear distinction A-symmetry modes ($287, 337\text{ cm}^{-1}$)
- **100nm:** Broad CZTS peak: mixture CTS/CZTS phase



Experimental approach

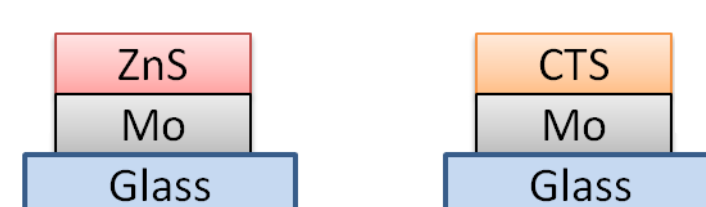
Properties of the experimental setup

- Heating stage: temperatures up to 600°C
- Inert atmosphere: Nitrogen is introduced
- Raman: Backscatter configuration
- Excitation wavelengths used: 325 and 532 nm



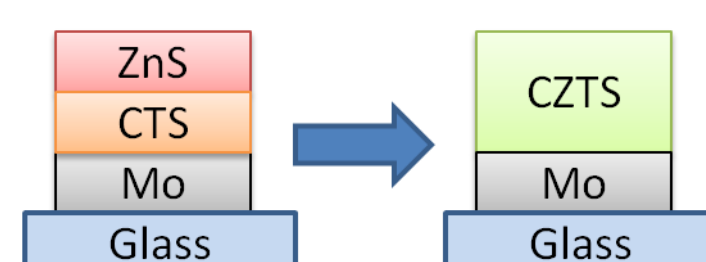
Method

1. Phase evolution and identification of prominent secondary phases ZnS and CTS



First, the secondary phases ZnS and CTS, that commonly appear in CZTS films, have been prepared by coevaporation and are characterized ex situ by GIXRD 0.5° and Raman spectroscopy. The temperature dependent evolution of the Raman spectra have been studied up to 550°C .

2. CZTS formation from stacked ZnS/CTS film



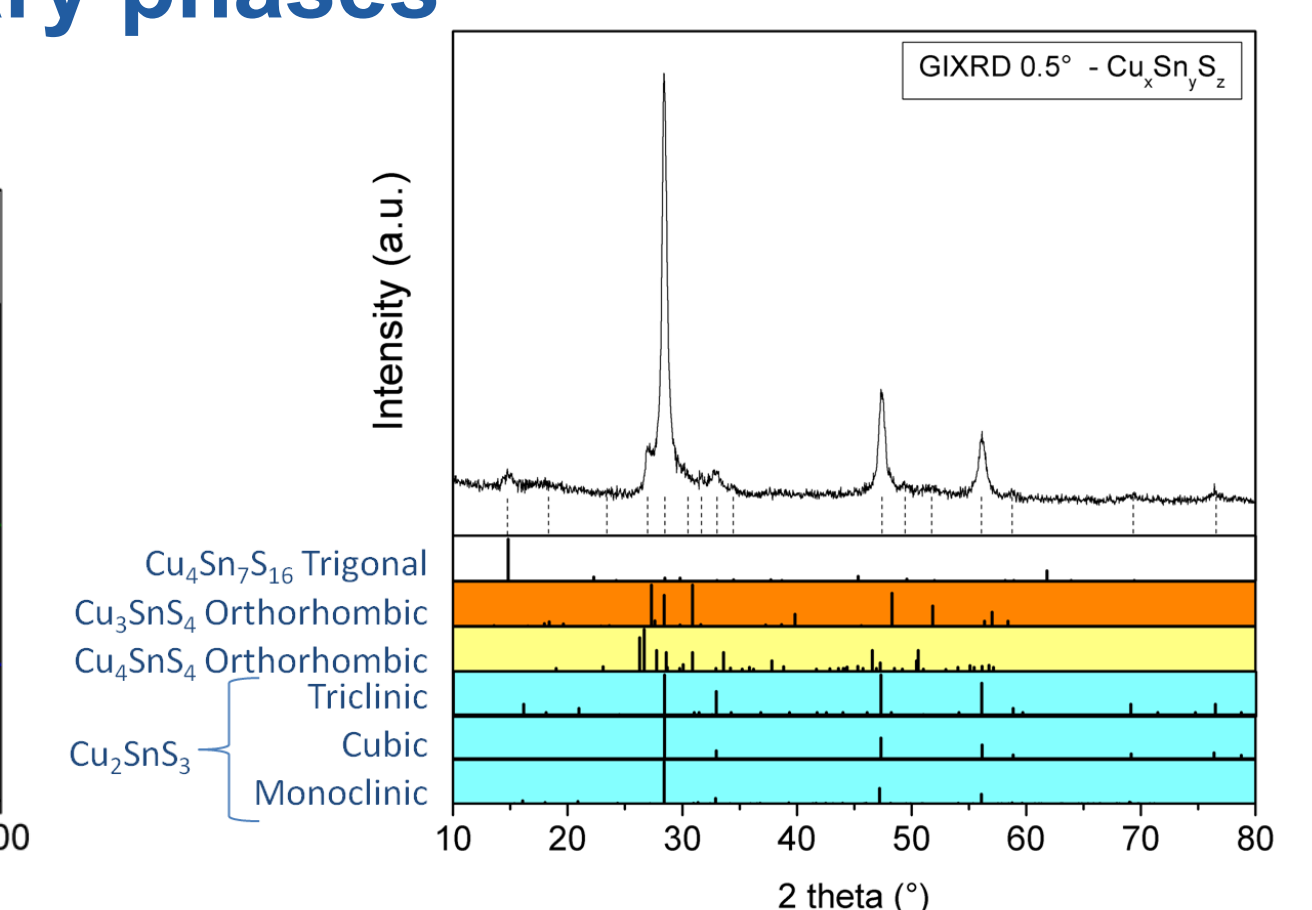
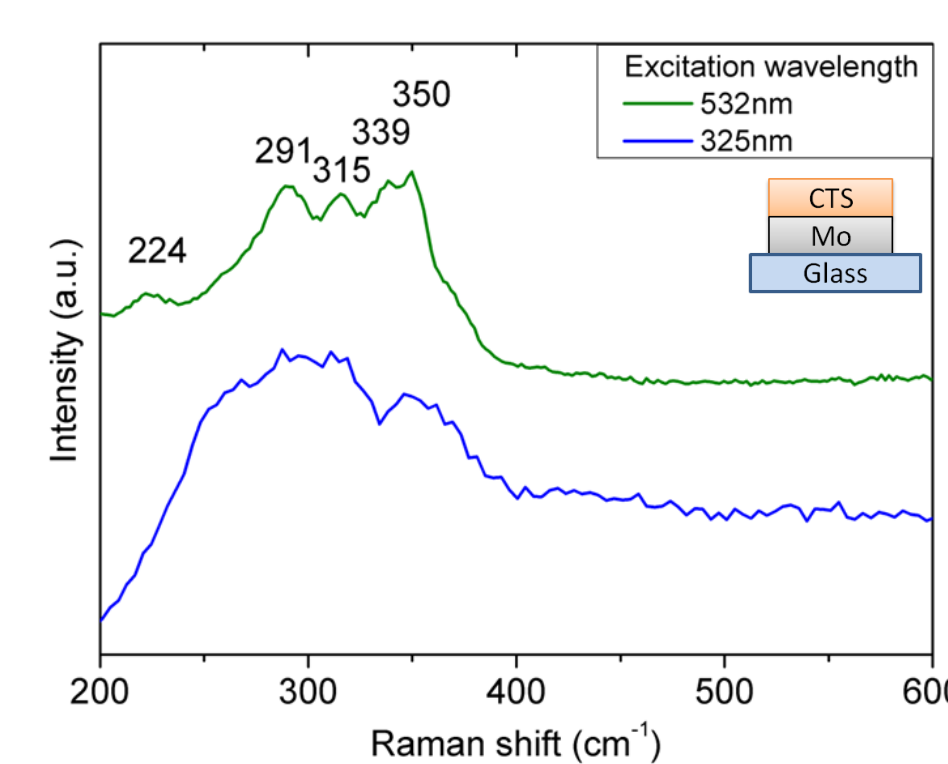
Secondly, a stacked film was created by sputtering a ZnS layer on top of the CTS film. Two different thicknesses of ZnS were studied; 100 nm and 300 nm. Thickness of the ZnS layer was confirmed with a Dektak reference measurement of a ZnS layer sputtered on Molybdenum in the same run. The stacked layer was heated upto 550°C to study the formation of CZTS.

Expected observations

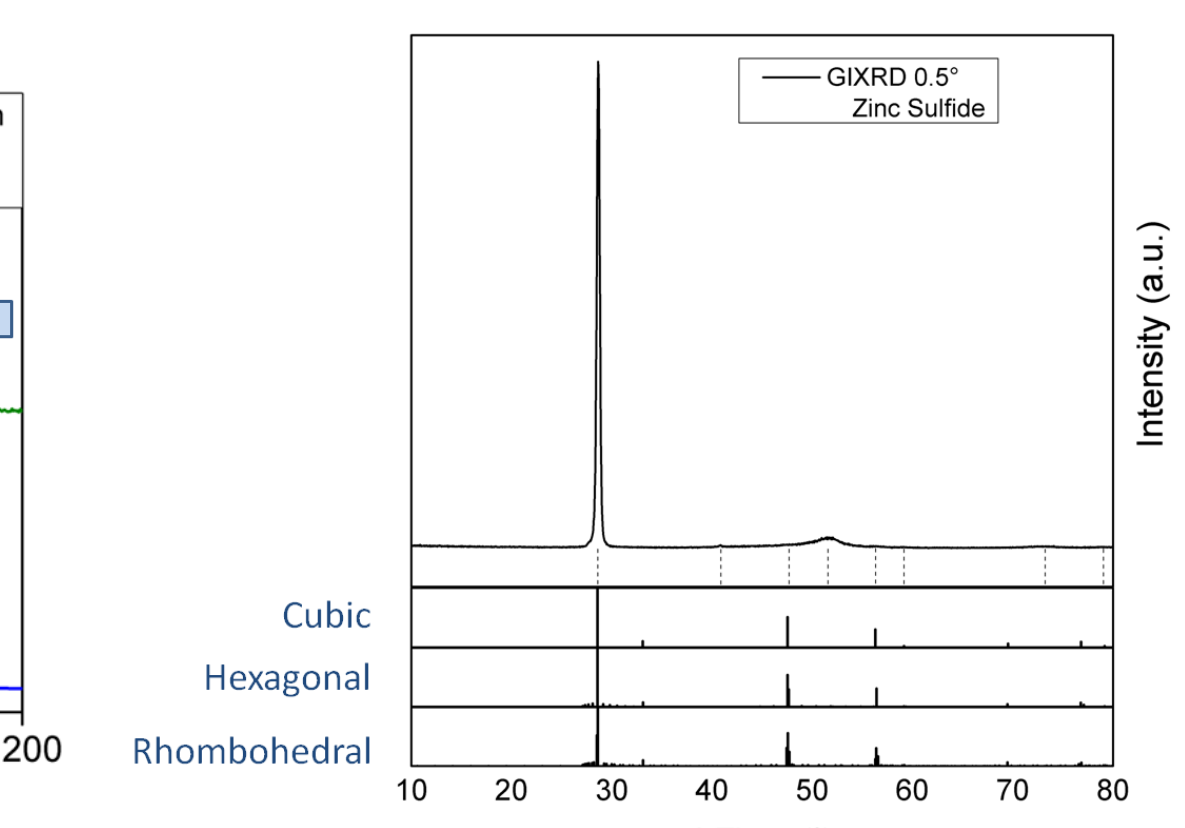
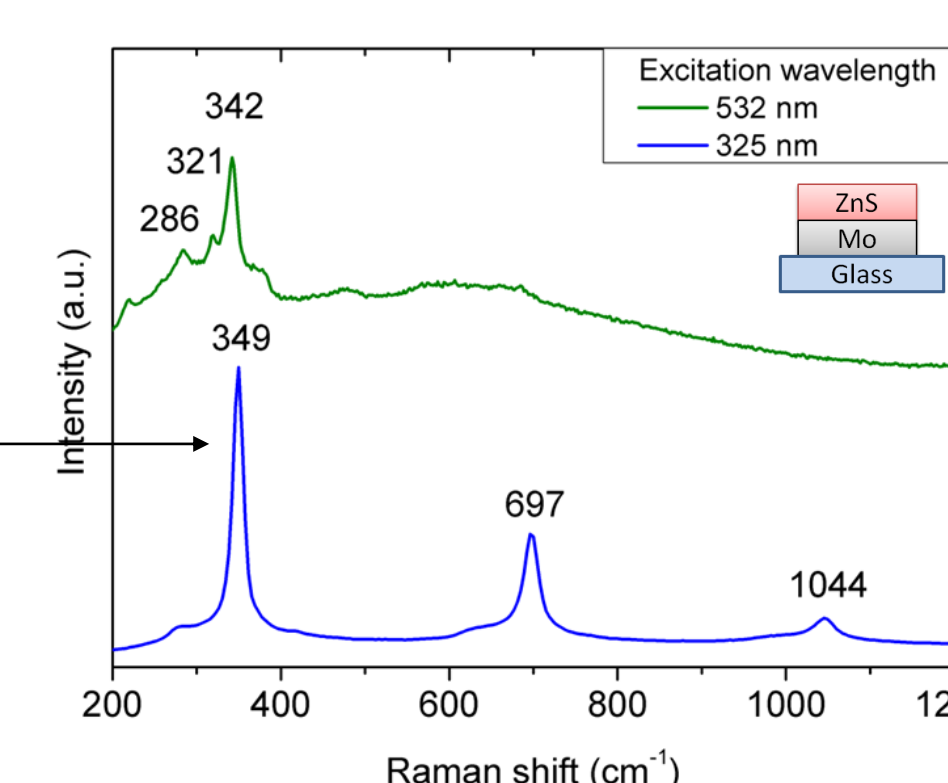
Temperature changes could induce structural changes in the material due to recrystallization, diffusion of elements and evaporation. Linewidth broadening and peak red shift in the Raman signal were explained by Balkanski (1983) by a model of a damped harmonic oscillator that included contributions from thermal expansion and phonon coupling.

Results - Ex situ characterization on secondary phases

- Dominant phase Cu_2SnS_3
- Minor structures of other CTS phases observed



- Dominant phase cubic ZnS
- Resonant enhancement of vibrational mode where photon energy coincides with bandgap energy



Conclusion

- In situ phase identification at high process temperatures is possible with Raman spectroscopy
 - ZnS up to 450°C
 - CTS up to 550°C
- Formation of CZTS from ZnS/CTS stack occurs around 450°C
- CZTS main A-mode can be monitored in situ at 550°C

References

- Raman on Cu_2SnS_3
Fernandes J, Phys. D: Appl. Phys. 43 (2010) 215403 (11pp)
Hao Guan et al. J Mater Sci: Mater Electron (2013) 24:1490–1494
Naoya Aihara, Japanese Journal of Applied Physics 53, 05FW13 (2014)
Chaiapathi, Phys. Status Solidi A 210, No. 11, 2384–2390 (2013)
- Raman on ZnS
Scott et al Vol 1, no. 8 Optics Communications 1970
Nielsen, Phys Rev Vol 182 no. 3 1969
Fairbrother, CrystEngComm, 2014
- Temperature dependent Raman on CZTS
Sarswat, Phys. Status Solidi B 248, No. 9, 2170–2174 (2011)
Om Pal Singh, Materials Chemistry and Physics 146 (2014) 452–455

The research leading to these results has received funding from the People Program (Marie Curie Actions) of the European Union's Seventh Framework Program FP7/2007-2013/ under REA Grant Agreement No. 316488 (KESTCELLS)



Stephan.vanduren@helmholtz-berlin.de
www.helmholtz-berlin.de

Impurities in Chalcopyrite Photovoltaic: Changing the perception from an absolute to a relative and cost efficiency perspective

SPONSORED BY THE



project: SEKUMAT-CIS
code: 16V0166

Motivation:

The basic intension of the presented research action is to overcome resource-economic bottlenecks of the further technological development and market rollout of CIGS PV Products. The envisaged approach to overcome these bottlenecks is to find possibilities to use precursor material with element specific purity levels. This approach followed the idea that knowing the impurities elements which have a substantial influence on the device characteristic allows to modified recycling and cleaning processes of precursor material which focused on impurities elements with substantial influence.

Background:

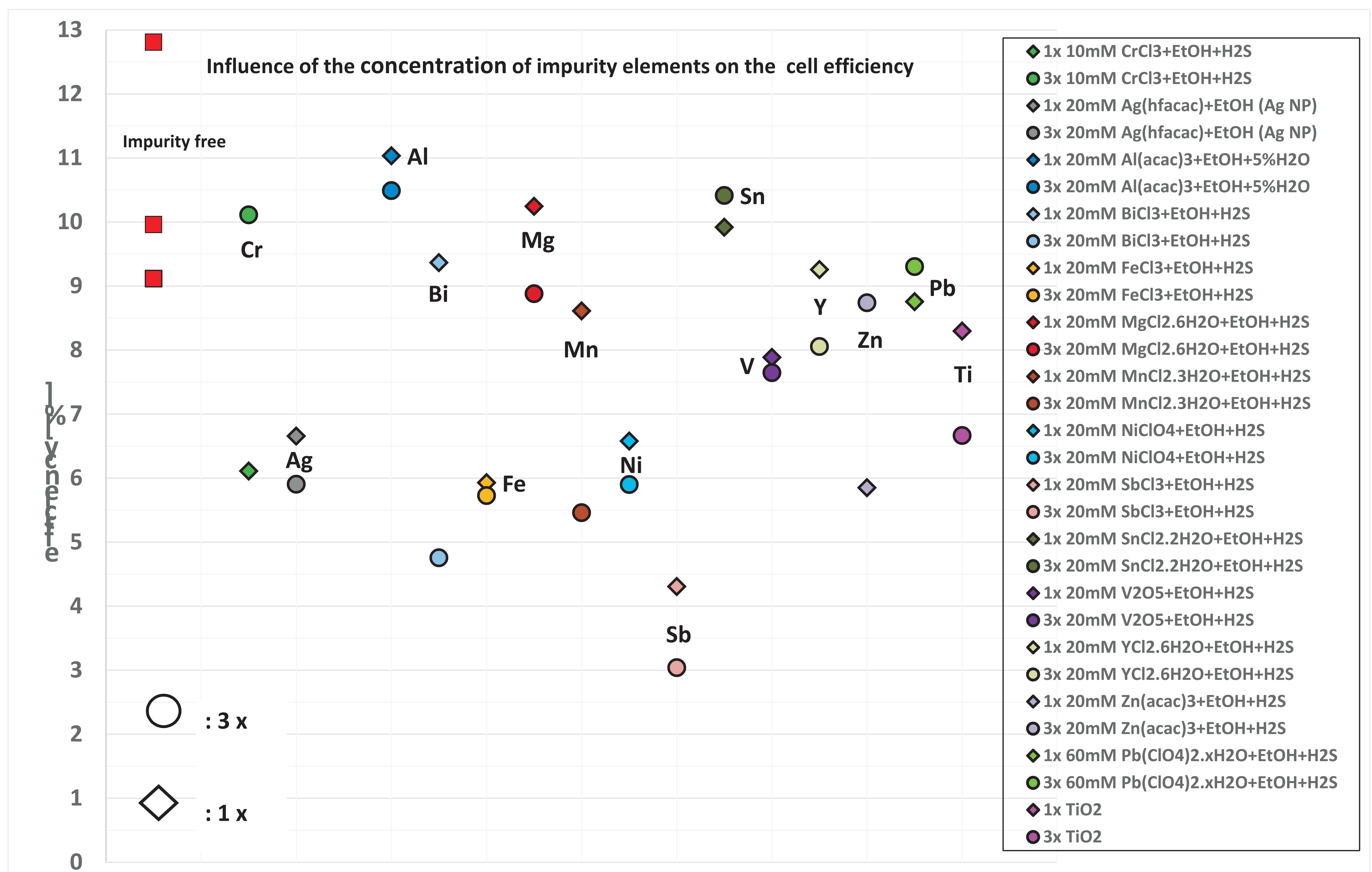
At the beginning of the research action it could be shown that marketable precursor material includes multiplicity of impurity elements [1]. Furthermore it has shown that impurity profiles of the target are nearly complete transferred to the substrate with some concentration effects while using evaporation deposition. [2]. As a preliminary result it could be shown that the purity of the Indium target has only a small influence on the efficiency of the prepared solar cells. That means using high purity material does not lead automatically to an improvement of the cell efficiency in the same dimension.

Some impurities like Fe are well known to severely deteriorate the efficiency of chalcopyrite devices when contained in the absorber material in relevant concentrations. In opposition to that, possible impurity elements like Na, Ka or Sb are known to improve the device properties by improving the crystalline structure of the absorber.

To explore the specific influence of the individual impurity element on the device characteristic deliberate impurities have been introduced to the precursor. These artificial contaminations of the precursor were realized by ILGAR-Technique which allowed a coating with the dissolved impurities.

Experimental:

Several impurities elements were applied in different concentration on the precursor surface by ILGAR deposition.



Conclusion and Outlook:

As a result of this work information about the specific influence of impurity elements in indium precursor material can be given. It can be shown that some impurities elements have a significant higher influence on the cell performance than other. Furthermore it seems that the achievable improvement of cell efficiency does not fully justify the higher cost of high purity indium. Lowering the overall purity of the precursor material and sparsen the element specific purity can have a significant contribution on reduction the manufacturing costs of CIGS-PV.

References:

- [1] „Impurities in Chalcopyrite Photovoltaic Absorbers originating from precursor materials“. Volker Hinrichs, Volker Handke, et al. 29th EUPVSEC, 22 - 25 September 2014, Amsterdam, The Netherlands
 [2] „LA-ICP-Mass Spectrometry of Impurities in Indium Feedstock Material and their Influence on Cu(In_xGa(1-x))Se₂ PV-Device Performance!“. Volker Hinrichs, Volker Handke, et al: 6th World Conference on Photovoltaic Energy Conversion

Process and Quality Control of Cu(In,Ga)Se₂ Co-Evaporation via White Light Reflectometry

MOTIVATION

Optical process analysis becomes an increasingly important area for the deposition of complex semiconductor alloys like Cu(In,Ga)Se₂. It allows a better understanding as well as better control of the semiconductor growth. Here we present an optical analysis technique, which is capable of providing in-situ data about deposition rate, roughness, band gap as well as Urbach energy. Additionally we used energy dispersive X-ray diffraction to correlate the obtained optical properties to the structural properties, like roughness and crystalline phase transitions [1][2].

PROCESS CONTROL

Fig.1: The foundation of the method is to analyze the specular reflection spectrum from a CIGSe layer deposited on a Mo substrate, which is shown together with the fitted spectrum. First, different properties are obtained from different parts of the spectrum, as marked by the circles. Then the whole spectrum is fitted with the refractive index as a fitting parameter. The process is repeated until convergence is achieved.

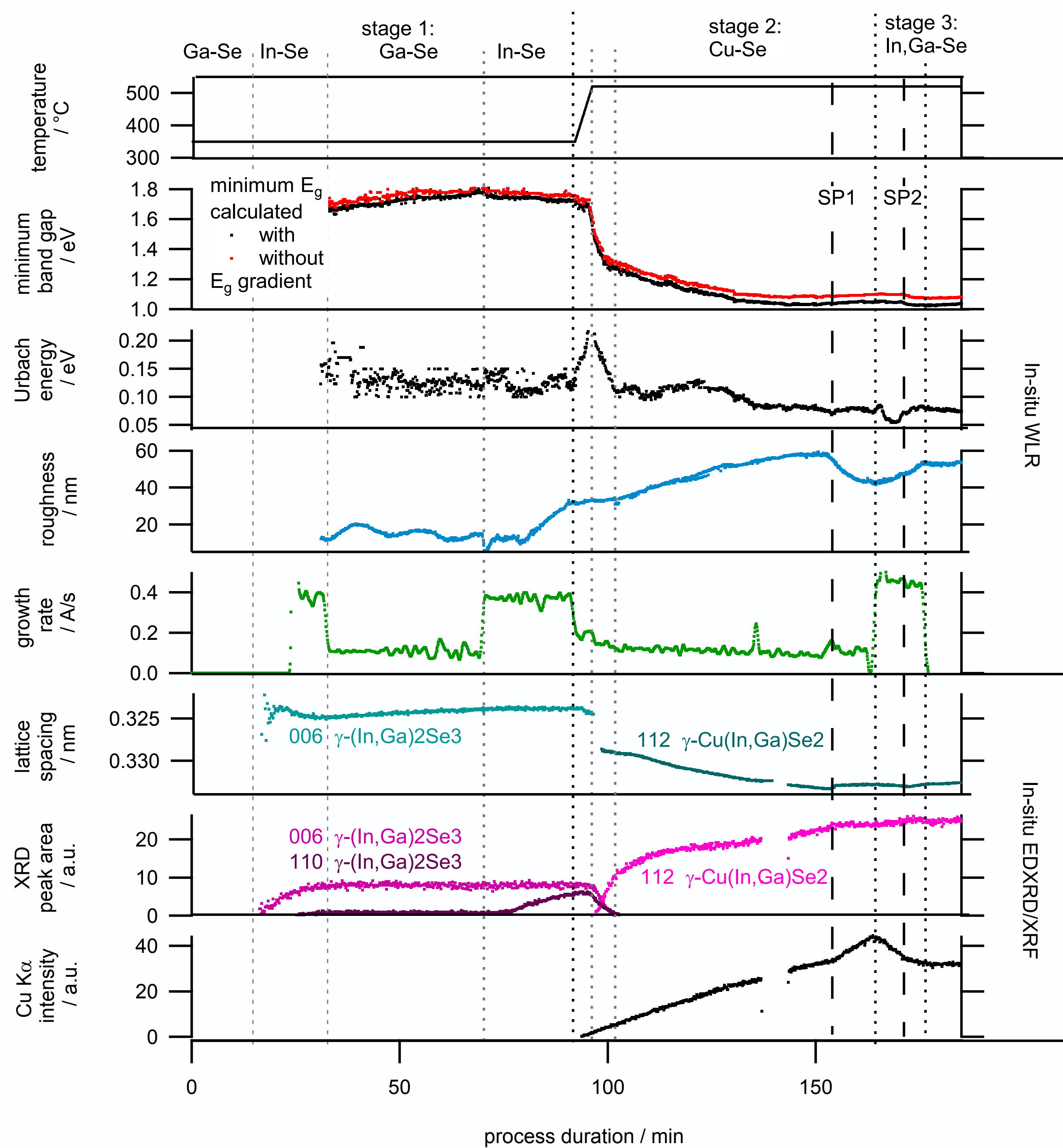
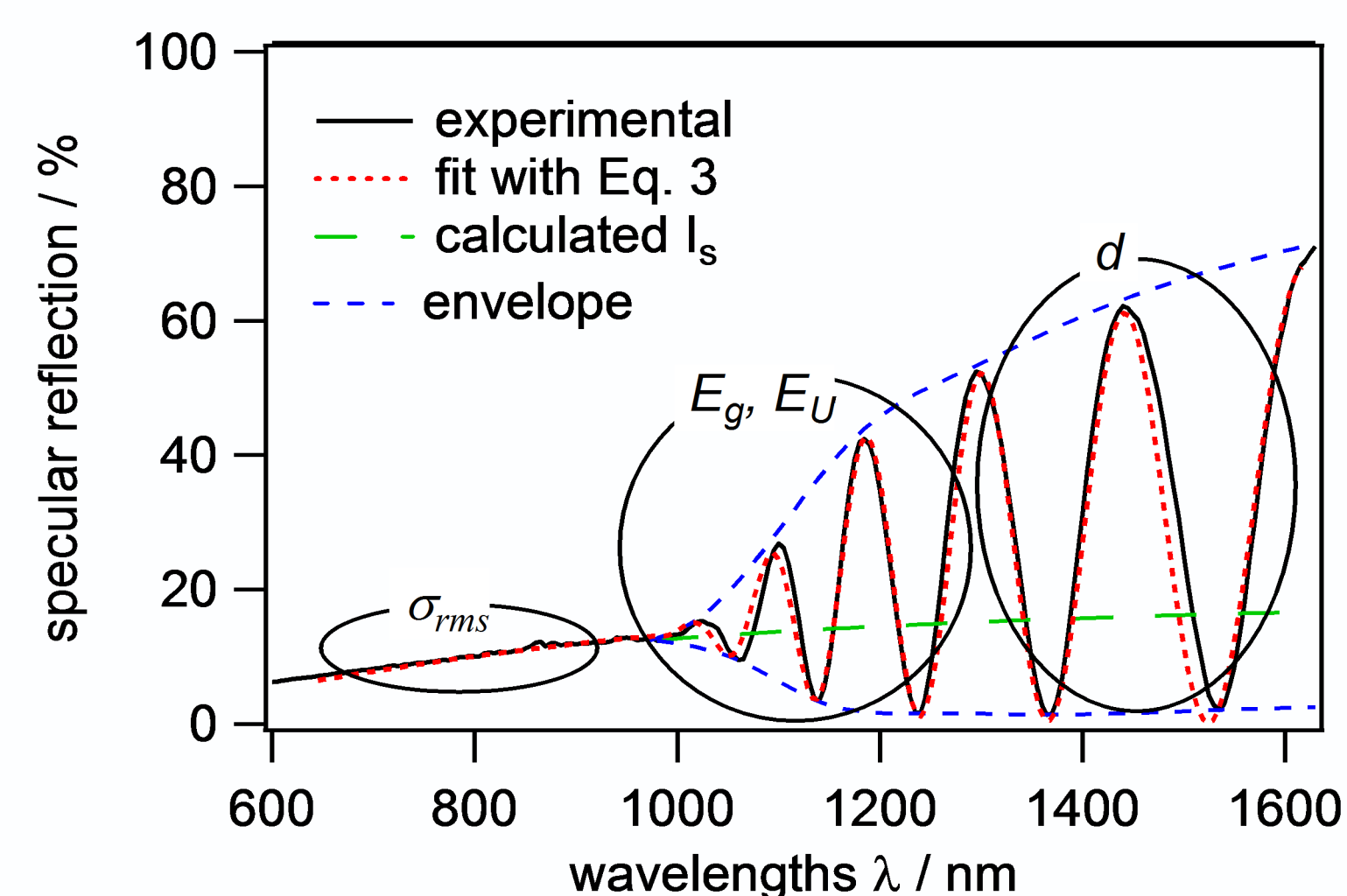


Fig.2: Optical and structural properties obtained in real time by in-situ white light reflection (WLR) and EDXRD/XRF during a multi-stage deposition process of Cu(In,Ga)Se₂. In the first and third stage In-Ga-Se is deposited and in the second stage Cu and Se.

CONCLUSION AND OUTLOOK

- A method is presented that is capable of providing in-situ data about the growth rate, roughness, band gap energy as well as Urbach energy during thermal co-evaporation of CIGSe thin films.
- The film roughness indicates the crystalline phase development in the bulk, as well as indirectly the secondary phases on the surface.
- The measurement of the minimum band gap energy during the process enables the control over the final minimum band gap energy by controlling the gallium flux during stage 2.
- The dip in the Urbach energy during the third stage may open new pathways for future improvement of absorber quality.

EXPERIMENTAL SETUP

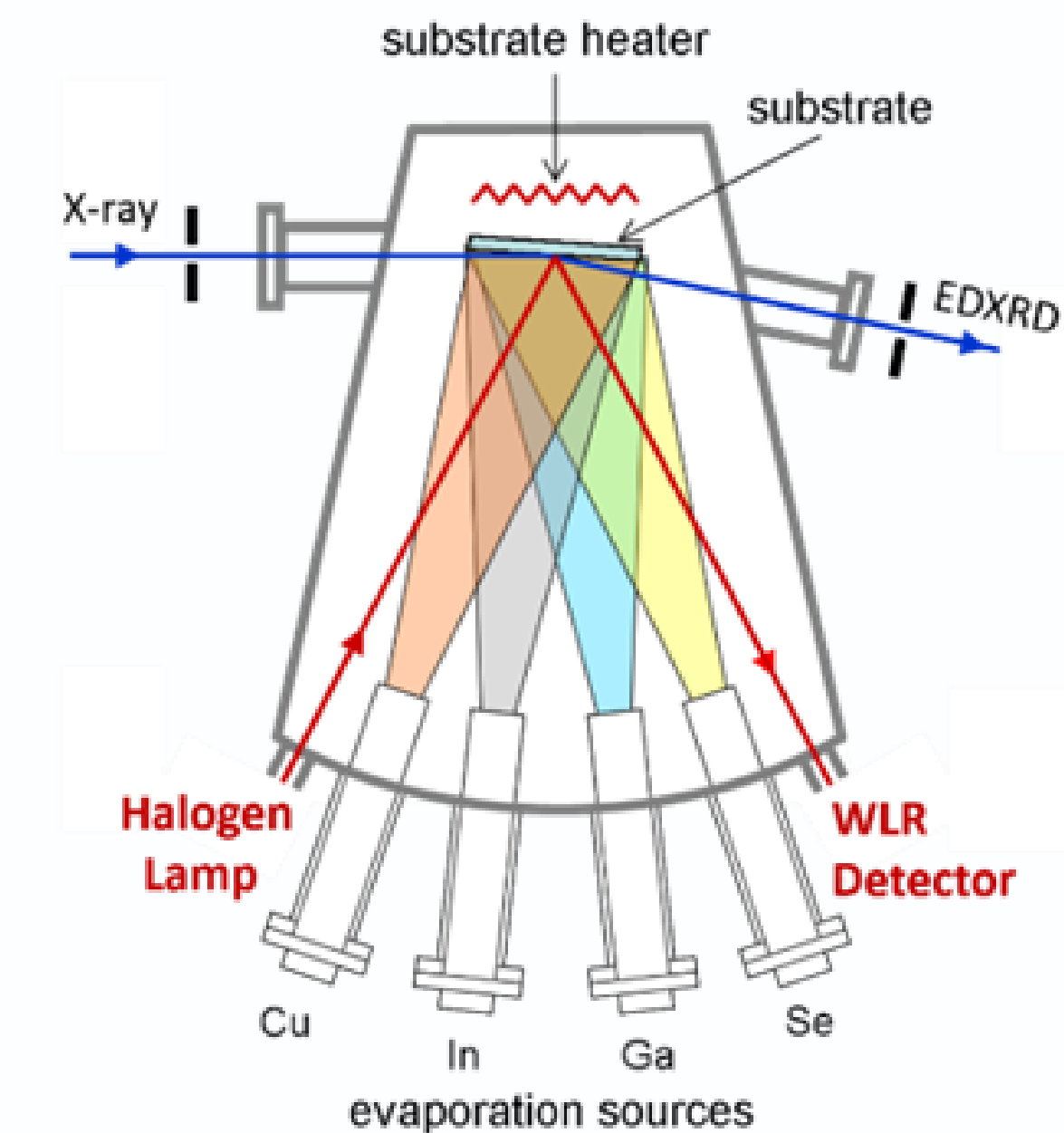


Fig.3: Schematic drawing of the PVD chamber and the in-situ characterization tools used to grow and analyze the CIGS film at the same time. The three-stage co-evaporation process [3] of the CIGS deposition were performed at 520 °C.

CORRELATION WITH ED-XRD

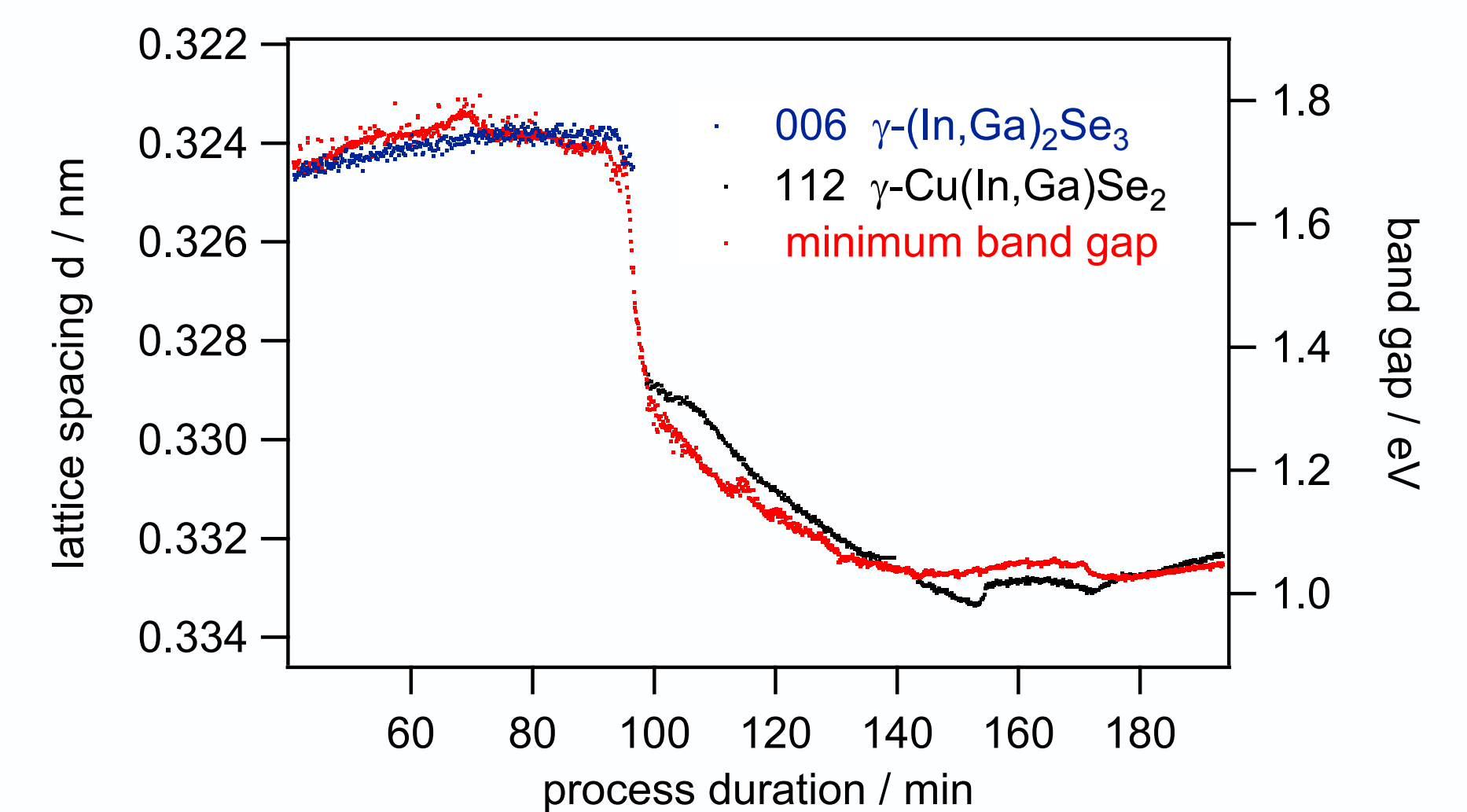


Fig.4: The minimum band gap correlates well with the dominant XRD peak position of 110 g-(In,Ga)₂Se₃ and the 112 g-Cu(In,Ga)Se₂ peak. phase development in the bulk.

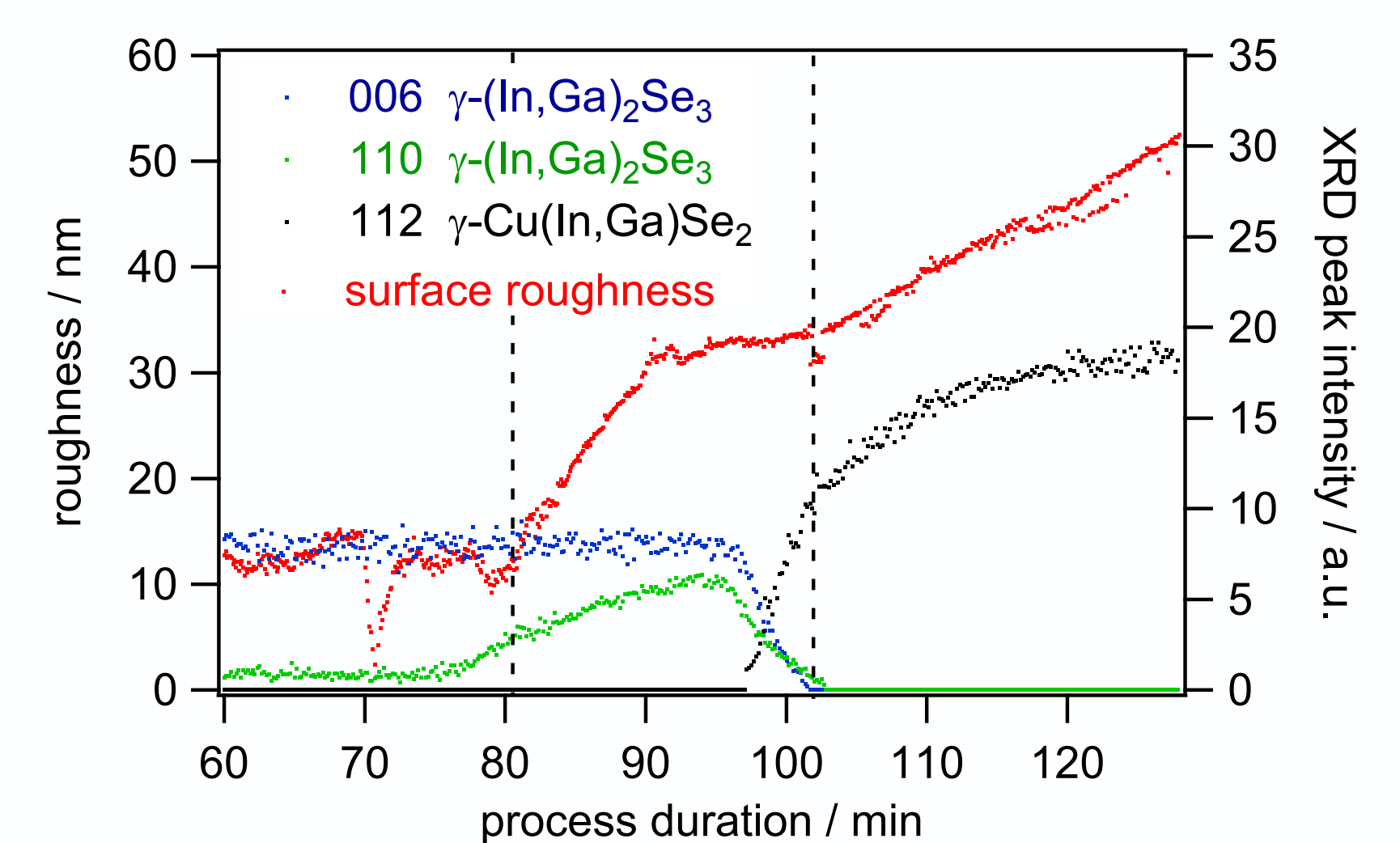


Fig.5: The surface roughness in comparison to the dominant XRD peak intensities. The changes in roughness can be well correlated to the crystalline phase transitions.

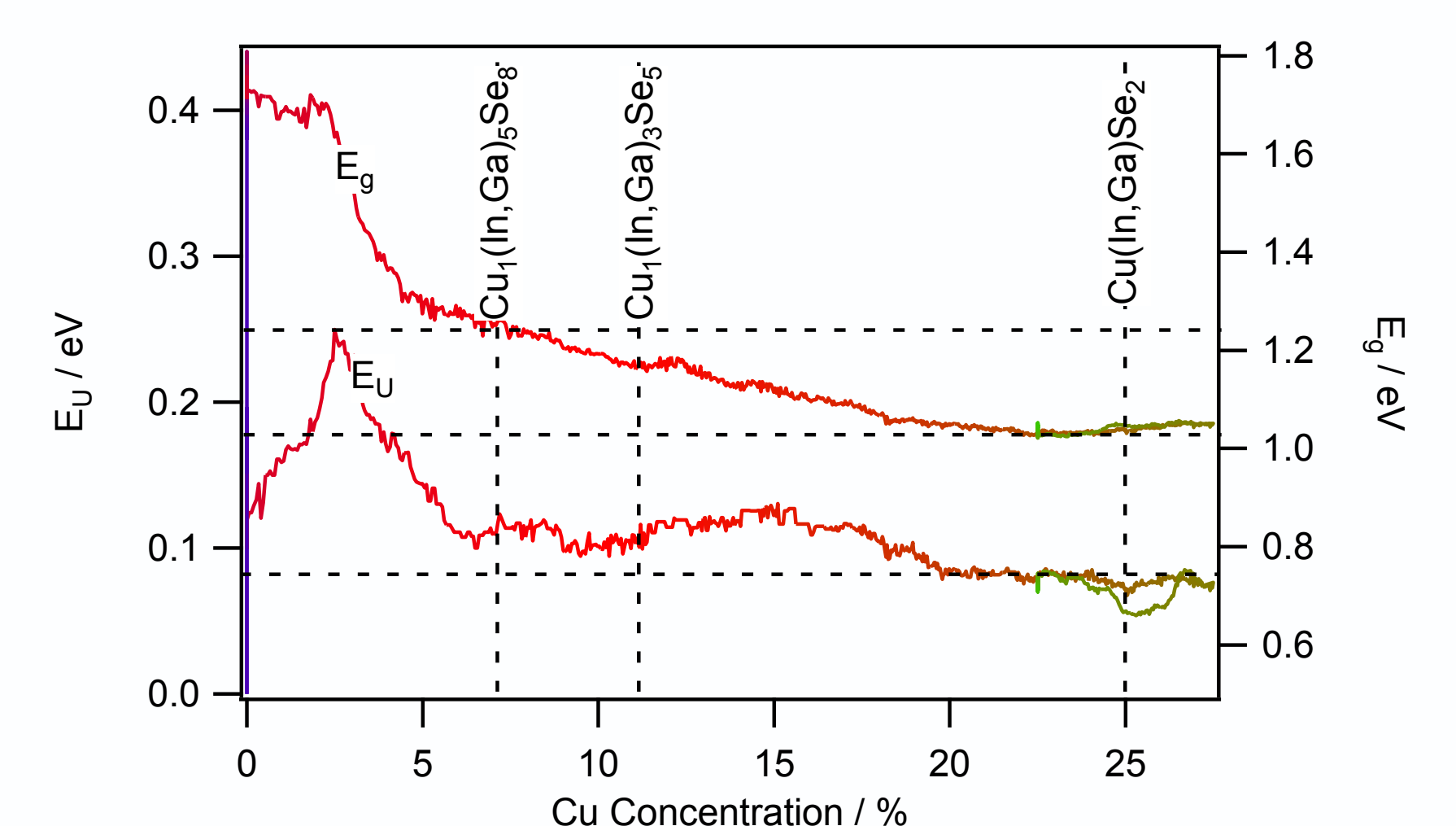


Fig.6: Urbach energy and minimum band gap plotted versus the Cu concentration in the growing film. The Urbach energy is minimized during the Cu-rich phase at a Cu concentration above 25%.

Literature:

- [1] Patent filed
[2] Paper submitted to Advanced Energy Materials
[3] K. Ramanathan, M. A. Contreras, C. L. Perkins, S. Asher, F. S. Hasoon, J. Keane, D. Young, M. Romero, W. Metzger, R. Noufi and others., „Properties of 19.2% efficiency ZnO/CdS/CuInGaSe₂ thin-film solar cells,“ Progress in Photovoltaics: Research and Applications, Bd. 11, Nr. 4, pp. 225-230, 2003.

Temperature dependence of the opto-electronic and structural properties of the MgAg₃-MoO_{3-x} system as recombination zone in tandem organic solar cells

A. R. Jeong, S. Fengler, S. Wiesner, M. A. Gluba, M. Ch. Lux-Steiner, and M. Rusu

Institut für Heterogene Materialsysteme, Helmholtz-Zentrum Berlin für Materialien und Energie GmbH, Lise-Meitner Campus, Hahn-Meitner-Platz 1, 14109 Berlin, Germany

HZB Helmholtz Zentrum Berlin

Abstract

- High efficiency tandem organic solar cells require efficient recombination zones for the series connection of their individual sub-cells.
- Temperature induced changes in work function and structure have been investigated by Kelvin probe force microscopy and Raman spectroscopy.
- Surface properties of MgAg₃-MoO_{3-x} system are correlated with variation of MoO_{3-x} characteristics depending on annealing temperature.

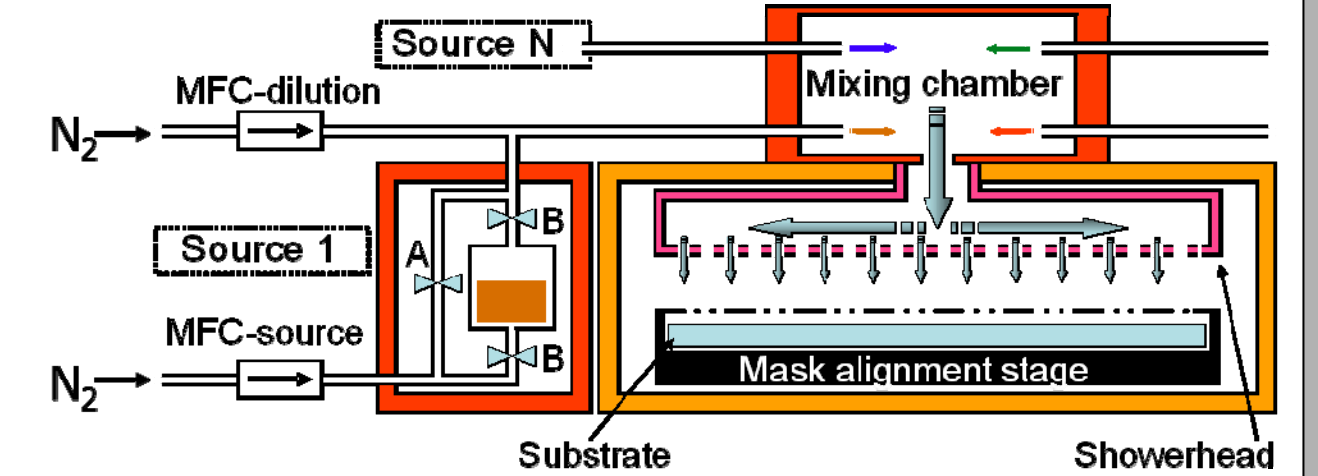
Experimental

Thin-film Preparation

- Zinc phthalocyanine (ZnPc) and C₆₀ layers by organic vapour phase deposition (OVPD)^[3]
- MoO_{3-x} as hole transport layer by PVD in high vacuum (~10⁻⁷ mbar)
- Mg:Ag layers by physical vapour deposition

OVPD Method^[6]

- Carrier gas: N₂
- Reactor pressure p: 0.6 mbar
- Substrate temperature T: 151°C



Characterization

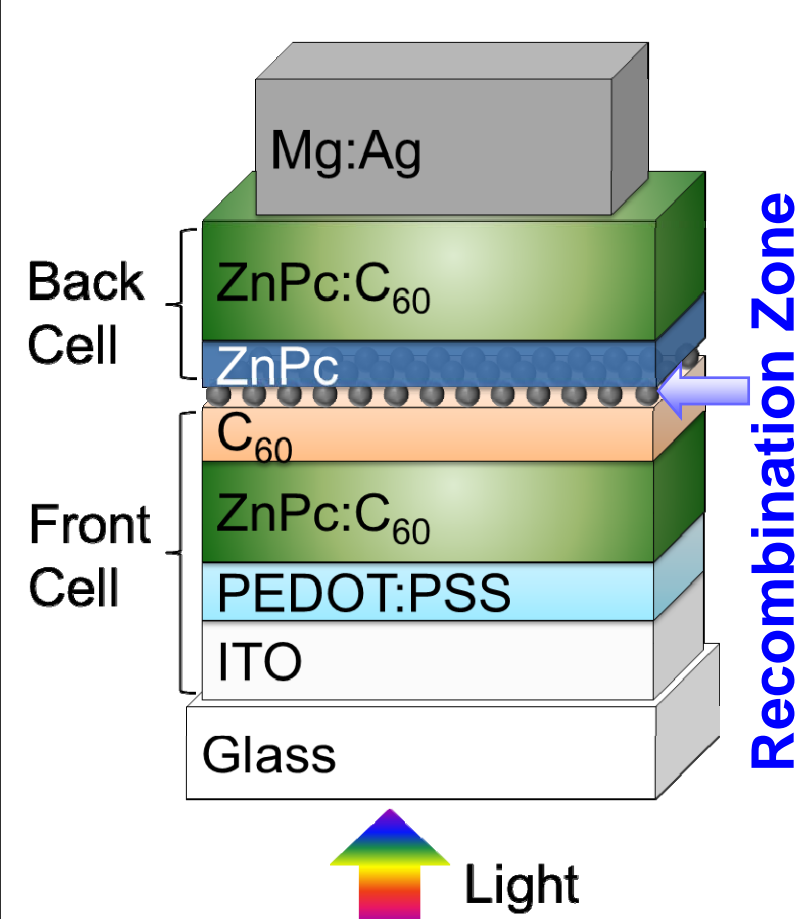
- Electric and photoelectric properties of OPVs by I-V measurements in the dark and illumination (100 mW/cm² (Ha-Lamp), 25°C), external quantum efficiency (EQE)
- Work function by ultra high vacuum Kelvin probe force microscopy (UHV-KPFM) (~10⁻¹⁰ mbar)
- Raman spectroscopy, X-ray photoemission spectroscopy

Ultra high vacuum (UHV) KPFM

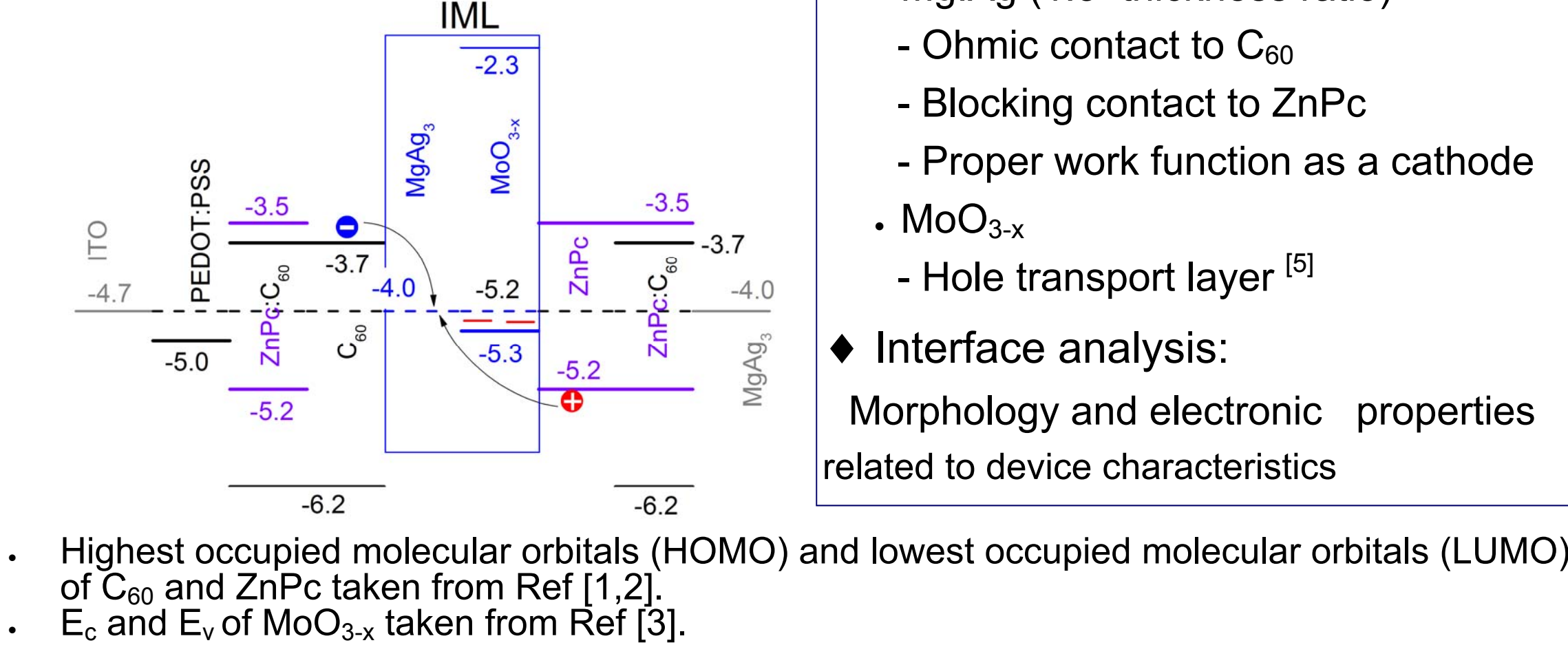
- Work function of the sample measured by KPFM
- $\Phi_{sample} = \Phi_{tip} + eV_{CPD}$
- (e: elementary charge, V_{CPD}: contact potential difference)
- Sample transport from N₂ filled glove box to UHV KPFM (~10⁻¹⁰ mbar) without air exposure

Motivation

Tandem OPV device



Band alignment of tandem device

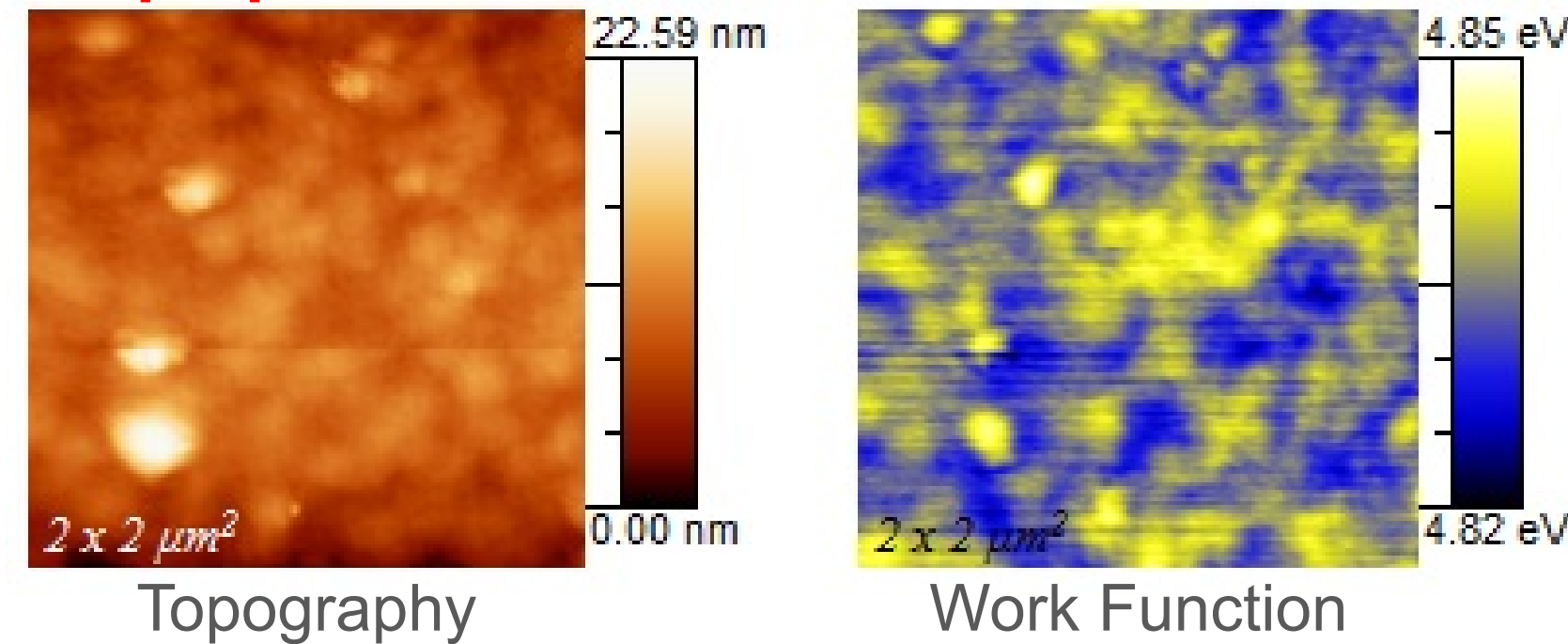


- MgAg₃-MoO_{3-x} intermediate layer
 - Mg:Ag (1:3 thickness ratio)^[4]
 - Ohmic contact to C₆₀
 - Blocking contact to ZnPc
 - Proper work function as a cathode
- MoO_{3-x}
 - Hole transport layer^[5]
- Interface analysis:
 - Morphology and electronic properties related to device characteristics

Electronic properties of MgAg₃-MoO_{3-x} system

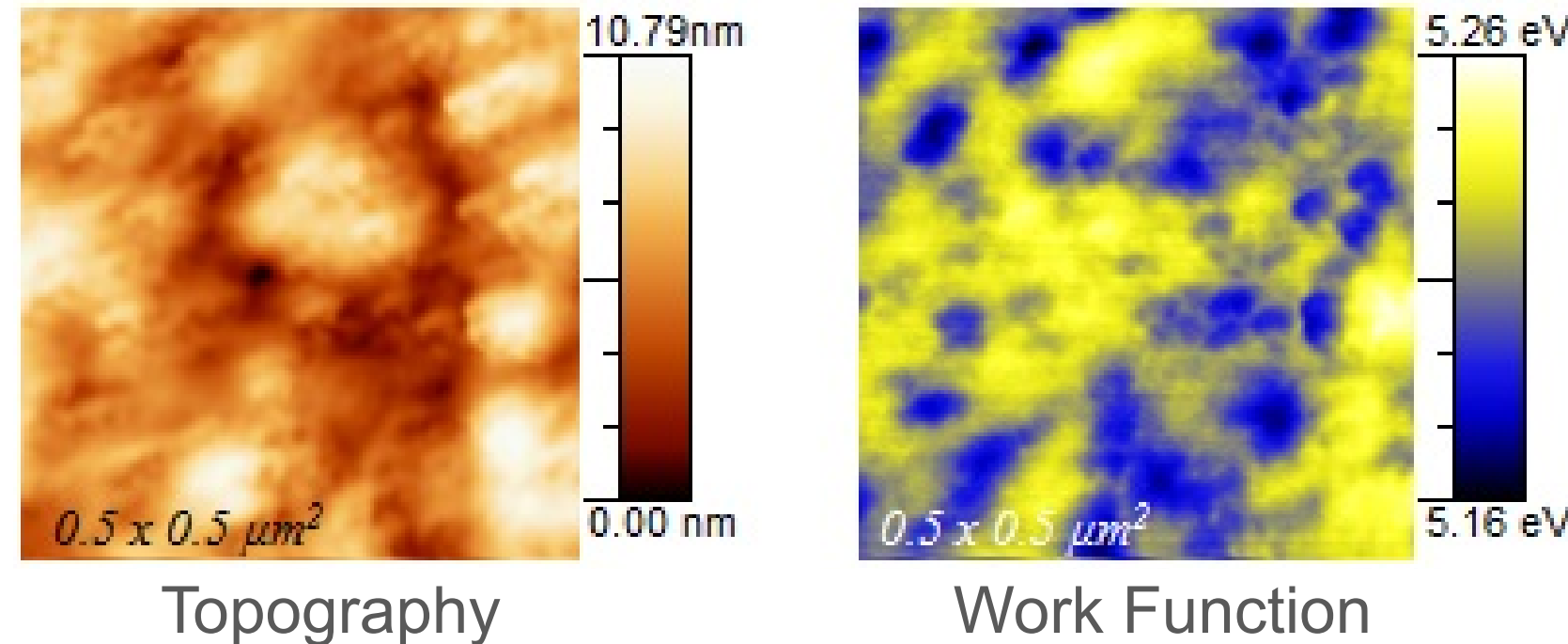
- ITO / PEDOT:PSS / 60 nm ZnPc:C₆₀ / 10 nm C₆₀ / **0.8 nm MgAg₃ - 3 nm MoO_{3-x}**

As-prepared



Surface materials	Work function (eV)	
	As-prepared	Annealed
C ₆₀	4.45 ± 0.01	4.54 ± 0.01
MgAg ₃	4.23 ± 0.01	4.03 ± 0.01
MoO _{3-x}	4.83 ± 0.01	5.21 ± 0.01
MgAg ₃ -MoO _{3-x}	4.83 ± 0.01	5.21 ± 0.01

Annealed at 150°C, 30min

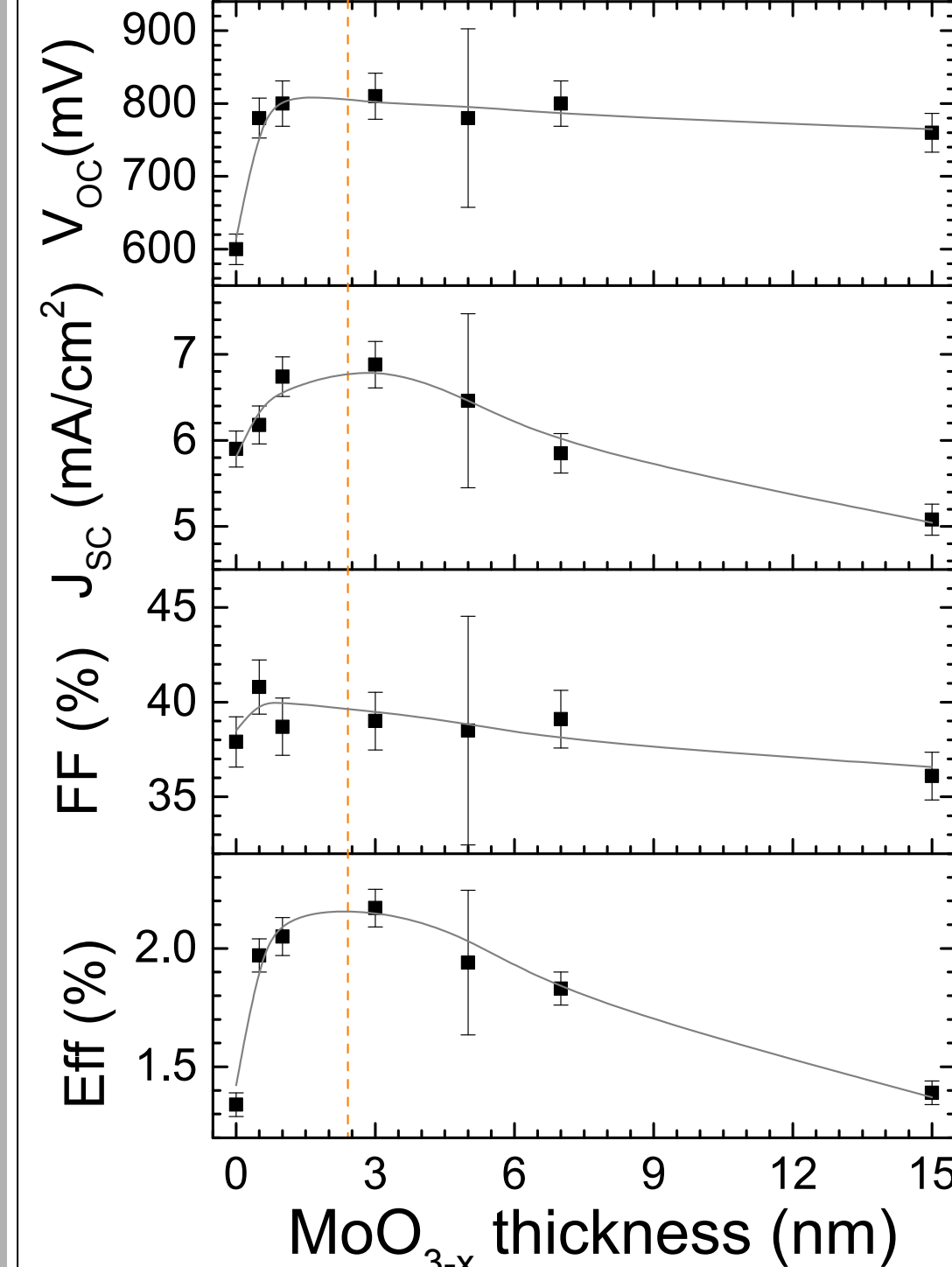


- Annealing process conducted under the same conditions as the OVPD process for tandem cell preparation
- Investigating local morphology features and electronic properties by UHV-KPFM
- Appropriate work function and band alignment for the recombination zone

Optimization of Recombination Zone

PV Parameters of organic tandem solar cells

Variation of MoO_{3-x} thickness at fixed 0.8 nm MgAg₃



MgAg ₃ (nm)	MoO _{3-x} (nm)	V _{oc} (mV)	J _{sc} (mA/cm ²)	FF (%)	Eff (%)
0.8	5	790	5.61	39.0	1.7
0	5	390	10.38	38.6	1.6
0.8	3	810	6.88	39.0	2.2
0.8	0	600	5.90	37.9	1.3
Front		430	9.66	35.8	1.5
Back		440	10.26	39.9	1.8

- Maximum Eff. and Voc**
- ⇒ **2.2% and 810 mV with optimized recombination zone (close to the sum of Voc's of the front and back cells)**
- Recombination zone with single material
- ⇒ MoO_{3-x} only: does NOT function as recombination zone
- ⇒ MgAg₃ only: acts as recombination zone, but not optimized
- EQE (J_{sc}) of the tandem device is nearly half of the reference due to reduced light intensity in the back cell and not optimized absorber positions in the optical field across the device.

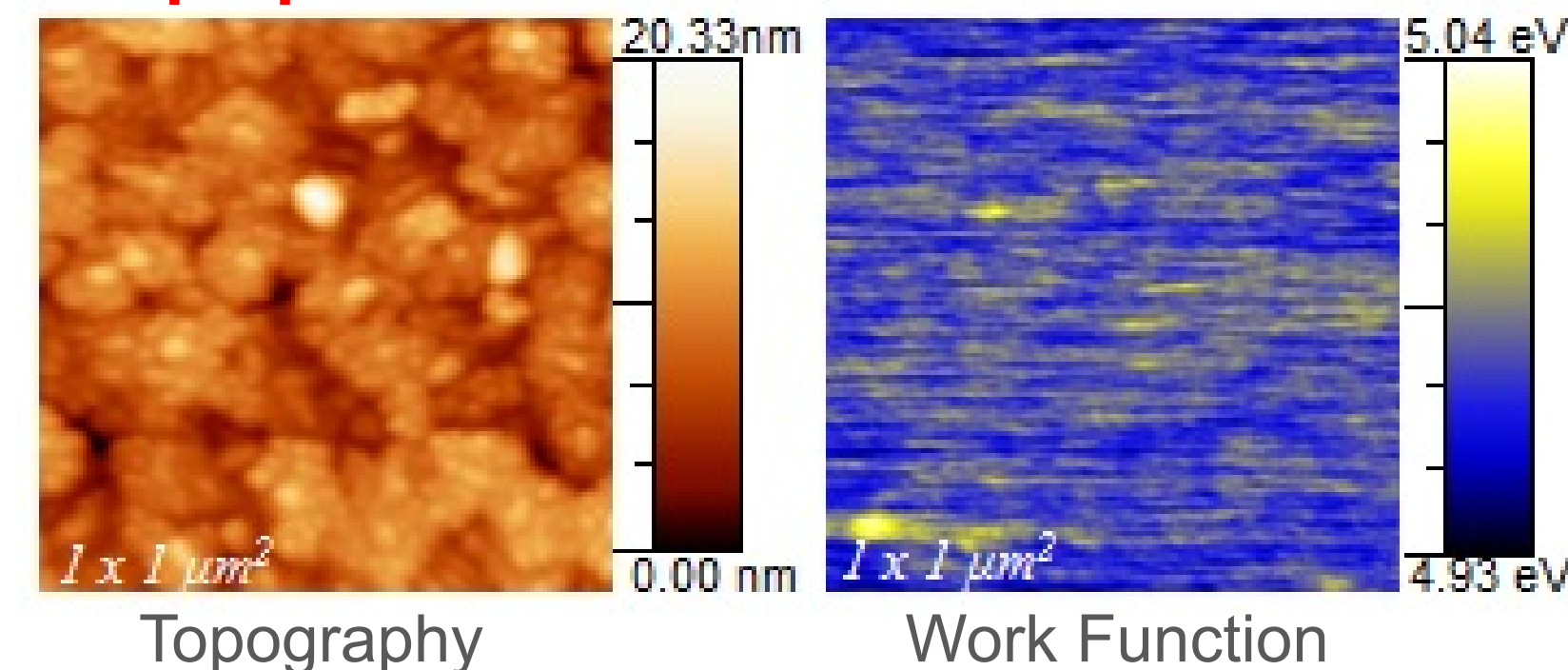
Physical properties of MoO_{3-x}

Electronic properties

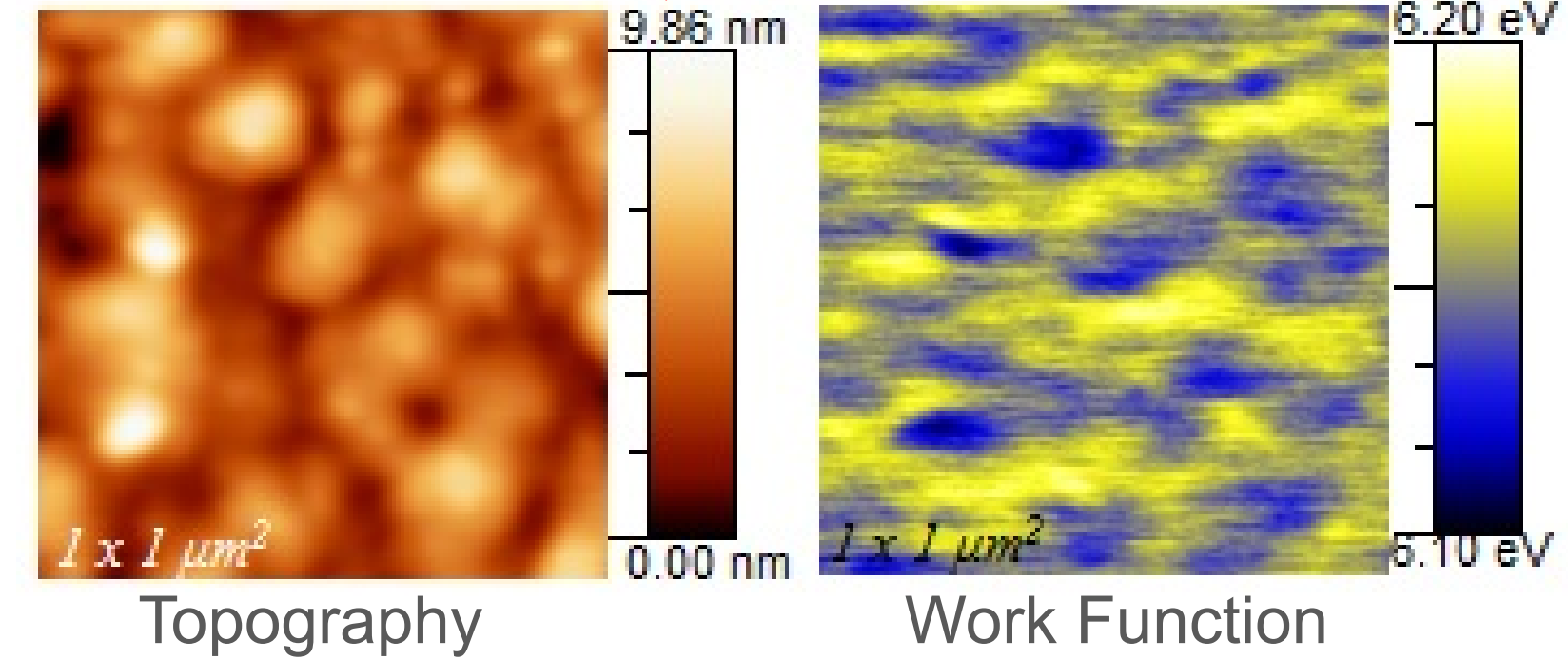
KPFM analysis

- ITO / 15 nm MoO_{3-x}

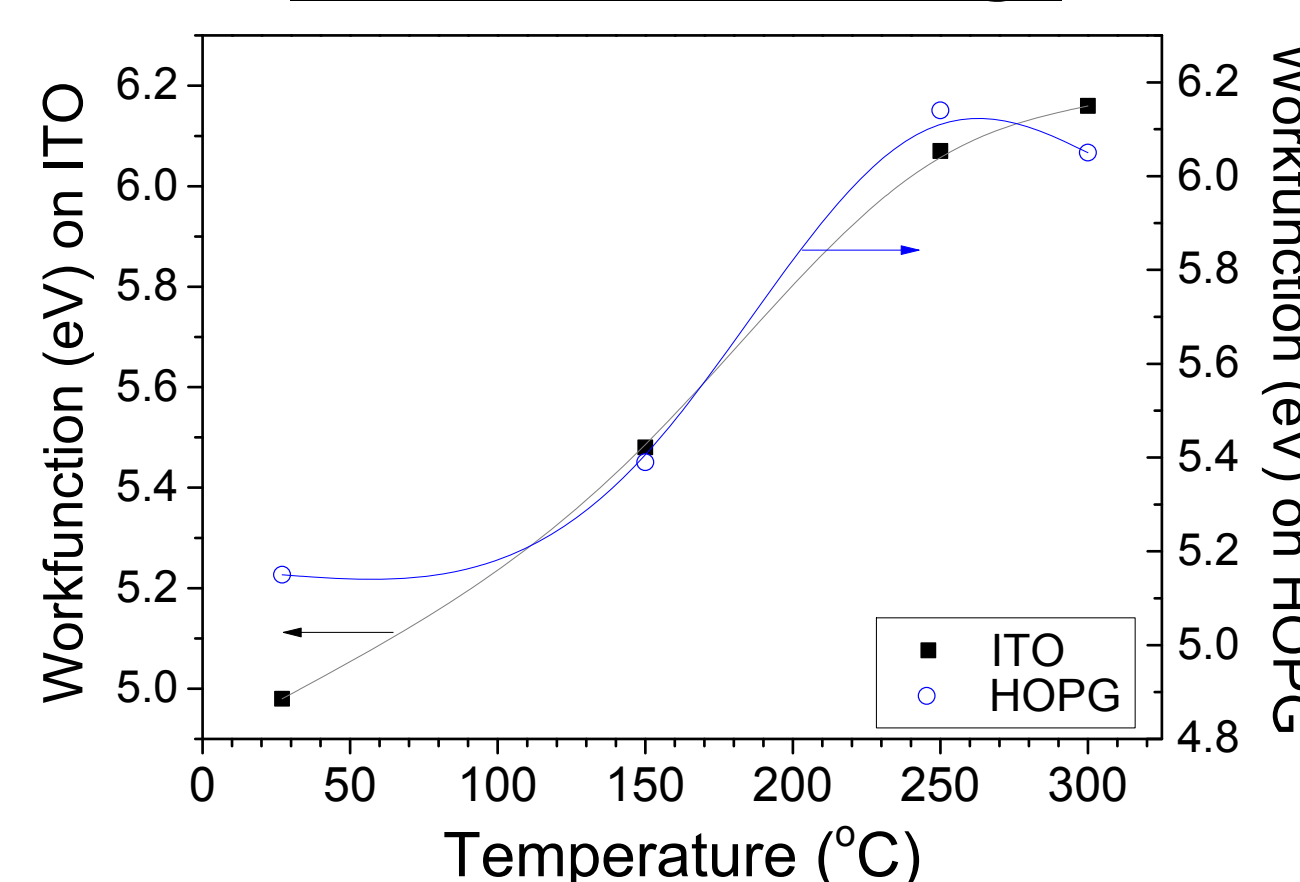
As-prepared



Annealed at 300°C, 30min



Temperature induced work function change



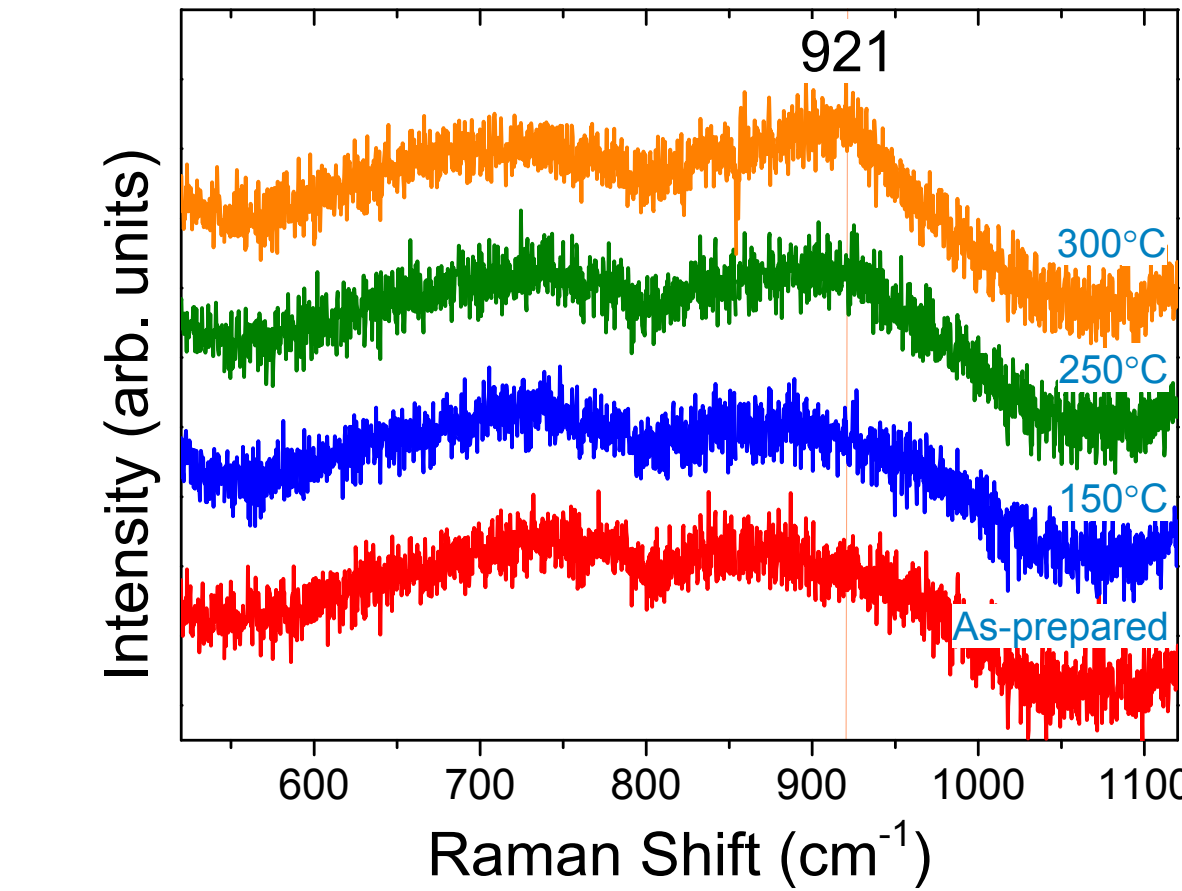
- Temperature induces work function increase regardless of the substrate.

XPS analysis

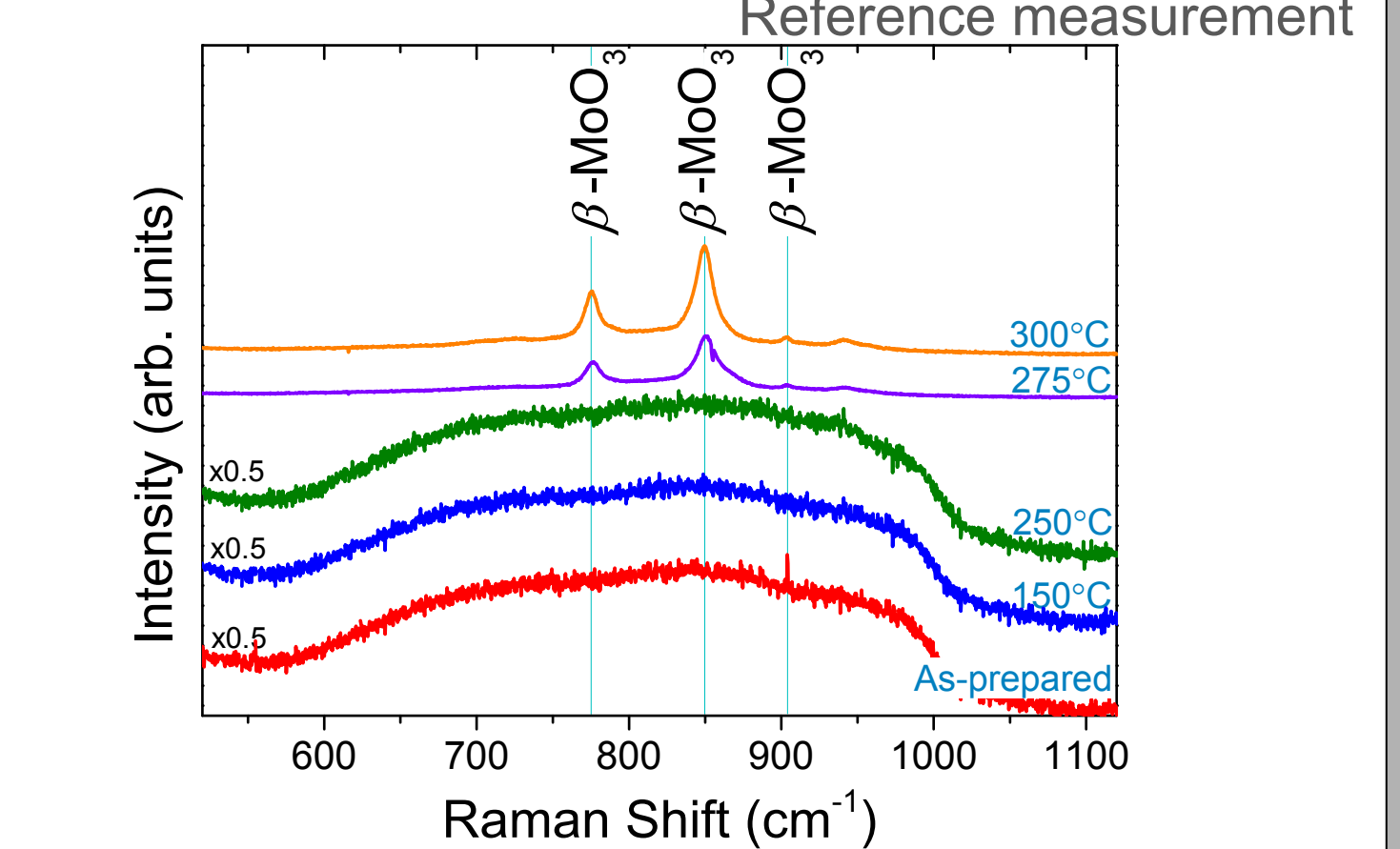
Oxygen vacancies are created by annealing Mo⁶⁺ (30°C) → Mo⁵⁺/Mo⁴⁺ (310°C).
⇒ Oxygen vacancies can influence work function and distort the structure.^[7]

Structural properties Raman analysis

- ITO / 15 nm MoO_{3-x}



- ITO / 200 nm MoO_{3-x}



Crystallization of MoO_{3-x}

- The broad signal from 800 to 1020 cm⁻¹ is related to the MoO₃ frame.^[8]
- Increase of Raman band at 917, 935, 921, 918, 930 cm⁻¹ indicates crystallization by annealing above 250°C.
- Evolution of Raman band at ~921 cm⁻¹ indicates increasing degree of crystallinity of 15 nm MoO_{3-x} films above 250°C.
- Increase of Raman line width: probably formation of nano-crystallinities in amorphous matrix and/or strain induced distortion of crystal structure.^[9]

Conclusion

- The efficient 0.8 nm MgAg₃-3 nm MoO_{3-x} recombination zone for tandem solar cell has been studied by KPFM for surface morphology and work function.
- Suitable band alignment in tandem organic device has been proved at the interface of recombination zone.
- Temperature induced change in the electronic and structural of MgAg₃-MoO_{3-x} has been investigated, which is related to MoO_{3-x} properties.
- MoO_{3-x} shows structural changes after annealing over 250°C, which is correlated with the work function change of the layer and chemical composition.

References

- [1] K. L. Mutolo, E. I. Mayo, B. P. Rand, S. R. Forrest, and M. E. Thompson, *J. Am. Chem. Soc.* **128**, 8108 (2006).
- [2] Z. R. Hong, R. Lessmann, Maennig, Q. Huang, K. Harada, M. Riede, and K. Leo, *J. Appl. Phys.* **106**, 064511 (2009).
- [3] J. K. Larsen, H. Simchi, P. Xin, K. Kim, and W. N. Shafarman, *Appl. Phys. Lett.* **104**, 033901 (2014).
- [4] M. Rusu, S. Wiesner, I. Lauer, M. Ch. Lux-Steiner, J. N. Audinot, Y. Fleming, and M. Ch. Lux-Steiner, *Appl. Phys. Lett.* **97**, 07350 (2010).
- [5] W. Riedel, S. Wiesner, D. Greiner, V. Hinrichs, M. Rusu, and M. Ch. Lux-Steiner, *Appl. Phys. Lett.* **104**, 173503 (2014).
- [6] M. Rusu, S. Wiesner, T. Mete, H. Blei, N. Meyer, M. Heuken, M. Ch. Lux-Steiner, and K. Fostiropoulos, *Renewable Energy* **33**, 254 (2008).
- [7] B. Dasgupta, W. P. Goh, Z. E. Ooi, L. M. Wong, C. Y. Jiang, Y. Ren, E. S. Tok, J. Pan, J. Zhang, and S. Y. Chiam, *J. Phys. Chem. C* **117**, 9206 (2013).
- [8] L. Seguin, M. Figlarz, R. Cavagnat, and J.-C. Lassgues, *Acta Part A* **51**, 1323 (1995).
- [9] K. Kalantar-zadeh, J. Tang, M. Wang, K. L. Wang, A. Shailos, K. Galatsis, R. Kojima, V. Strong, A. Lech, W. Wlodarski, and R. B. Kaner, *Nanoscale* **2**, 429 (2010).

The authors would like to thank X. Liao, R. G. Wilks, and M. Bär for XPS study. We gratefully acknowledge support by the Helmholtz-Gesellschaft Deutscher Forschungszentren e.V. (HGF) under the project „Hybrid-PV“ and European Union's 7th Framework Programme under project SMARTONICS No.310229.

Dr. Ah Reum Jeong

ahreum.jeong@helmholtz-berlin.de

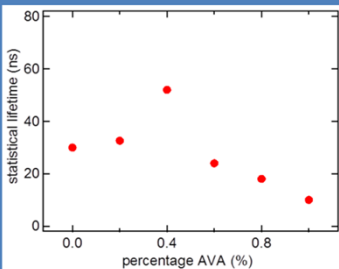
www.helmholtz-berlin.de

Influence of $\text{HOOC}(\text{CH}_2)_4\text{NH}_3\text{I}$ on phase formation, morphology and electronic properties in the solution processed $\text{CH}_3\text{NH}_3\text{PbI}_3 / \text{CH}_3\text{NH}_3\text{PbCl}_3$ system

Motivation and samples

preparation route of $\text{CH}_3\text{NH}_3\text{PbI}_3$ (MAPbI₃) for high-efficiency solar cells
preparation from a solution containing $\text{CH}_3\text{NH}_3\text{I}$ (MAI) and PbCl_2 in a mole ratio of 3:1
separation of $\text{CH}_3\text{NH}_3\text{PbCl}_3$ (MAPbCl₃) induced by adding $\text{HOOC}(\text{CH}_2)_4\text{NH}_3\text{I}$ (AVAI) to the precursor solution.

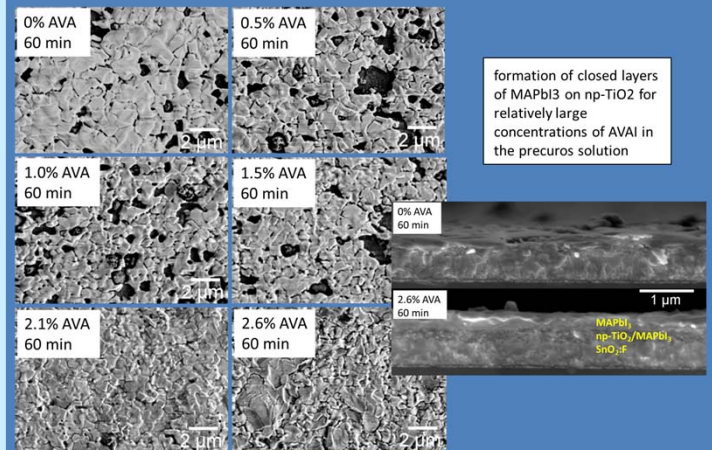
closed films on ultra-thin np-TiO₂ with large crystallized regions and low density of defects in MAPbI₃



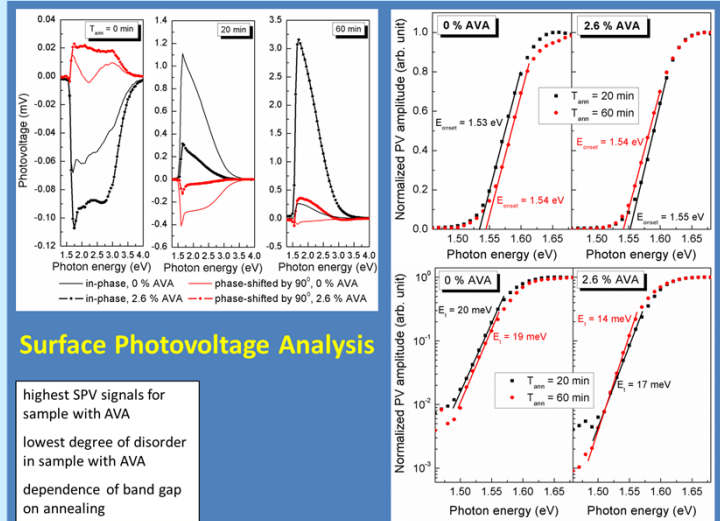
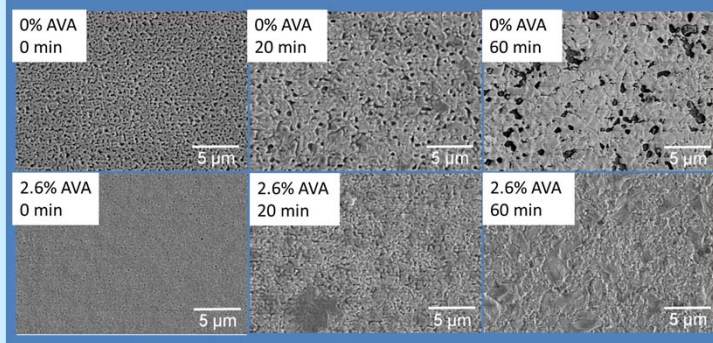
PL analysis

maximum PL lifetime for 0.4 wt% (1 mol%) of AVAI in the precursor solution
reduced PL lifetime for high concentrations of AVAI

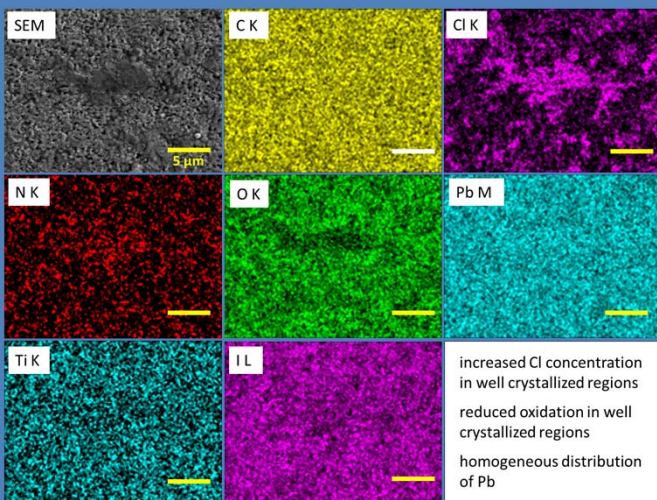
Role of the concentration of AVA



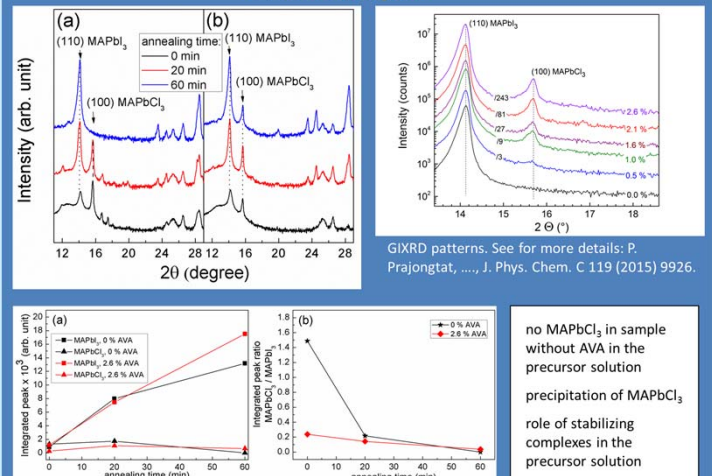
Role of annealing time



EDX Analysis



GIXRD analysis



Al-DOPED ZnO NANOSTRUCTURED ELECTRODES FOR SMALL MOLECULE ORGANIC SOLAR CELLS

S. Wiesner^a, W. Riedel^{a,b}, D. Greiner^c, M. Rusu^a, M. Ch. Lux-Steiner^{a,b}

^aInstitut für Heterogene Materialsysteme, Helmholtz-Zentrum Berlin für Materialien und Energie GmbH, Lise-Meitner Campus, Hahn-Meitner-Platz 1, 14109 Berlin, Germany

^bFreie Universität Berlin, Department of Physics, Arnimallee 14, 14195, Germany

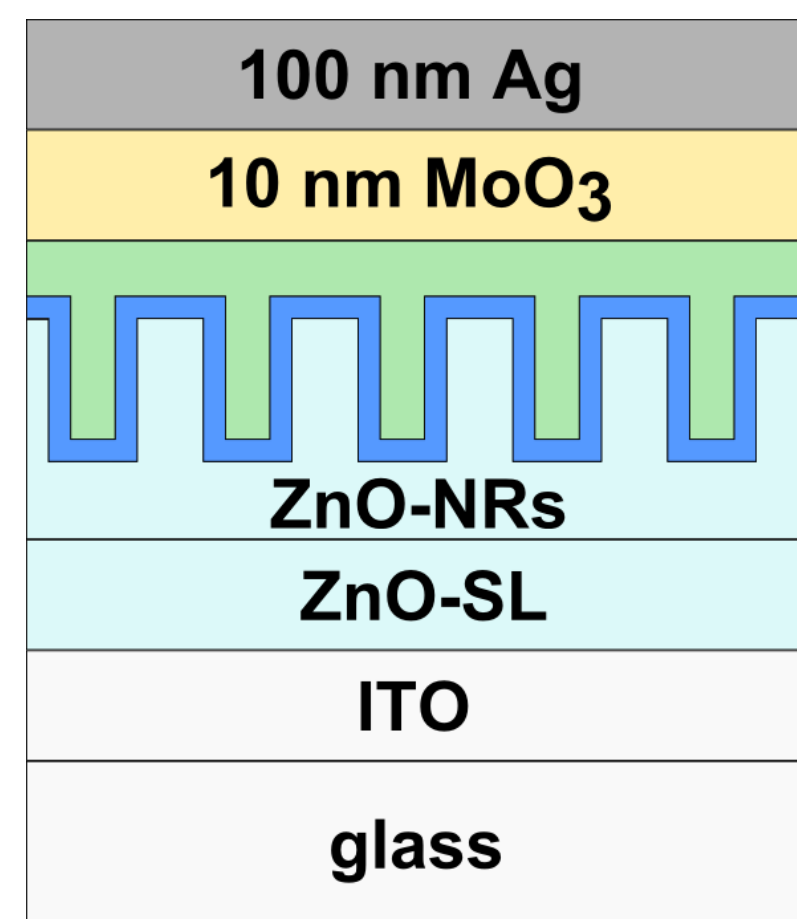
^cInstitut Kompetenz-Zentrum Photovoltaik Berlin, Helmholtz-Zentrum Berlin für Materialien und Energie GmbH, Wilhelm-Conrad Röntgen Campus, Schwarzschildstr. 3, 12489 Berlin, Germany

HZB Helmholtz
Zentrum Berlin

Motivation and Approach

The application of nanostructured transparent conductive oxide (TCO) electrodes to organic solar cells (OSCs) is motivated by the creation of effective pathways for charge carriers and the need of an increased optical thickness. In this work we focus on optimizing the conductivity of applied ZnO-nanorods (ZnO-NR) prepared by electrochemical deposition onto ITO substrates covered with a sputtered ZnO-seed layer (ZnO-SL). We investigate the effect of Al incorporation into the ZnO-NRs and the sputtered ZnO-SLs on the morphology and the composition and correlate their physical properties with the photovoltaic (PV) parameters of solar cells with C₆₀/ZnPc:C₆₀ active layer stacks on top of the nanostructures. To achieve Al incorporation into the ZnO-NRs during electrochemical deposition from aqueous solution, Al(NO₃)₃ was added to the solution in varied concentrations. ZnO-SLs were Al doped during sputtering process from an ZnO:Al target.

Experimental



$$\Phi_{\text{ZnO-NR}} = 3.9 \pm 0.1 \text{ eV}^{[1]}$$

50 nm C₆₀
80 nm ZnPc:C₆₀

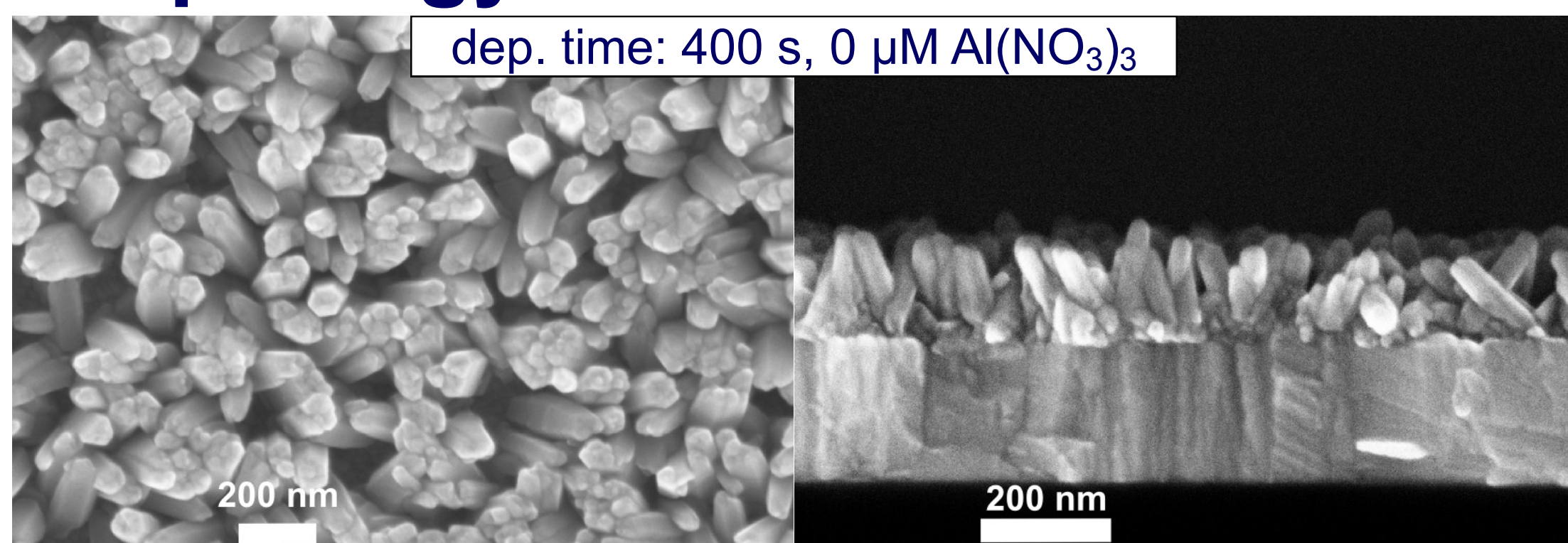
Preparation:

- ZnO, ZnO:Al (2 wt% Al₂O₃ in sputter target) seeding layer (SL) by rf-sputtering
- ZnO nanorods (ZnO-NRs) by electrochemical deposition at 75 °C^[2]
 - aqueous solution for ZnO-NR growth: 5 mM Zn(NO₃)₂
 - Al incorporation: 0...15 μM Al(NO₃)₃
 - deposition time: 400 s
- C₆₀ and ZnPc:C₆₀ layers by organic vapour phase deposition (OVPD)^{[3], [4]}
- MoO₃ as hole transport layer by PVD in high vacuum (~10⁻⁷ mbar)
- Ag back contact by PVD in high vacuum (~10⁻⁷ mbar)

Characterisation:

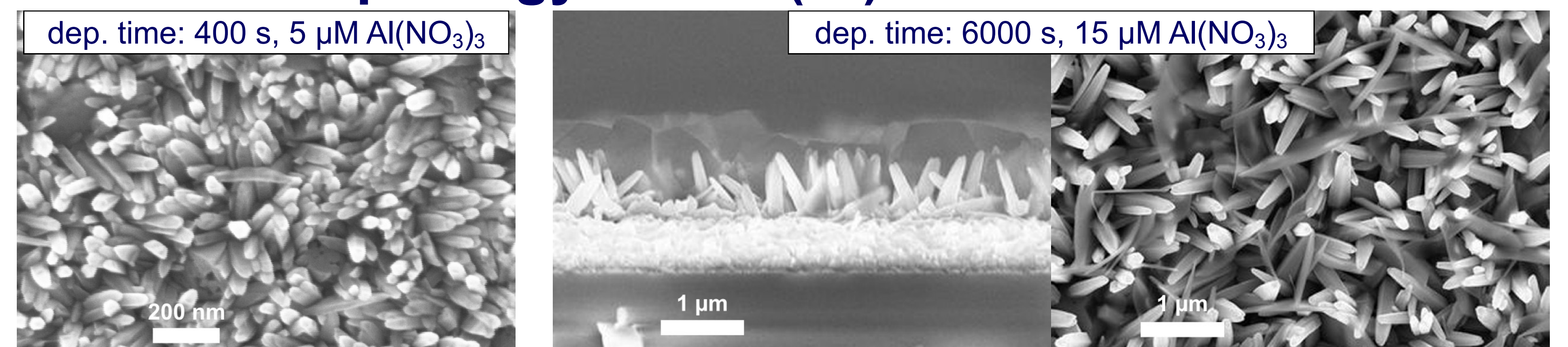
- Film morphology by scanning electron microscopy (SEM)
- Al:Zn ratio by laser-induced breakdown spectroscopy (LIBS) and X-ray photoelectron spectroscopy (XPS)
- Al content of ZnO nanostructures by energy dispersive X-ray spectroscopy (EDX)
- Electric and photoelectric properties of OSCs by J-V measurements [100 mW/cm² (Ha-Lamp), 25 °C]

Morphology of i-ZnO nanostructures



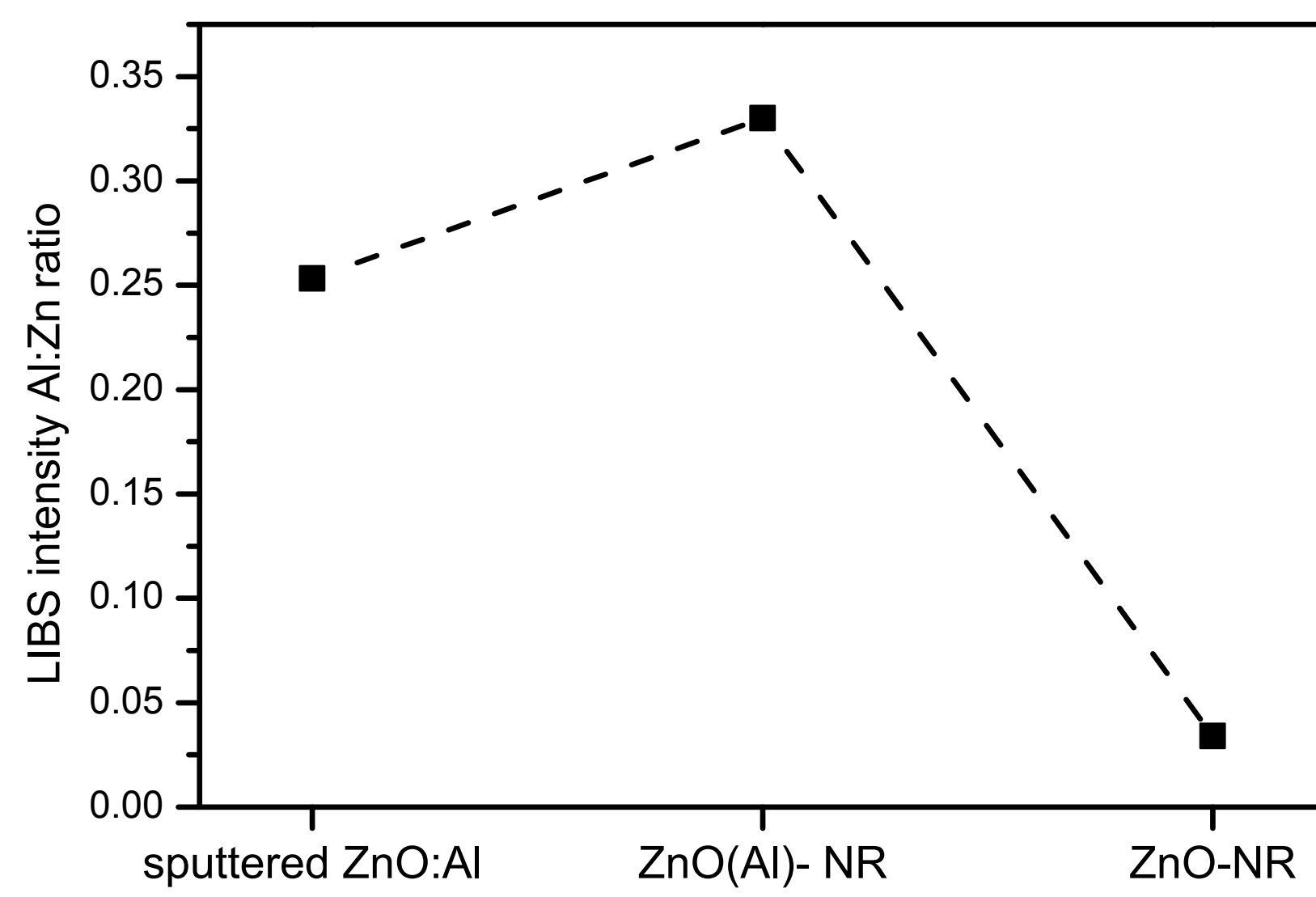
- NR diameter adjustable: 50-250 nm
- NR length adjustable: 100-2000 nm

Morphology of ZnO(AI) nanostructures



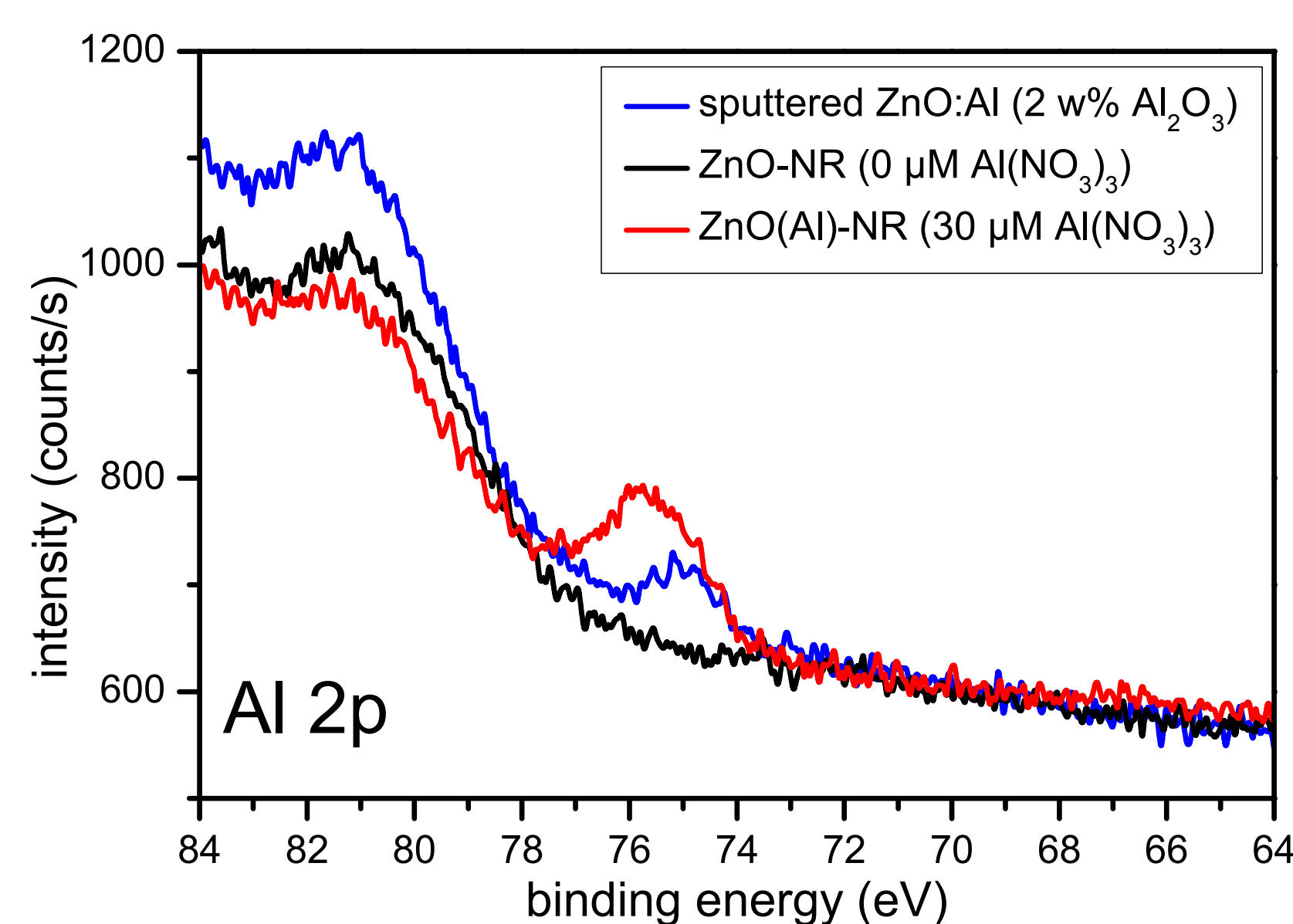
- Addition of Al(NO₃)₃ to solution → growth of “nanosheets” with larger height
- Number of „nanosheets” depends on Al(NO₃)₃ concentration

Al content in ZnO nanostructures and sputtered ZnO:Al films



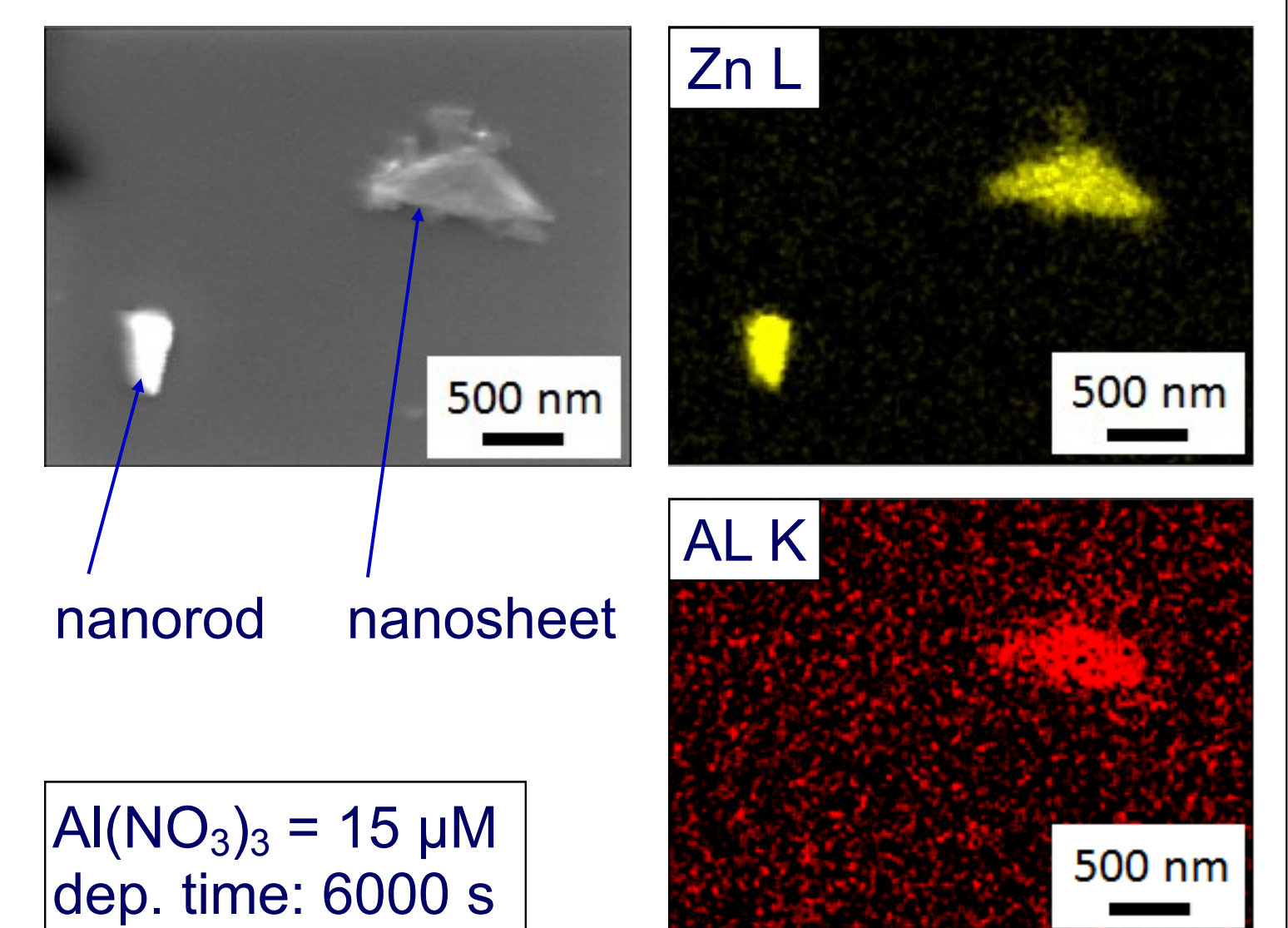
LIBS:

- Al content in ZnO(AI)-NRs higher than in sputtered ZnO:Al layers
- Al content of Al free prepared ZnO-NRs approx. one order of magnitude lower



XPS:

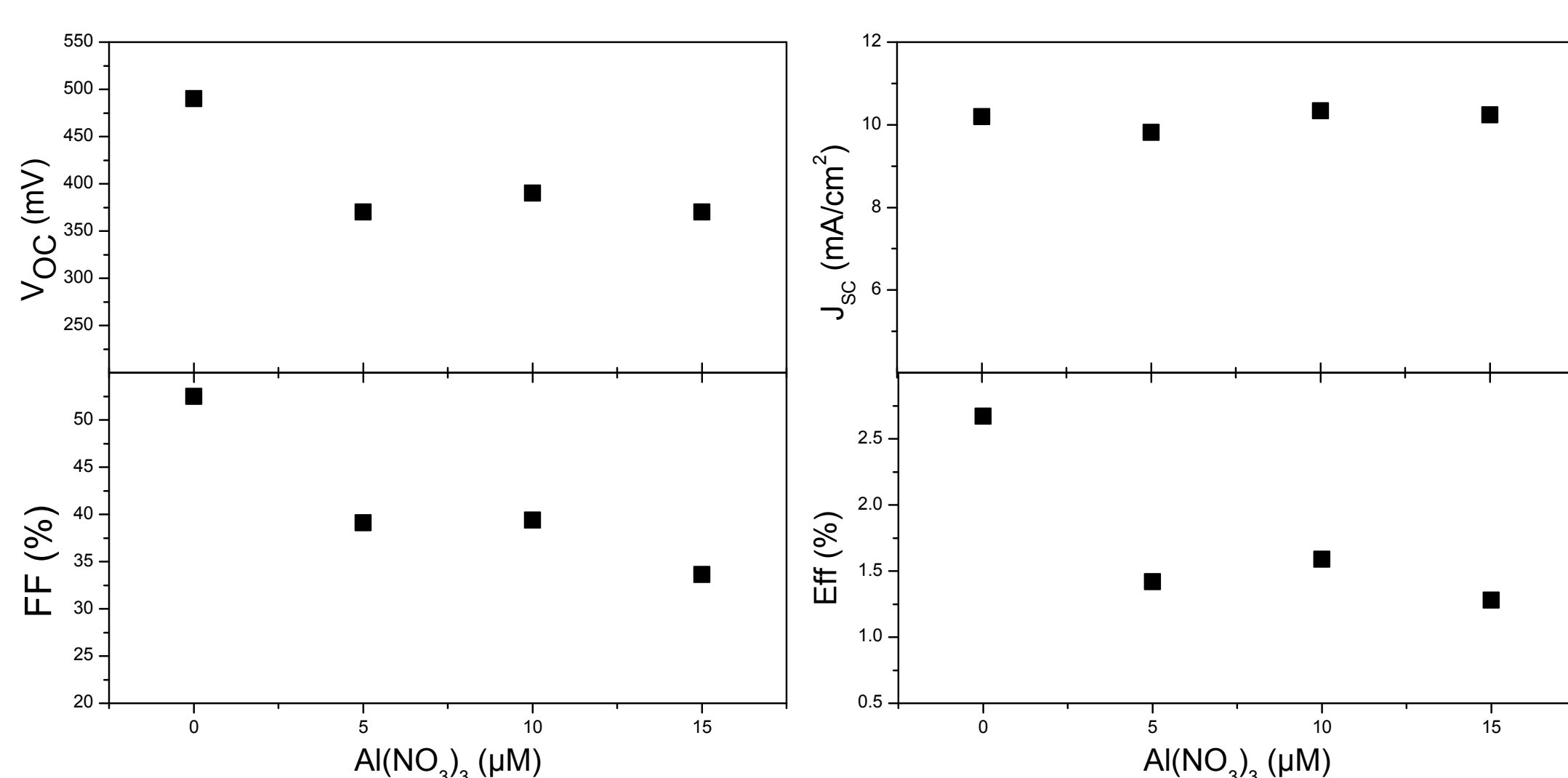
- ZnO(AI)-NRs prepared with reduced Al precursor concentration
- Al 2p intensity higher than that of sputtered ZnO:Al films



EDX on ZnO(AI) nanostructures:

- Nanosheets contain both Al and Zn
- Nanorods contain mainly Zn

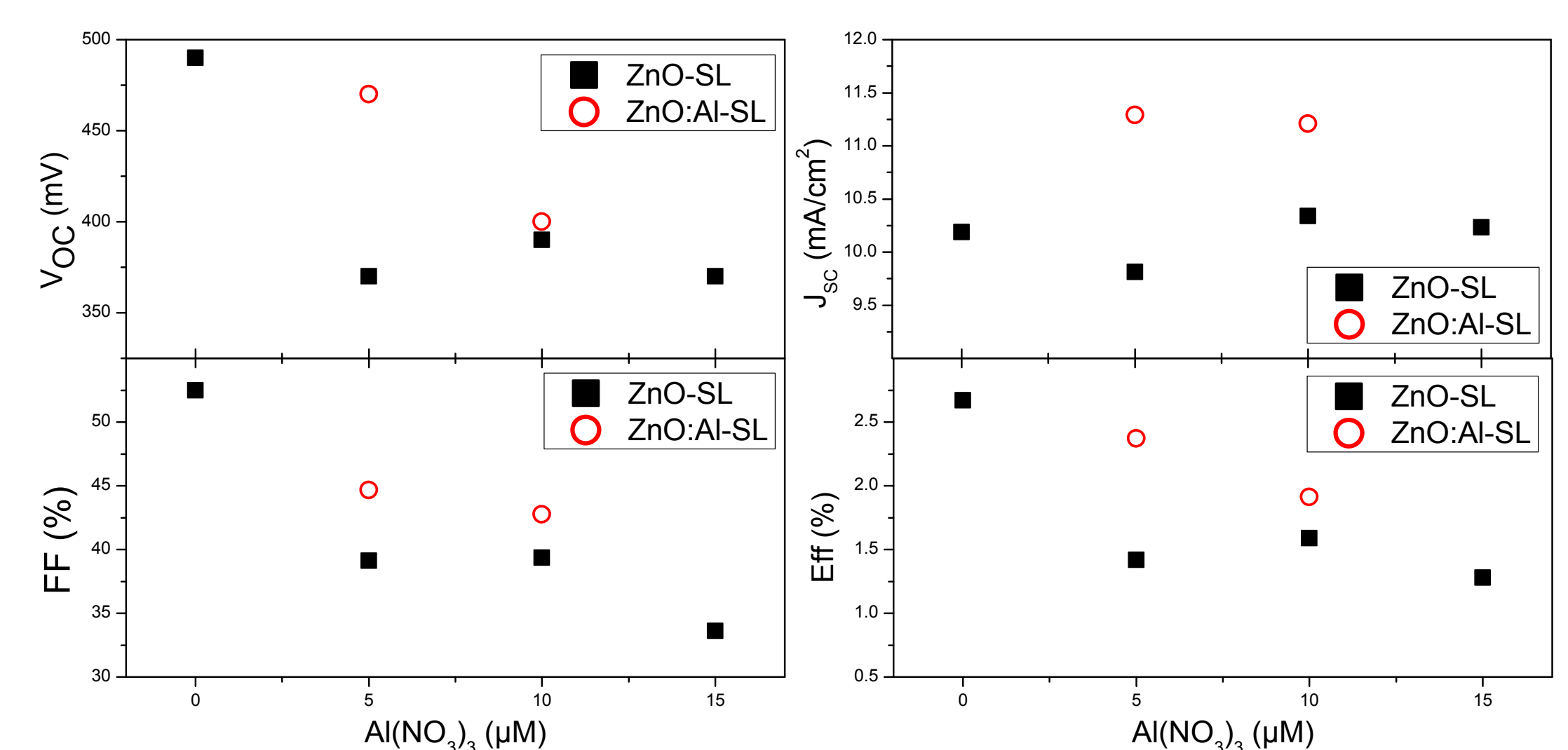
Al treated ZnO-NRs on ZnO-SLs



Al(NO ₃) ₃ -conc. (μM)	R _{sh} (Ω x cm ²)
0	3766
5	87
10	99
15	83

- ZnO(AI)-NRs: reduced V_{OC}, FF and Eff compared to Al free prepared ZnO-NRs
- Formed „nanosheets” might cause shunting of the photovoltaic device → reduced R_{sh}

ZnO-SLs vs. ZnO:Al-SLs



- ZnO:Al-SL: improved PV parameters compared to ZnO-SL due to higher conductivity of the Al doped SL

Conclusion

- Formation of additional “nanosheets” during electrodeposition of ZnO nanostructures in the presence of an Al precursor with larger height than ZnO-NRs
- Incorporation of Al in nanostructures demonstrated, however a preferential accumulation in the “nanosheets” is observed
- Reduced performance of solar cells prepared on ZnO(AI) nanostructures, probably due to shunting of the photovoltaic device by the “nanosheets”
- Insertion of an Al doped ZnO-SL improves the device performance compared to undoped ZnO-SL

References:

- W. Riedel, S. Wiesner, D. Greiner, V. Hinrichs, M. Rusu and M. Ch. Lux-Steiner, *Applied Physics Letters* 104, 173503 (2014).
- W. Ludwig, W. Ohm, J.-M. Correa-Hoyos, Y. Zhao, M. Ch. Lux-Steiner and S. Gledhill, *Phys. Status Solidi A* 210, 1557 (2013).
- M. Rusu, S. Wiesner, T. Mete, H. Blei, N. Meyer, M. Heuken, M. Ch. Lux-Steiner, K. Fostiropoulos, *Renewable Energy* 33, 254 (2008).
- M. Rusu, J. Gasiorowski, S. Wiesner, N. Meyer, M. Heuken, K. Fostiropoulos, M. Ch. Lux-Steiner, *Thin Solid Films* 516, 7160 (2008).

We gratefully acknowledge support by the Helmholtz-Gesellschaft Deutscher Forschungszentren e.V. (HGF) under the project „Hybrid-PV”. The authors would like to thank J. Riedel for conduction of the LIBS measurements.

Sven Wiesner

sven.wiesner@helmholtz-berlin.de

www.helmholtz-berlin.de

Emitter patterning for IBC-SHJ cells using laser hard mask writing and self-aligning

S. Ring^{1*}, L. Mazzarella¹, P. Sonntag², S. Kirner¹, C. Schultz³, U. Schmeißer³, J. Haschke², L. Korte², B. Stannowski¹, B. Stegemann³, R. Schlattmann^{1,3}

¹ PVcomB/Helmholtz-Zentrum Berlin für Materialien und Energie, Schwarzschildstr. 3, D-12489 Berlin, Germany.

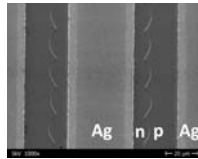
² Institute for Silicon Photovoltaics/Helmholtz-Zentrum Berlin für Materialien und Energie, Kekuléstr. 5, D-12489 Berlin, Germany.

³ University of Applied Science (HTW), Wilhelminenhofstraße 75a, D-12459 Berlin, Germany.

* Sven.Ring@helmholtz-berlin.de

Summary

- A laser-based emitter/absorber patterning method for IBCSHJ cells is presented
- Key features:
 - single step laser patterning
 - contact-free
 - lithography-free
 - gap-free repassivation
 - self-aligned contact layer deposition
 - sacrificial hard mask required
- Proof-of-concept cells show V_{oc} up to 665mV, FF is R_{oc} -limited (metalization w. lithography)

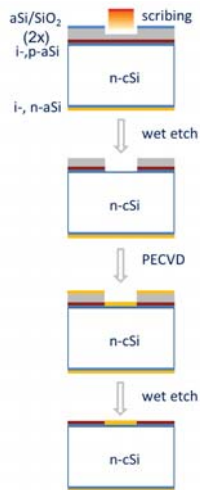


Motivation and Background

- Rear-contacted a-Si:H/c-Si heterojunction (SHJ) cells allow to combine high voltage and high short circuit current densities [1-5].
- Rear-contacted cell concepts however require patterning steps—usually separate patterning steps for emitter and absorber are used.
- Standard photolithography is too costly for production processes.
- Laser patterning is increasingly adopted in the PV industry e.g. for contact firing [6], and for patterning of emitter and BSF areas separately [7].
- Develop a fast and simple emitter patterning process for IBC-SHJ cells

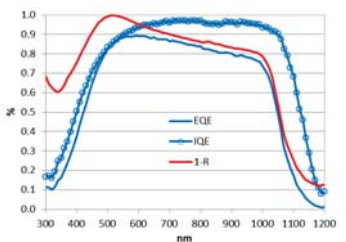
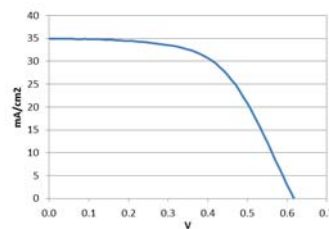
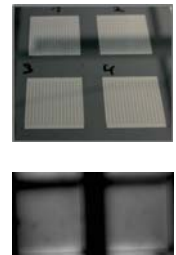
Patterning process scheme

- Full area deposition of Emitter, FSF, and hard mask stack
- Laser scribing of absorber contact area
Here: each finger consists of a single scribe line (355nm ps laser, flat top profile)
- Wet chemical etch sequence to
 - Fully open the laser scribed area
 - Emitter removal
 - Damage etch
- Full area deposition of BSF
- Lift-off etch to remove mask



Proof-of-concept cell

- Cell design: 1cm², pitch 600µm, 90% emitter coverage
- 1 Laser line (width 60 micron) per finger
- Lithographic patterning of ITO/Ag contacts
- PL image after metalization



- V_{oc} 620mV, FF, 58%, pFF 74%
- FF limited by R_{oc} (6 Ωcm^2)
- j_{sc} 33.2 mA/cm² determined from EQE
- IQE up to 0.95

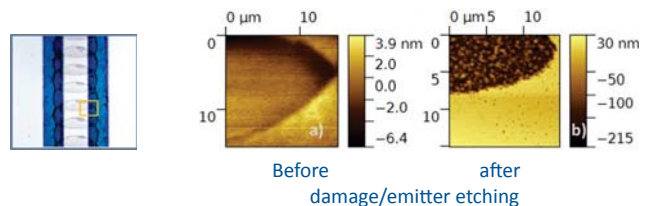
→ Indicates increased recombination at the rear side

References

- [1] M. Lu, S. Bowden, U. Das, and R. Birkmire, Appl. Phys. Lett., 91, 0635071, 2007.
- [2] A. Tomasi, B. Paviet-Salomon, D. Lachenal, S. M. de Nicolas, A. Descoedres, J. Geissbühler, S. De Wolf, and C. Ballif, IEEE J. Photovoltaics, 4 (4), 1046–1054, 2014.
- [3] N. Mingirulli, J. Haschke, R. Gogolin, R. Ferre, T. F. Schulze, J. Dusterhoft, N. P. Harder, L. Korte, R. Brendel, and B. Rech, Phys. Status Solidi-Rapid Res. Lett., 5, 159–161, 2011.
- [4] S. N. Granata, M. Aleman, T. Bearda, J. Govaerts, M. Brizzi, Y. Abdulraheem, I. Gordon, J. Poortmans, and R. Mertens IEEE J. Photovoltaics, 4(3), 807, 2014.
- [5] K. Masuko, M. Shigematsu, T. Hashiguchi, D. Fujishima, M. Kai, N. Yoshimura, T. Yamaguchi, Y. Ichihashi, T. Mishima, N. Matsubara, T. Yamanishi, Takahama, M. Taguchi, E. Maruyama, and S. Okamoto, IEEE J. Photovoltaics, 4(6), 1433, 2014.
- [6] T. Desrues, I. Martín, S. De Vecchi, S. Abolmasov, D. Diouf, A. Lukyanov, P. Ortega, M. Colina, M. Versavel, M. Tusseau, F. Souche, T. Nychporuk, M. Gueunier-Farret, D. Muñoz, M. Lemiti, J. P. Kleider, P. Roca i Cabarrocas, R. Alcubilla, Y. Schlumberger, and P.J. Ribeyron, 28th PVSEC 1135, 2013.
- [7] S. De Vecchi, T. Desrues, F. Souche, D. Munoz, and M. Lemiti, SPIE Vol. 8473, 2012

Acknowledgments

We appreciate technical assistance from K. Bhatti, K. Mack, K. Jacob, M. Wittig, M. Hartig, C. Klimm, and E. Conrad, and funding from the European Union's Seventh Programme for research, technological development and demonstration under grant agreement No 608498 (project HERCULES).



- AFM measurement reveals rough surface structure
- Etching reveals laser damage, partially responsible for enhanced recombination
- Etch processes need to be optimized further

Modifying the Sulfur Gradient in Sequentially Processed CIGSe Absorber under Atmospheric Pressure Using Elemental Chalcogenides

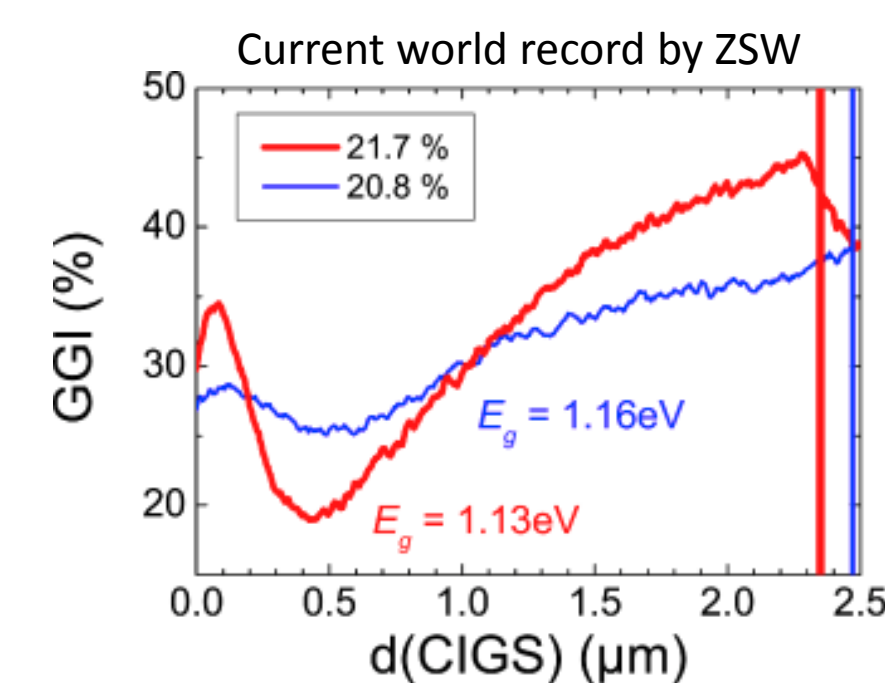
Christian Wolf^{1*}, Humberto Rodriguez-Alvarez², Sebastian S. Schmidt¹, Tim Kodalle¹, Dieter Greiner¹, Hans-Werner Schock¹, Christian A. Kaufmann¹, Rutger Schlatmann¹

¹PVcomb/Helmholtz-Zentrum Berlin für Materialien und Energie GmbH, Schwarzschildstr., D-12489 Berlin, Germany

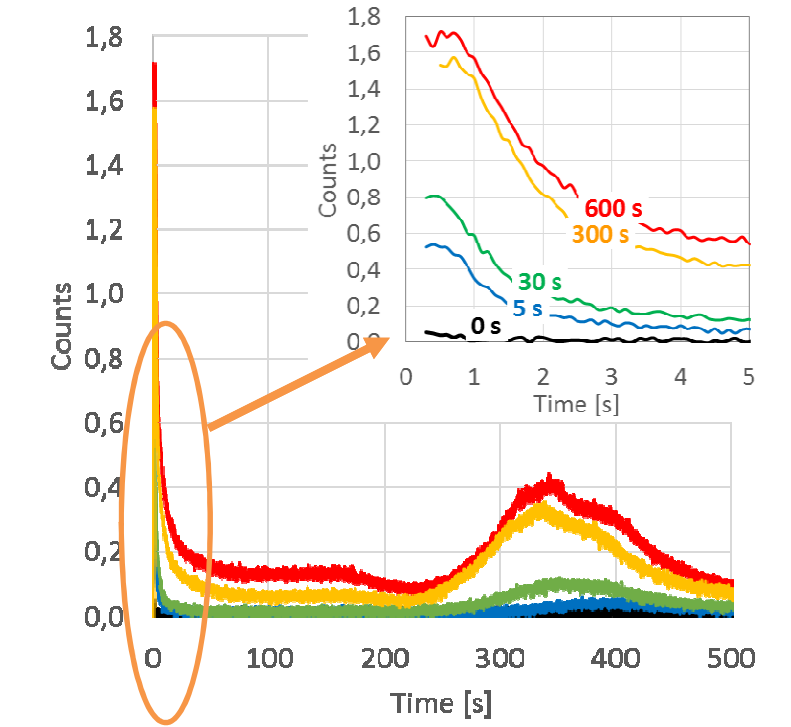
*Corresponding author: Christian.wolf@pvcomb.de

Motivation

- **Designing band gap** profile is crucial for high efficiencies [1][2].
- In sequentially processed thin-film CIGSe absorbers Ga tends to accumulate at back contact.
- To adjust interface near band gap, S is incorporated in sequentially deposited CIGSe absorbers → **Sulfurization after Selenization „SAS“**
- First tests: SAS of complete absorbers lead to agglomeration of **S at back contact** and no possibility to influence S-depth profile
- Solution: less aggressive sulfurizations requires unfinished absorbers to get a decent amount of sulfur in the absorber → **Sulfurization of partially selenized absorber**



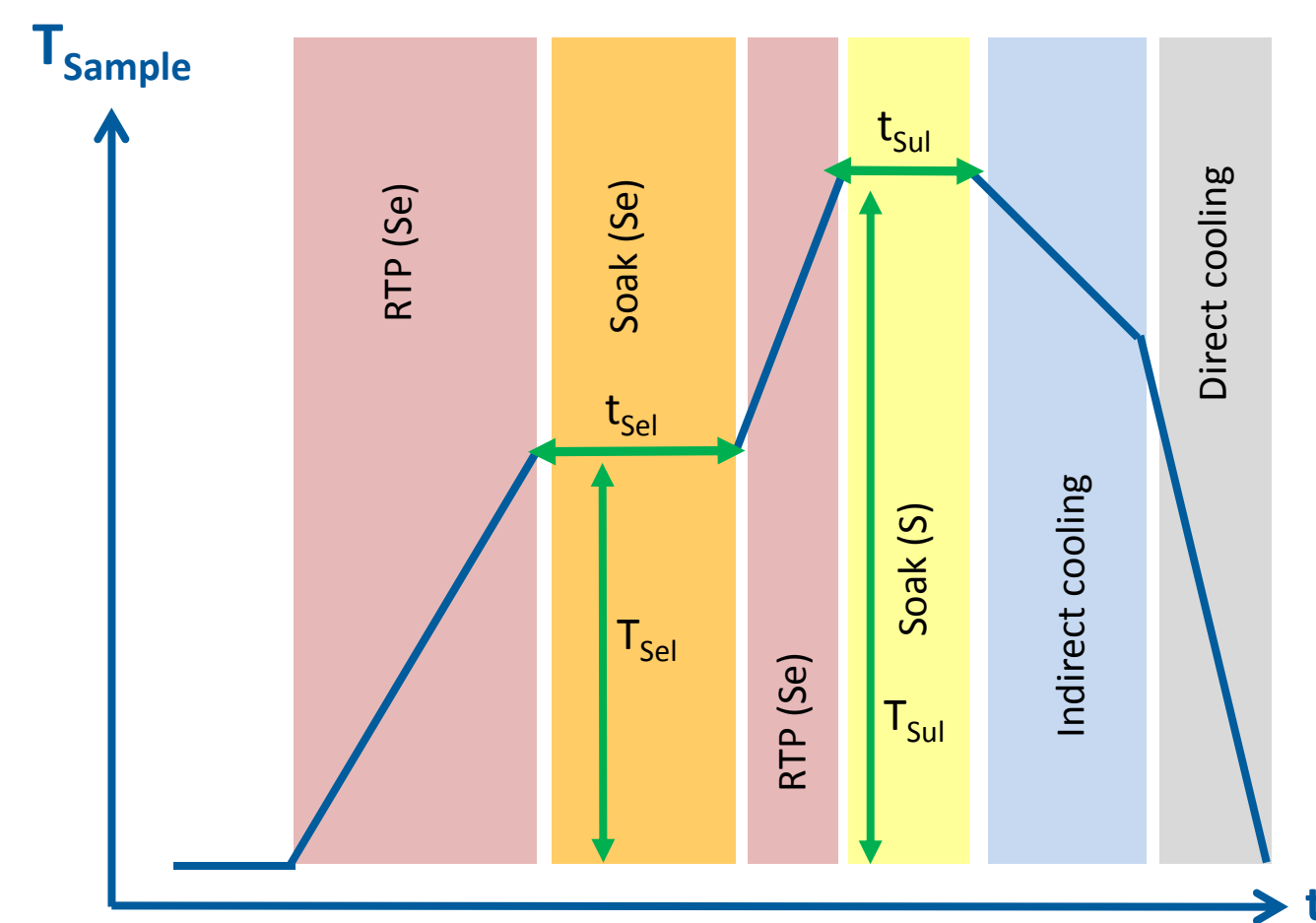
Example of GGI (= band gap) of recent record solar cell by ZSW show increasing band gap to the absorber front [1]



First experiments at PVCOMB about sulfurization of complete CIGSe absorbers at 580 °C showed significant accumulation of sulfur at the back contact (at 350 s sputter time in shown GDOES depth profile)

Sulfurization of partially selenized CIGSe absorbers

- **Procedure:**
 1. Sputtering of Mo/CIG on glass
 2. Partial selenization
 3. XRF measurement → Se content
 4. Sulfurization
 5. XRF measurement → S/(S+Se)
 6. GDOES measurement → Depth profiles
- **Variations:**



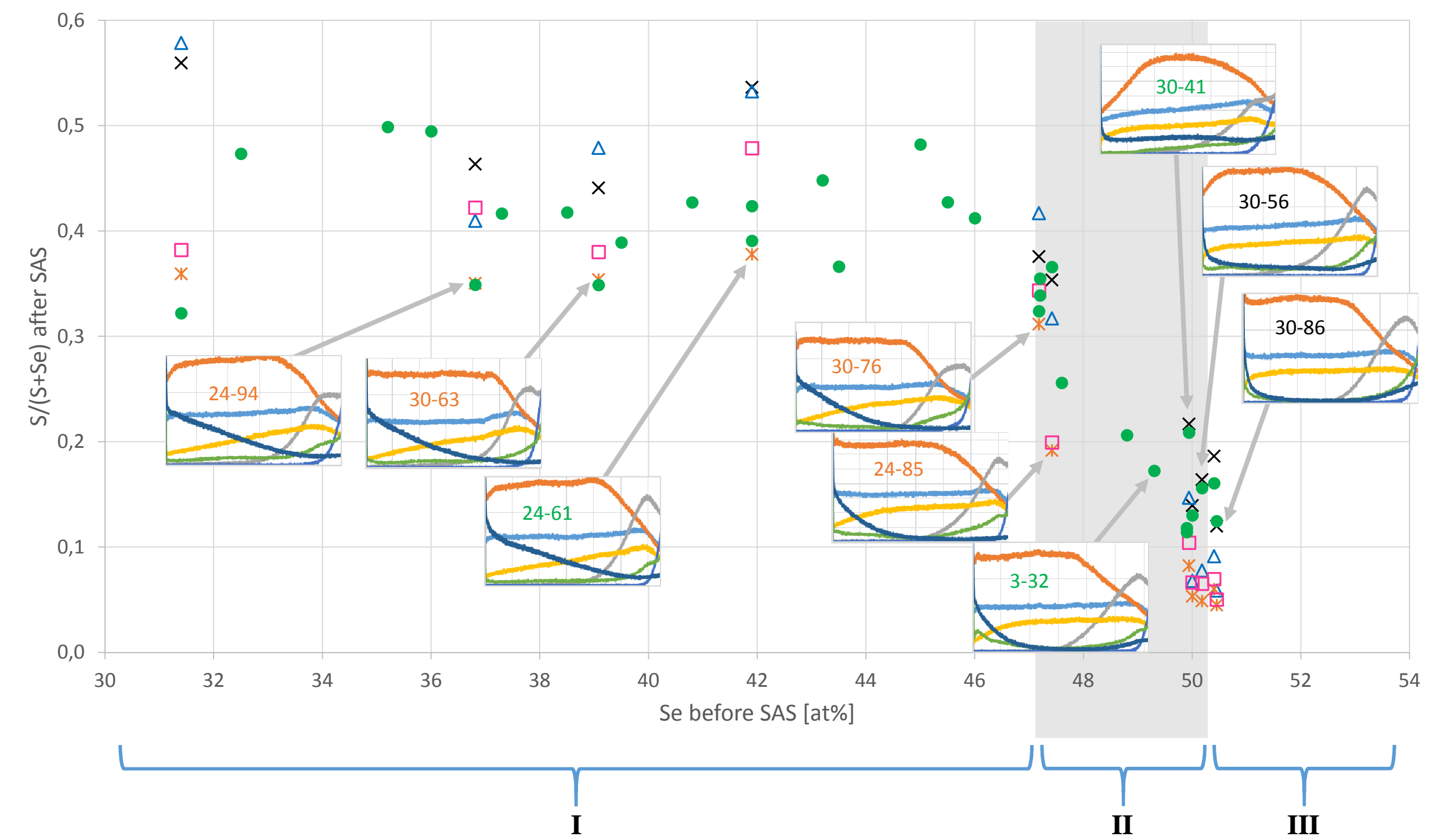
Sulfurization after Selenization – sketch of temperature profile and possible settings

Equipment:

- Industrial like in-line RTP furnace by Smit Thermal Solutions
- Selenization/Sulfurization in N₂ atmosphere at atmospheric pressure
- Elemental chalcogen sources

Parameter	Description	Range
T _{Se1} [°C]	Temperature of Selenium soak	360 – 580
T _{Se} [°C]	Temperature of Selenium source	350 – 420
t _{Se1} [min]	Duration of Selenium soak	1 – 30
T _{Sul} [°C]	Temperature of Sulfur soak	450 – 580
T _S [°C]	Temperature of S source	190 – 210
t _{Sul} [min]	Duration of Sulfur Soak	1 – 20

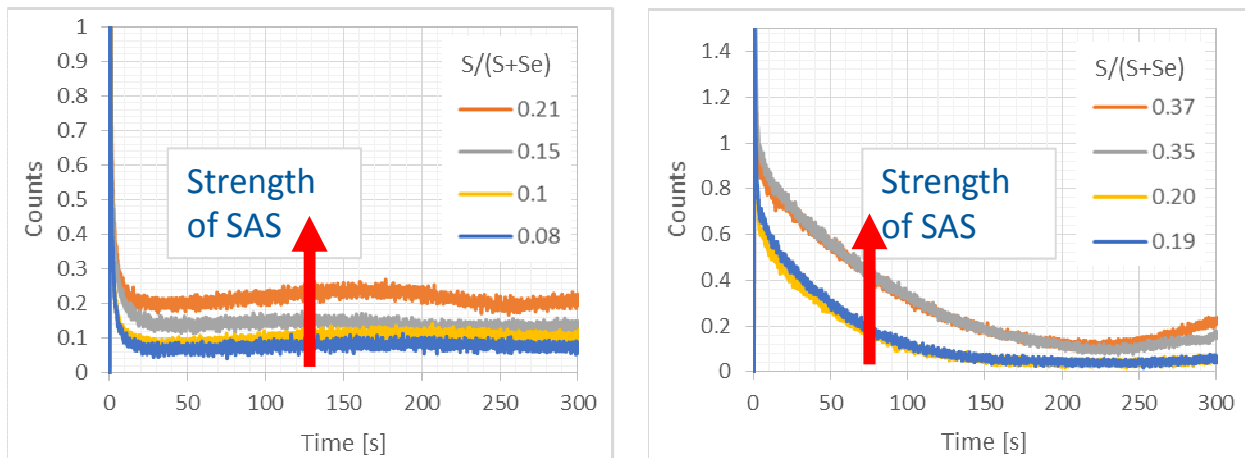
Composition and depth profiles



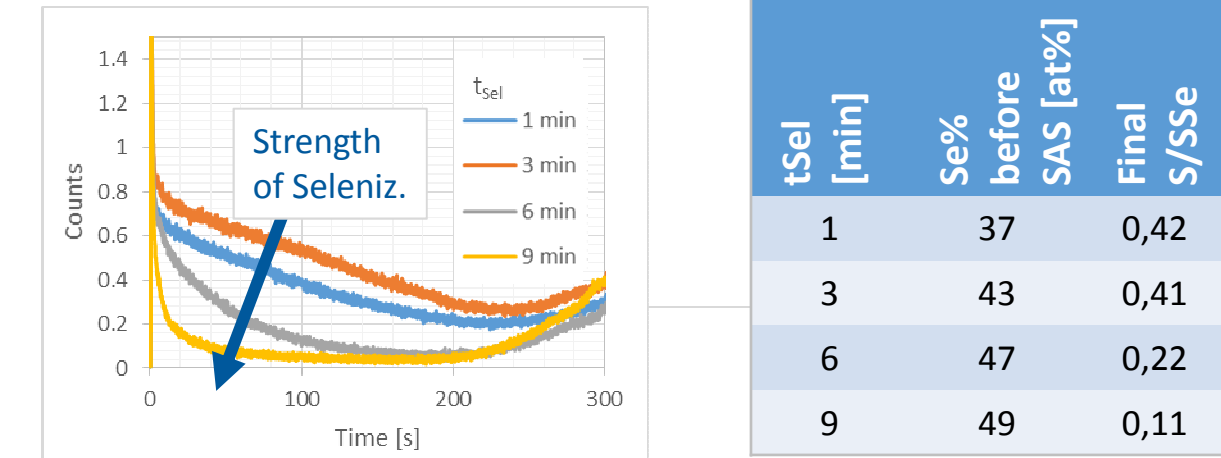
Sulfur concentration in finished CIGSe absorbers versus Se concentration before sulfurization and selected GDOES depth profiles of resulting CIGSe (each color of ID corresponds to one set of sulfurization parameters) with different intervals of Se concentration (see table below)

Se [at%]	Influence	Description
I < 47	Only little influence on S profile	<ul style="list-style-type: none"> • S amount decreases nearly linear from front contact to back contact • Similar sulfurizations get similar S/(S+Se)
II 47 - 51	Profile adjustable	<ul style="list-style-type: none"> • From steep to flat • S/(S+Se) smaller with increasing Se content of partially selenized absorbers
III >51	Only little S incorporation	<ul style="list-style-type: none"> • Aggressive Sulfurization necessary • Agglomeration of S at back contact

Sulfur amount and S depth profile



GDOES depth profiles of CIGSe for different SAS (Variation: T_{Sul}, T_S, t_{Sul}) Left/Right: Different selenizations

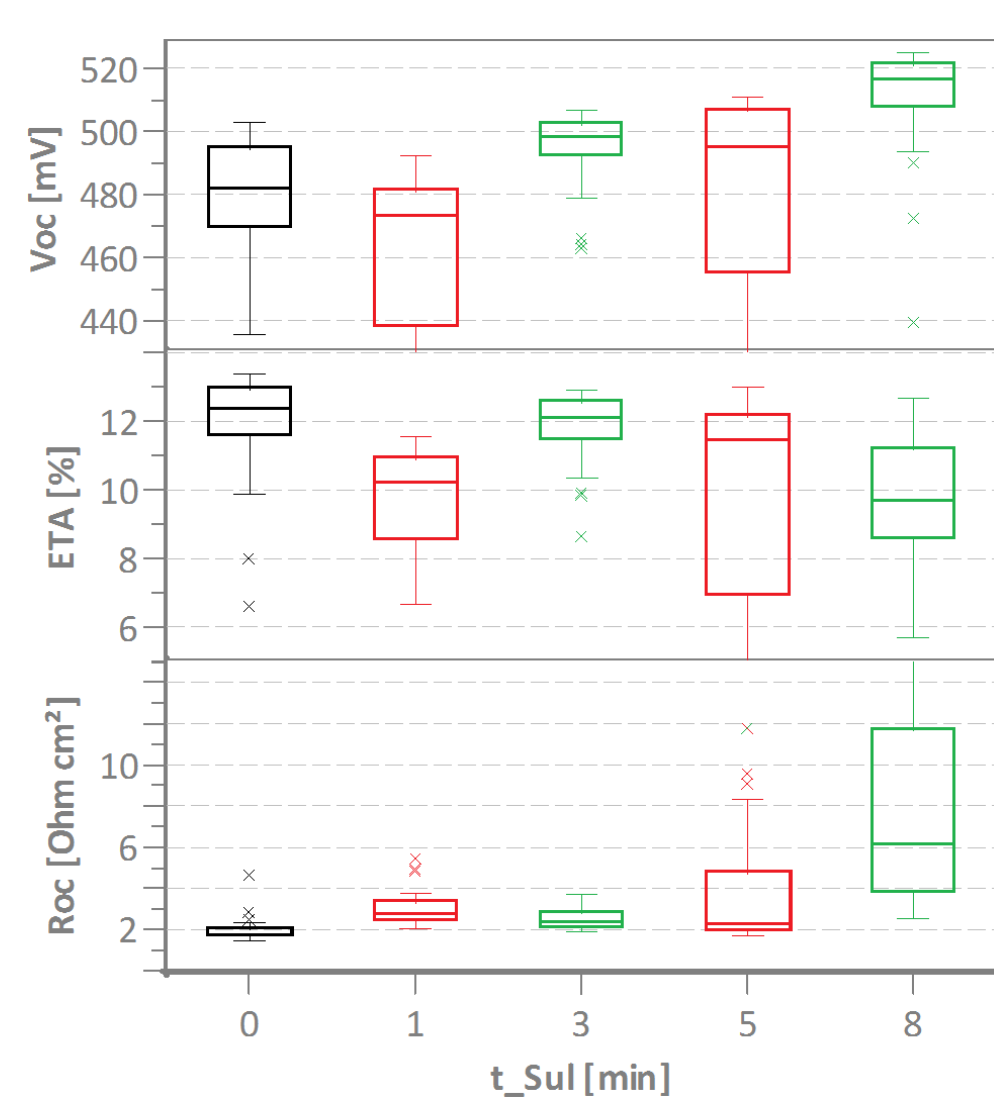


Example of GDOES depth profiles and XRF results of CIGSe for different Selenizations (Variation: duration of Se-soak Constant: T_{Se1}, T_{Se}, SAS)

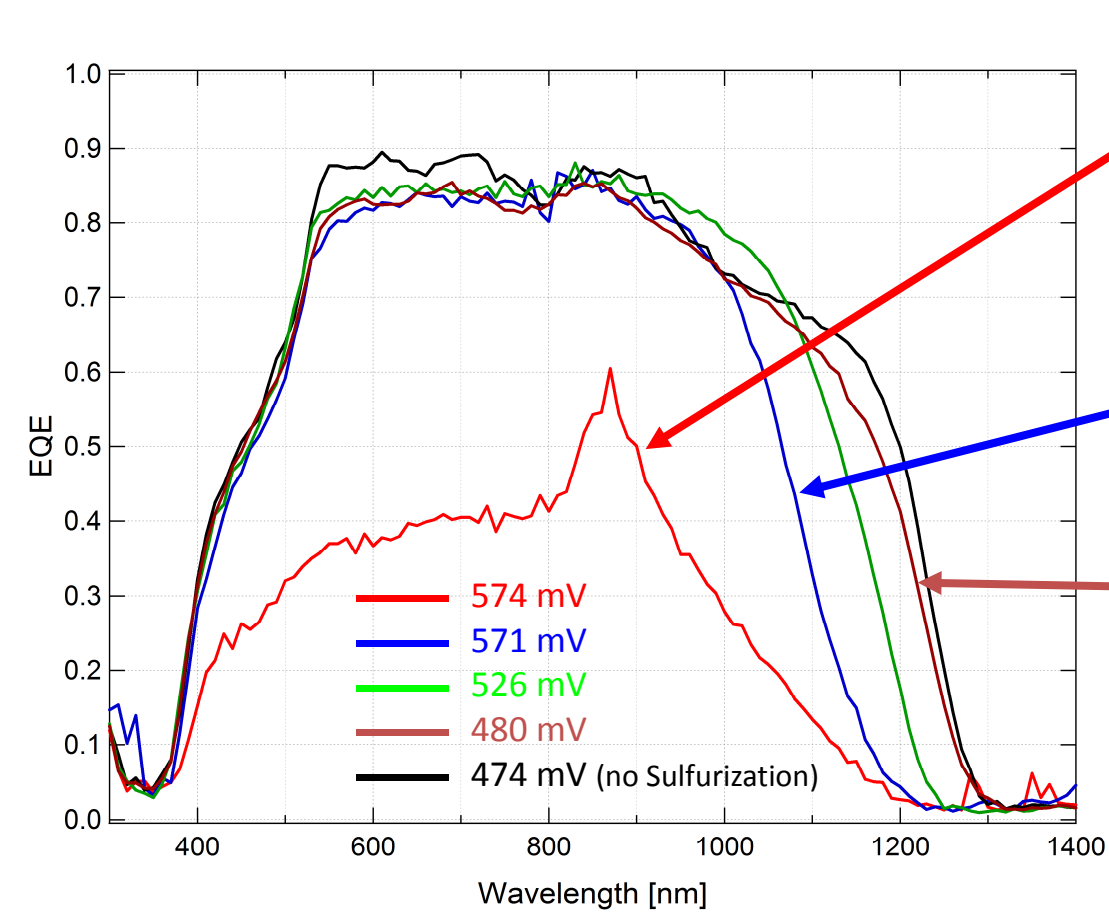
- S amount is adjusted by sulfurization settings
- Nearly no influence on shape of S profile by SAS setting

- S profile and incorporated amount depends on Se content after selenization

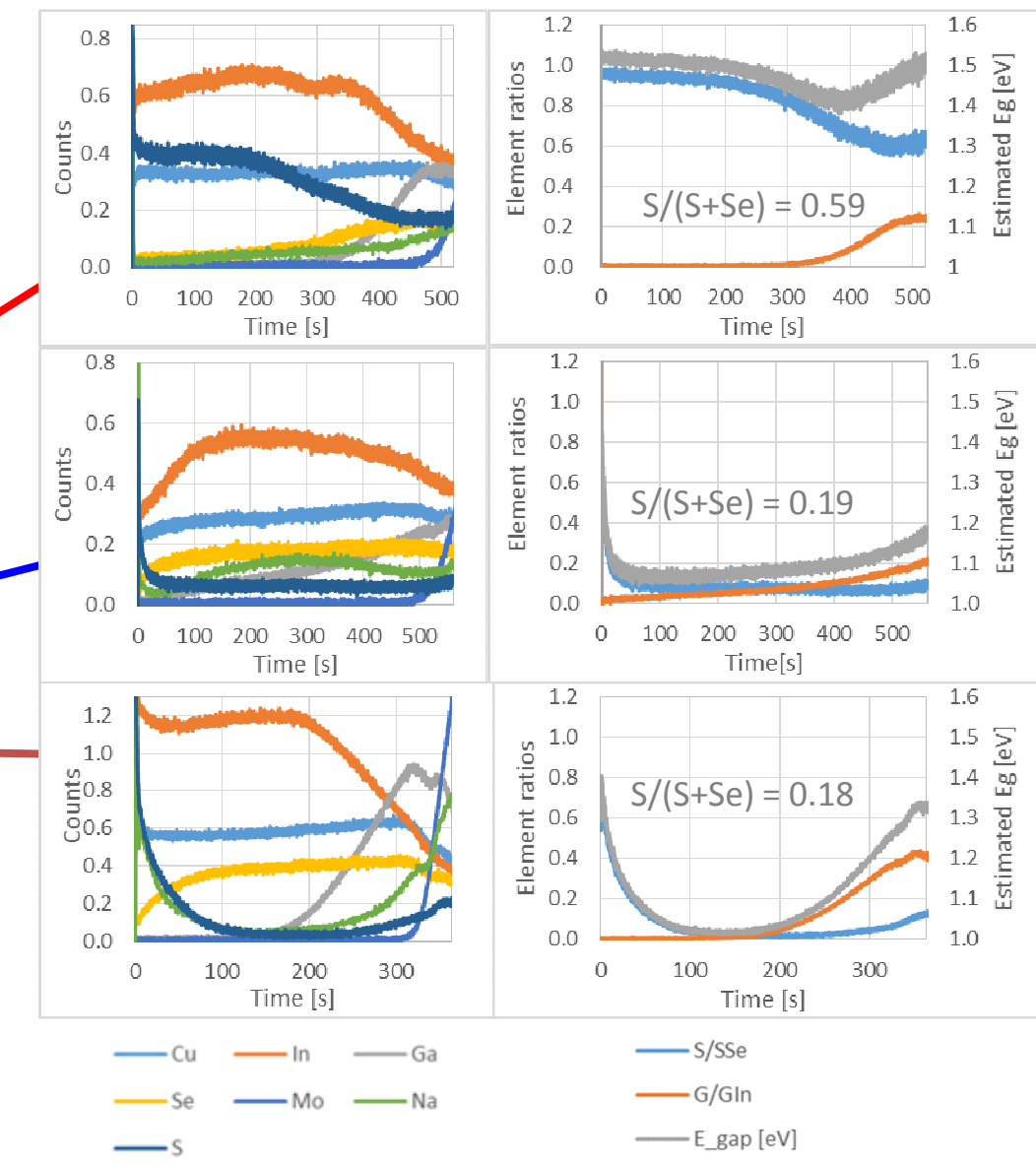
Influence on IV characteristic



IV results for different selenizations and sulfurizations (t_{Sul} = 0 was baseline reference without sulfurization) Selenization settings chosen to achieve different S profiles



EQE spectra of samples out of different selenization and sulfurization experiments with given open circuit voltage of the respective cell



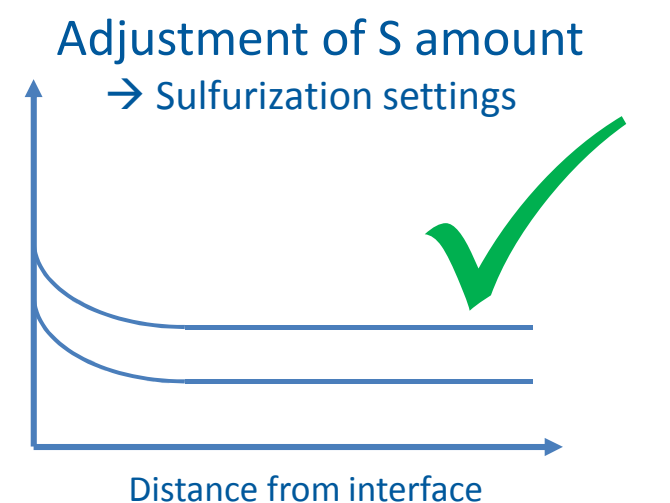
GDOES depth profiles and estimation of band gap using total composition (XRF), depth profiles (GDOES) and formula for E_g^{CIGSe}(Ga, S) from [3]

- E_{gap} can be increased by increasing S/(S+Se) ...
- ... yet not as much as expected [4]
- Constant profile helps increasing minimum band gap
- Increased S/(S+Se) leads to higher serial resistance (back contact barrier?)

Conclusion and outlook

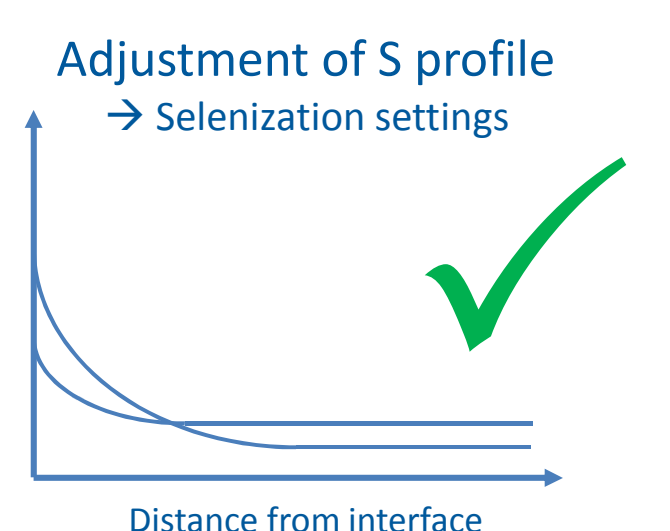
Our experiments point towards a promising way to control the surface near band gap profile via incorporation of elemental sulfur during our sequential in-line absorber formation in N₂ atmosphere under ambient pressure

Desired influence on S depth profile:



Further challenges:

- Shift resulting band gap minimum further to absorber surface [5]
- Change Ga gradient during sequentially absorber formation
- Avoid chalcogenization of back contact
- Adjustment of buffer and i:ZnO to sulfurized absorbers
- Investigation of role of alkali metals



References

- [1] P. Jackson, D. Hariskos, R. Wuerz, O. Klowski, A. Bauer, T.M. Friedmeier, M. Powalla; Properties of Cu(In,Ga)Se₂ solar cells with new record efficiencies up to 21.7%; (2015); physics status solidi (RRL) – Rapid Research Letters Volume 9, Issue 1, pages 28–31
- [2] T.Hara, T.Maeda, S.Minoura, Y.Sago, S.Niki, H.Fujihara; Quantitative Assessment of Optical Gain and Loss in Submicron-Textured Cu(In,Ga)Se₂ Solar Cells Fabricated by Three-Stage Coevaporation; (2014) Phys. Rev. Applied 2, 034012
- [3] M. Bar, W. Bohne, J. Röhrich, E. Strub, S. Lindner, M. C. Lux-Steiner, Ch.-H. Fischer, T. P. Niesen, F. Karg; Determination of the band gap depth profile of the ternary Cu(In_{0.9}Ga_{0.1})Se₂ chalcopyrite from its composition gradient; (2004) J. Appl. Phys. 96, 3857
- [4] M.Turcu, I.M.Kötschau, U.Rau; Composition dependence of defect energies and band alignments in the Cu(In_{0.9}Ga_{0.1})Se₂ alloy system (2002) Journal of applied physics, 91, 1391-1399.
- [5] M. Gloeckler, J.R. Sites. Band-gap grading in Cu(In,Ga)Se₂ solar cells. Journal of Physics and Chemistry of Solids, Volume 66, Issue 11, November 2005, Pages 1891–1894

TECHNOLOGY TRANSFER FOR THIN-FILM PHOTOVOLTAICS

Complete Manufacturing Process in Pilot-Lines

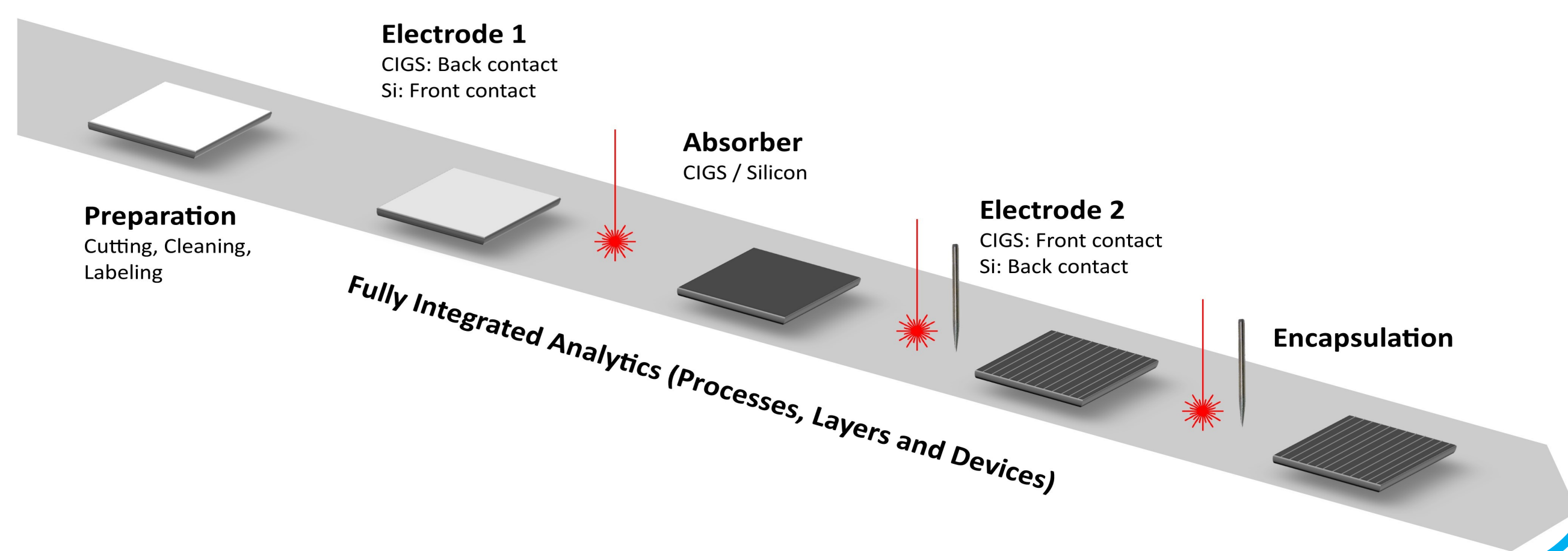
Two dedicated pilot-lines for research on 30 x 30 cm² PV modules (Thin-film Silicon & CIGSe)



Applied R&D on Processes, Cells & Modules

Improvement of state-of-the-art technologies

Development of new cell concepts



Projects, Education and Training

Reliable partner for industry & research institutes

Providing industry with highly skilled thin-film

PV professionals





Characterization of CZTS films grown using vacuum and solution based methods, through UPS, XPS and XANES measurements

G. Gordillo¹, R. A. Becerra¹, S. D. Cruz², C. L. Calderón¹, P. B. Perez³, E.A. Ramirez¹, I. Lauer mann⁴

¹ Grupo de Materiales Semiconductores y Energía Solar, Universidad Nacional de Colombia, Bogotá, Colombia

² Facultad de Ciencias Físico Matemáticas, Universidad Autónoma de Nuevo León, Monterrey, México

³ Departamento de Física Aplicada, CINVESTAV-IPN, Mérida, Yuc., México

⁴ Helmholtz Zentrum Berlin für Materialien und Energie



Email: ggordillo@unal.edu.co

Abstract

This work describes novel procedures to grow $\text{Cu}_2\text{ZnSnS}_4$ (CZTS) thin films using vacuum and solution based methods. The solution based approach includes sequential deposition of Cu_2SnS_3 (CTS) and ZnS films, where the CTS compound is synthesized in a one step process by simultaneous precipitation of Cu_2S and SnS_2 in a thiosulphate solution, using diffusion membranes to control the supply of Cu^+ and Sn^{4+} cations, in order to promote growth in heterogeneous phase. The vacuum based approach includes simultaneous evaporation of metallic precursors from one coaxial crucible in the presence of sulfur supplied from an effusion cell.

XPS (X-ray photoelectron spectroscopy) depth profile analysis revealed that the CZTS films prepared by co-evaporation using a coaxial source of evaporation built with an advanced design, show high homogeneity in chemical composition throughout the volume. X-ray absorption near edge structure (XANES) measurements at the sulfur K-edge indicate that the growth method does not significantly affect the band structure and that the absorbing atom in both types of CZTS samples exhibits the same oxidation state. The influence of the preparation method on the work function of CZTS films was also studied by ultraviolet photoelectron spectroscopy (UPS).

Preparation methods

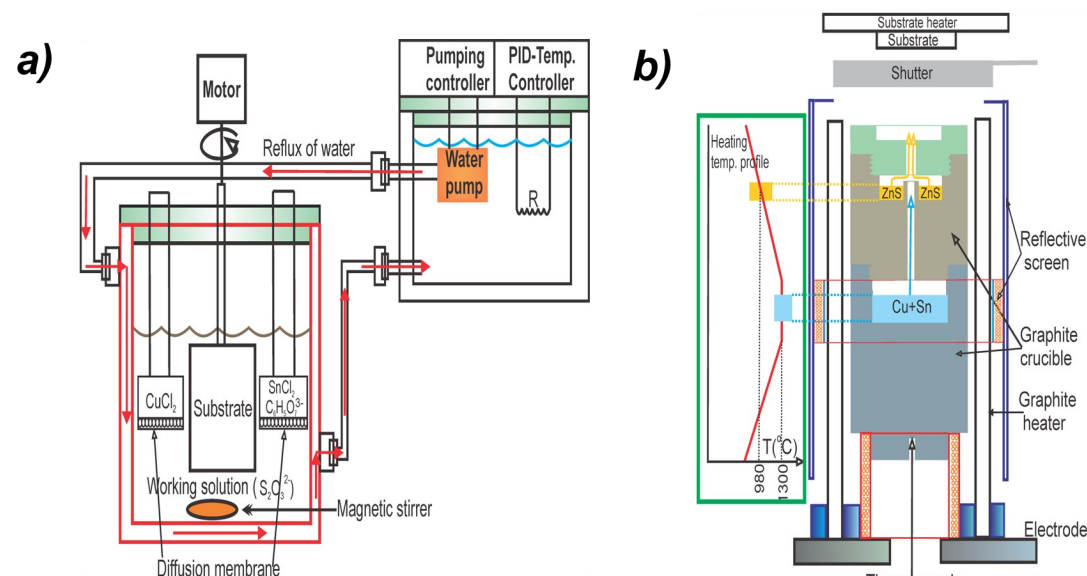


Fig. 1. Scheme of the systems used for the preparation of CZTS thin films by (a) CBD and b) co-evaporation

Results

XPS Analysis

The elemental composition homogeneity in the volume of CZTS films grown by both methods was studied through XPS measurements carried out at three different depths (sputter time of 0.5, 5 and 10 min respectively).

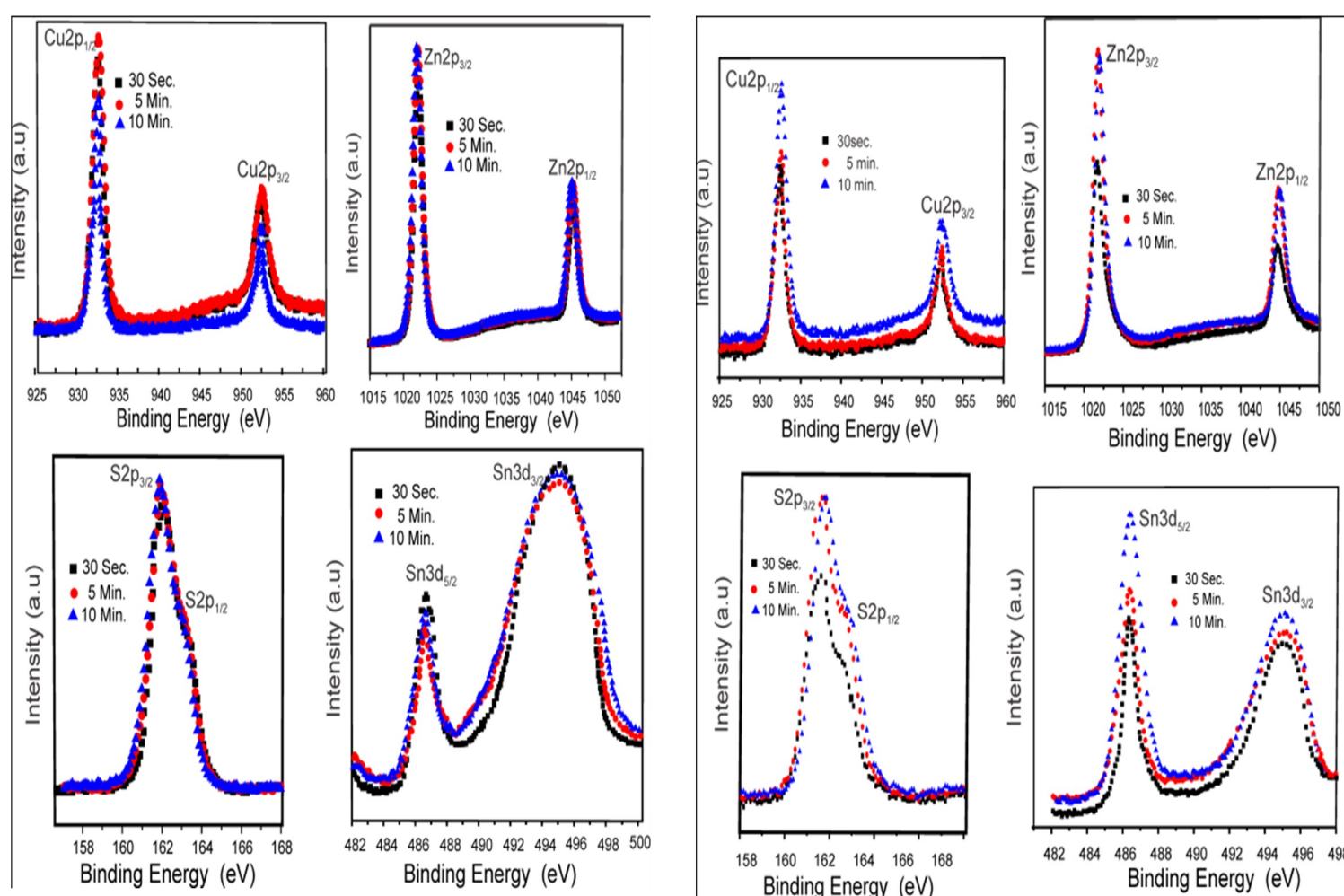


Fig. 2: XPS high resolution core level spectra of the Cu_{2p}, Zn_{2p}, Sn_{3d} and S_{2p} peaks measured at three different depths of typical CZTS thin films prepared by co-evaporation

Fig. 3: XPS high resolution core level spectra of the Cu_{2p}, Zn_{2p}, Sn_{3d} and S_{2p} peaks measured at three different depths of typical CZTS thin films prepared by CBD

XANES measurement

Normalized XANES spectra at the sulfur K-edge of CZTS prepared by co-evaporation and by CBD are compared in Fig. 4. Both types of samples exhibit a strong pre-edge peak at 2470 eV of similar intensity and shape, indicating that the growth method does not significantly affect the band structure and that the absorbing atom in both types of CZTS samples exhibits the same oxidation state.

Differences in the intensity between 2472 and 2480 eV could be attributed to multiple scattering of photoelectrons ejected at low kinetic energy, where the scattering cross section of co-evaporated CZTS samples is larger than that of the prepared ones by CBD

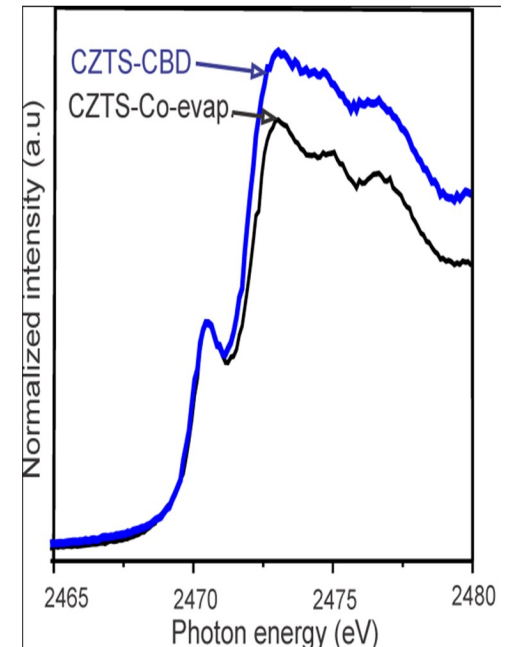


Fig. 4: XANES spectra at the sulfur K-edge of CZTS thin films prepared by co-evaporation and CBD respectively

UPS measurements

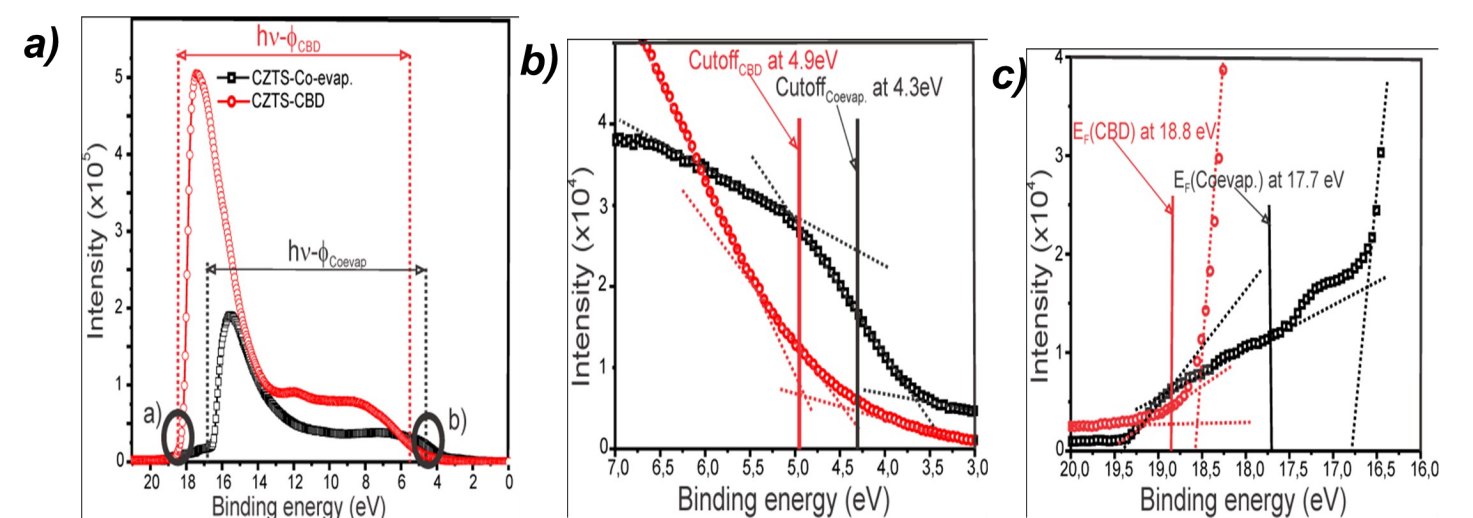


Fig. 5: a) Comparison of the He I UPS spectrum of a typical $\text{Cu}_2\text{ZnSnS}_4$ thin film prepared by co-evaporation with that of a typical CZTS sample prepared by CBD. Also shown is inelastic cutoff (circle a) and Fermi edge (circle b). The relation between spectrum width, $h\nu$ and work function ϕ is illustrated. b) Shows a detailed spectrum of inelastic cutoff region. It also shows the cutoff energy with a vertical bar; c) is similar to b), but shows Fermi edge region.

TABLE 1: Values of ϕ , spectrum width, E_F and E_{vac} from UPS measurements for CZTS films deposited by Co-evaporation and CBD

Sample	$h\nu - \phi$ (eV)	ϕ (eV)	E_F (eV)	E_{vac} (eV)
CZTS - Coevap.	13.4	7.8	3.5	11.3
CZTS - CBD	13.9	7.3	2.4	9.7

Conclusion

Single phase $\text{Cu}_2\text{ZnSnS}_4$ thin films with kesterite type structure were grown by co-evaporation and by sequential deposition of Cu_2SnS_3 and ZnS thin films following a new solution based route.

XANES and XPS analysis revealed that the oxidation states of the constituent elements of CZTS samples prepared by both methods correspond to the $\text{Cu}_2\text{ZnSnS}_4$ phase; XPS measurements revealed additionally that the evaporated CZTS films present a very good homogeneity in chemical composition along all the volume, while the samples grown by CBD are significantly more inhomogeneous. It was also found from XANES that the preparation method do not significantly affect band structure. UPS analysis allowed us to prove that the work function and density of states in the valence band of the films of CZTS is affected by the method of growth; samples prepared by CBD have a work function lower than those prepared by co-evaporation and greater density of states.

ACKNOWLEDGEMENTS: This work was supported by Colciencias (Contract #038/2013) and Universidad Nacional de Colombia, Sede Bogotá, Facultad de Ciencias, Grupo GMS&ES, Bogotá DC, Colombia (Proy. 20287 supported by DIB).

Improvement of Elemental Vapor Distribution Systems in CIGS Sulfo-Selenization Furnaces

H.F. Myers*, P.v.d. Heuvel and P. Diepens

Smit Thermal Solutions, Son, The Netherlands

S.S. Schmidt, C. Wolf, H.Rodriguez-Alvarez, C.A. Kaufmann and R. Schlatmann

PVcomB, Berlin, Germany

S. Villain, A. Weber, S. Bodnar, C. Guillou and C. Broussillou

NEXCIS, Rousset, France

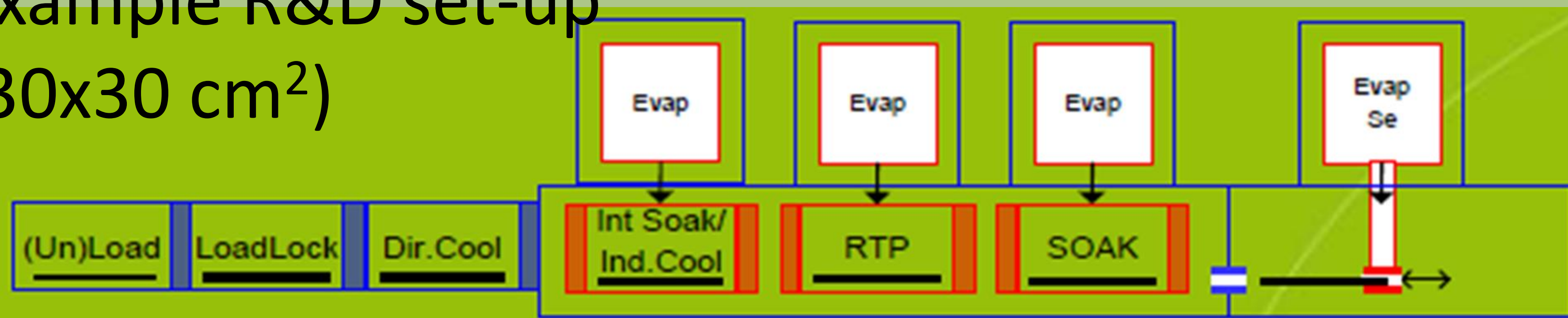
INTRODUCTION

Smit Thermal Solutions (formerly Smit Ovens), based Netherlands, develops custom-built chalcogenization platforms for CIGS. Three such systems, located at Solliance (High Tech Campus, Eindhoven), PVcomB (Berlin) and NEXCIS (Rousset, France), have been upgraded with advanced elemental chalcogen vapor-phase distribution systems. This work comprises a comparative study of the old and new vapor distribution systems in all three tools, exploring the homogeneity of Se concentration over the area of a panel, the Se usage, and the subsequent electrical results of the finished products.

SYSTEM OVERVIEW

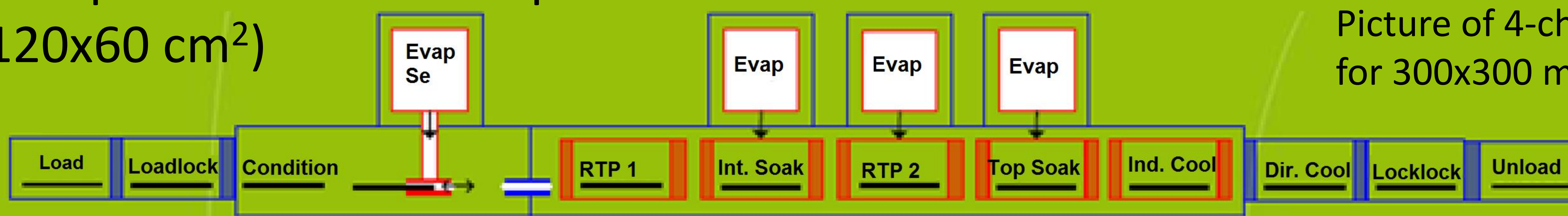
Modular heated reaction chambers with Se/S delivered to substrate by means of carrier gas (N or Ar).

Example R&D set-up
(30x30 cm²)



Picture of 4-chamber R&D system for 300x300 mm² substrates.

Example Pilot-scale set-up
(120x60 cm²)



IMPROVEMENT OF Se/S DISTRIBUTION SYSTEM

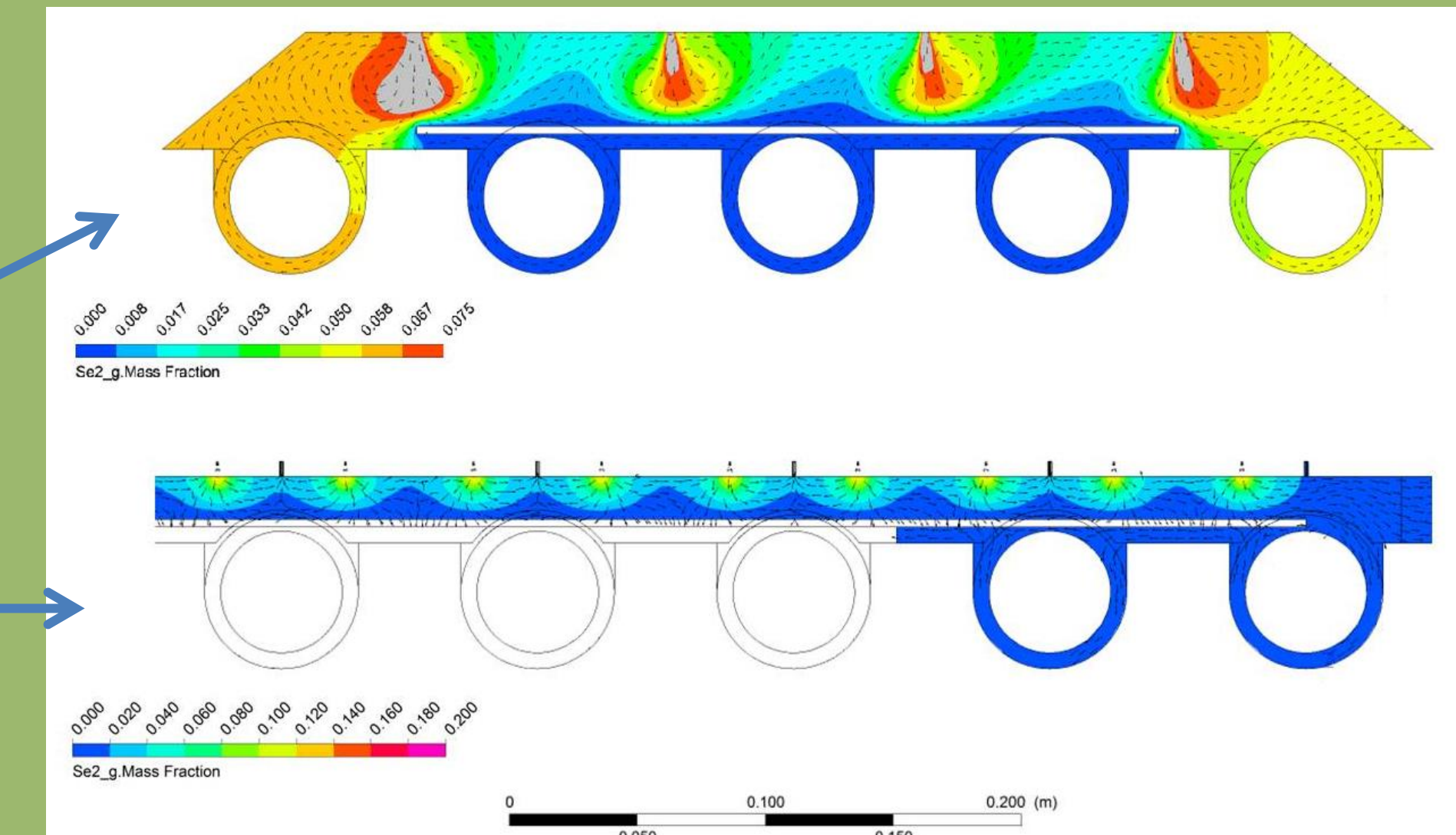
- Exhaust is from roof in new system, eliminating Se build-up in at sides (see CFD at right).
- Symmetric design for scalability to large-sized substrates.



Interior of old (left) and new (right) systems.

- Improved subheader network leads to more even Se flux at product surface.

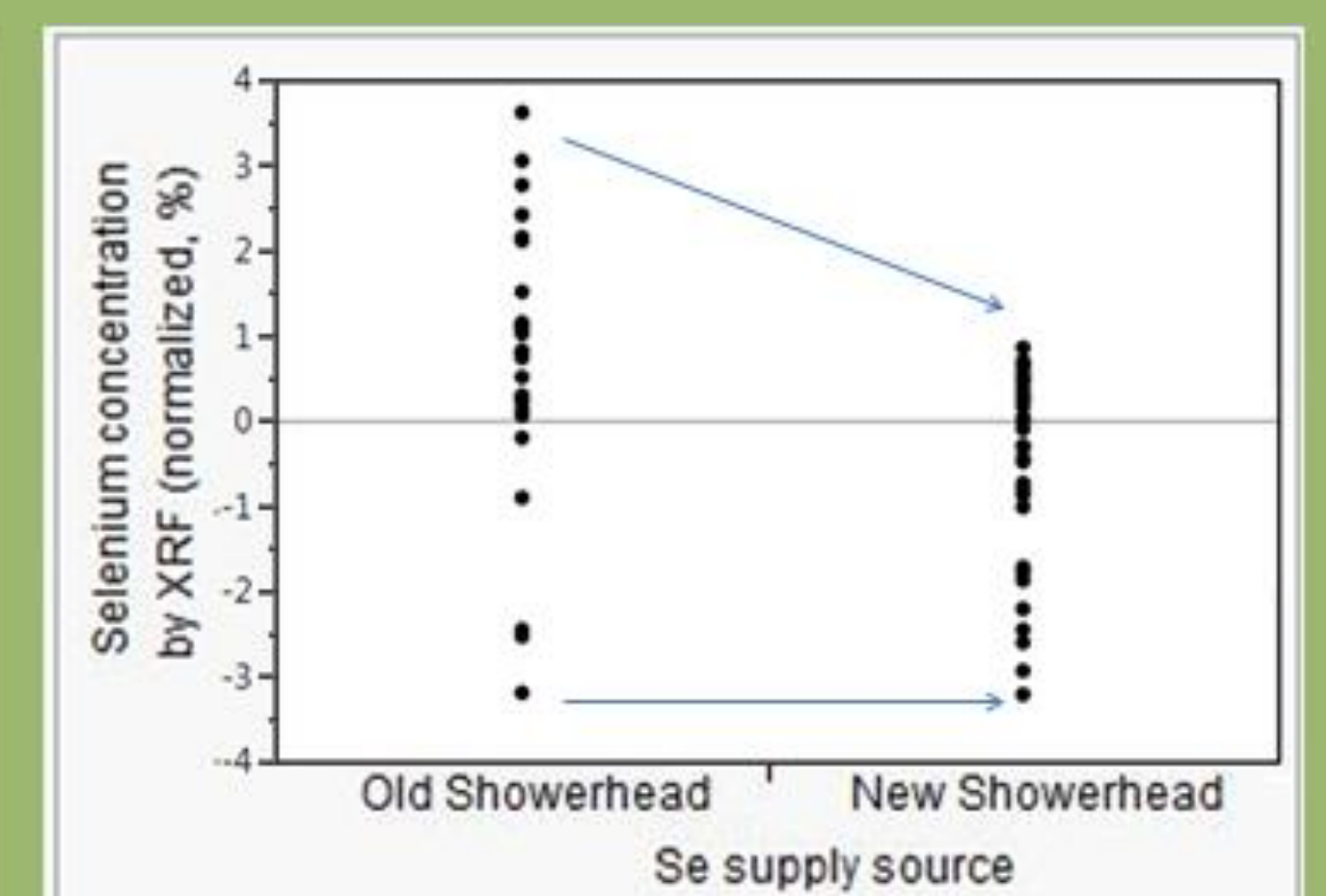
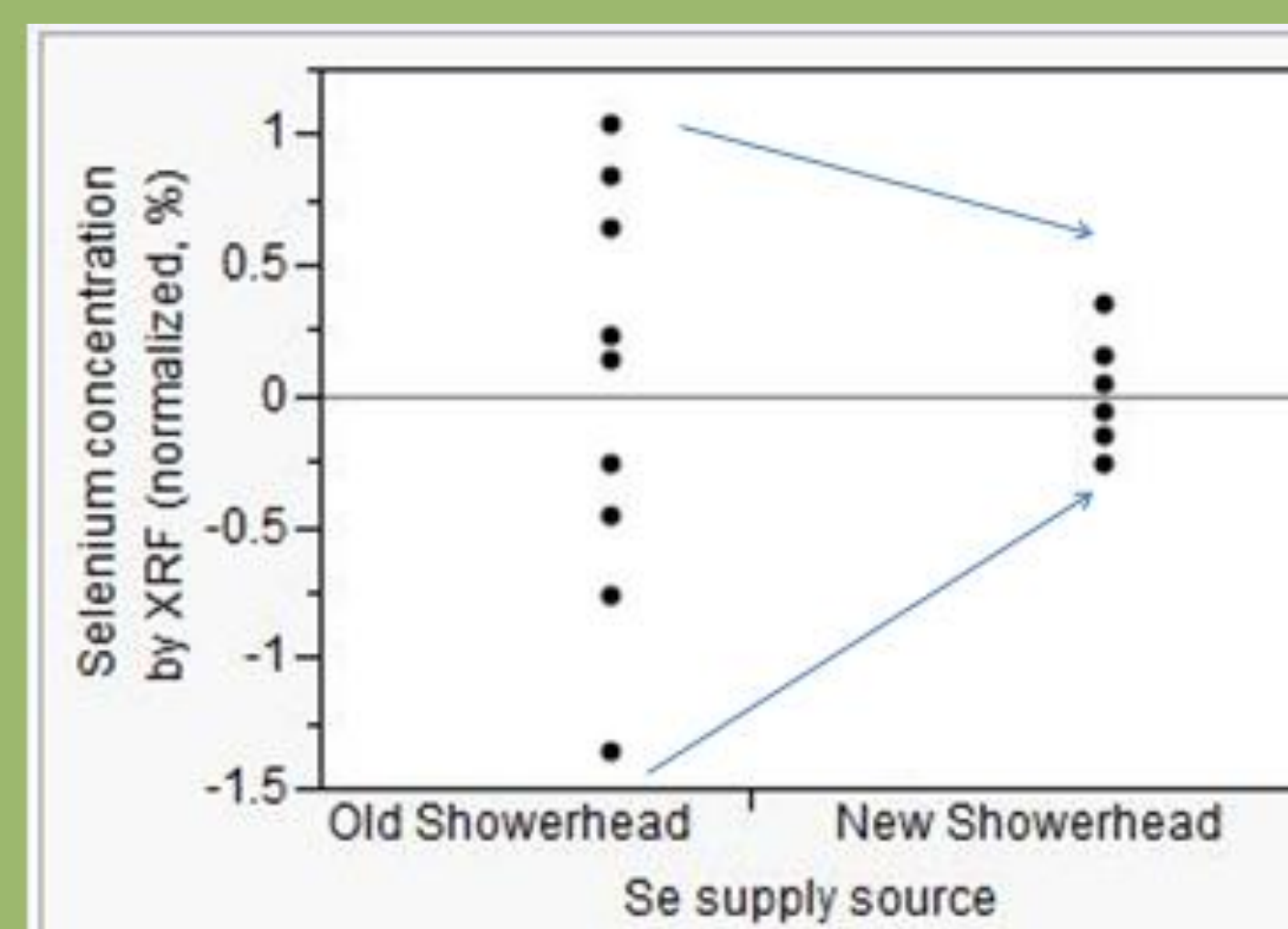
CFD analysis on old (top) vs new (bottom) distribution system, showing improved uniformity, particularly around edges.



BENEFITS OF IMPROVED Se/S DISTRIBUTION SYSTEM

Item	Current header/reactor		New header/reactor		Benefit
	delta		delta		
XRF Se Std dev.	0,8		0,39		Uniformity
Efficiency (mean)	x %	0%	x + 1.6 %	0%	Improved efficiency with reduced spread
Efficiency (median)	x + 1 %	1%	x + 1.8 %	0,2%	
Efficiency (max)	x + 3,2 %	3,2%	x + 3,5 %	1,9%	
Pick-up flow (optimized process)	16 slm		10 slm		Se flux 40%<, with improved uniformity

Increased Se compositional uniformity and corresponding higher average in small-area devices isolated from larger panels run in pilot-scale system at NEXCIS (1200x600 mm² total area, consisting of four 300x600 mm² modules). Further optimizing has resulted in a 17.3% champion device (CIGSSe).



Similar improvement and reduced spread seen in chalcogenide distribution using R&D systems at PVcomB (left) and Solliance (right – courtesy of C.H. Frijters and H. Steijvers of TNO)).

CONCLUSION

This article reports on the impact of hardware improvement on the material and optoelectronic properties of CIGS absorbers made from 2-step processes, in which metallic Cu-In-Ga precursors are reacted with Selenium and Sulfur vapors. Specifically, the next-generation chalcogenide distribution system was shown to improve material uniformity and overall performance while lowering costs. These results demonstrate that low-cost fabrication based on smart hardware design and innovative processes can provide high efficiency materials suitable for CIGS module production.

The e-learning platform of the FP7-SOPHIA Project: obtained results and perspective for its future exploitation

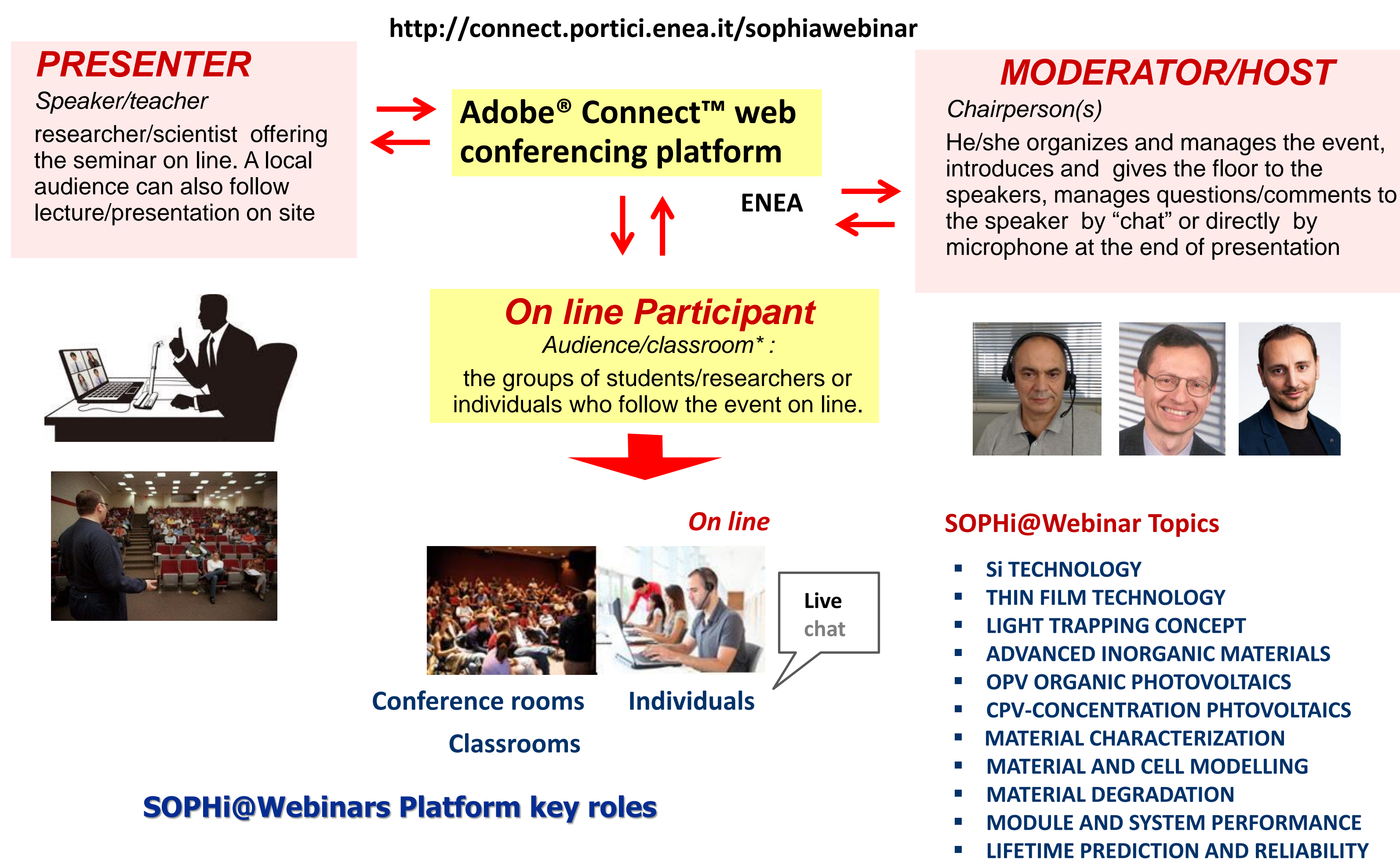
Francesco Roca¹, David Casaburi¹, Francesco Beone¹, Giuseppe Cipoletta¹, Giorgio Mencuccini¹, Luigi Pavia¹, Anna Vita¹, Iver Lauer⁸, Yael Augarten⁹, Ya Brigitte Assoa², Ignacio Antón Hernández¹², Fabien Bergeron², Suren Gevorgyan⁷, Jürgen Hüpkes⁹, Michael Koehl⁵, Jan Kroon³, Jens Merten², Siwanand Misara⁶, Tania Pettersen⁴, Martin Schubert⁵, Gerald Siefer⁵, Niger Taylor¹⁰, Ioannis-Thomas Theologitis¹¹, Philippe Malbranche²

¹ ENEA- Agenzia Nazionale per le Nuove Tecnologie, l'Energia e lo Sviluppo Economico Sostenibile, Italy; ² CEA-INES Commissariat à l'Energie Atomique Aux Energies Alternatives, France; ³ ECN-Stichting Energieonderzoek Centrum Nederland; ⁴ SINTEF ⁵ FH-ISE Fraunhofer-Institut für Solare Energiesysteme ; ⁶ FH-IWES Fraunhofer-Gesellschaft zur Förderung der Angewandten Forschung E.V., Germany; ⁷ Danmarks Tekniske Universitet; ⁸ Helmholtz-Zentrum Berlin für Materialien und Energie GmbH; ⁹ FZ-Jülich Forschungszentrum Juelich GmbH; ¹⁰ EC, Joint Research Centre, Ispra; ¹¹ SolarPower Europe, Belgium; ¹² UPM-IES Instituto De Energía Solar de la Universidad Politécnica de Madrid;

SOPHi@Webinar background:

FP7-SOPHIA, the European PV Research Infrastructure project coordinated by CEA-INES ended on 31st of January 2015. The project focused on strengthening and optimising the research capabilities of outstanding European Research Infrastructures by pulling together numerous scientists and researchers of more than 48 relevant Research Infrastructures to share a common vision and to conduct efficient and coordinated research work in the field of PV technologies. SOPHi@Webinar is the internal e-learning platform that has organized a set of online courses/seminaries/guest lectures in parallel to more conventional training initiatives held physically. It has also been opened to non-SOPHIA members

SOPHi@Webinars: the short-hand on e-learning platform



Electronic conferencing requires no more than a set of interconnected computers with suitable software and hardware. Participants can connect with conferences and workshops at their convenience, regardless of their time zone and geographical location,

Time saving and reducing travel costs

This is a great advantage for those who, perhaps due to financial constraints or lack of time, would be unable to attend physical events due to their own full booked agenda. Physical meetings can take place only when strictly necessary

Fluid and improved Communication

Video conferences enhance the possibilities for all to interactively review a subject, allowing them to share efficiently ideas, documents, conclusions and concerns.

No limitation on event location

E-conferences can be realized by laptops, tablets and mobile phones and can be followed from everywhere

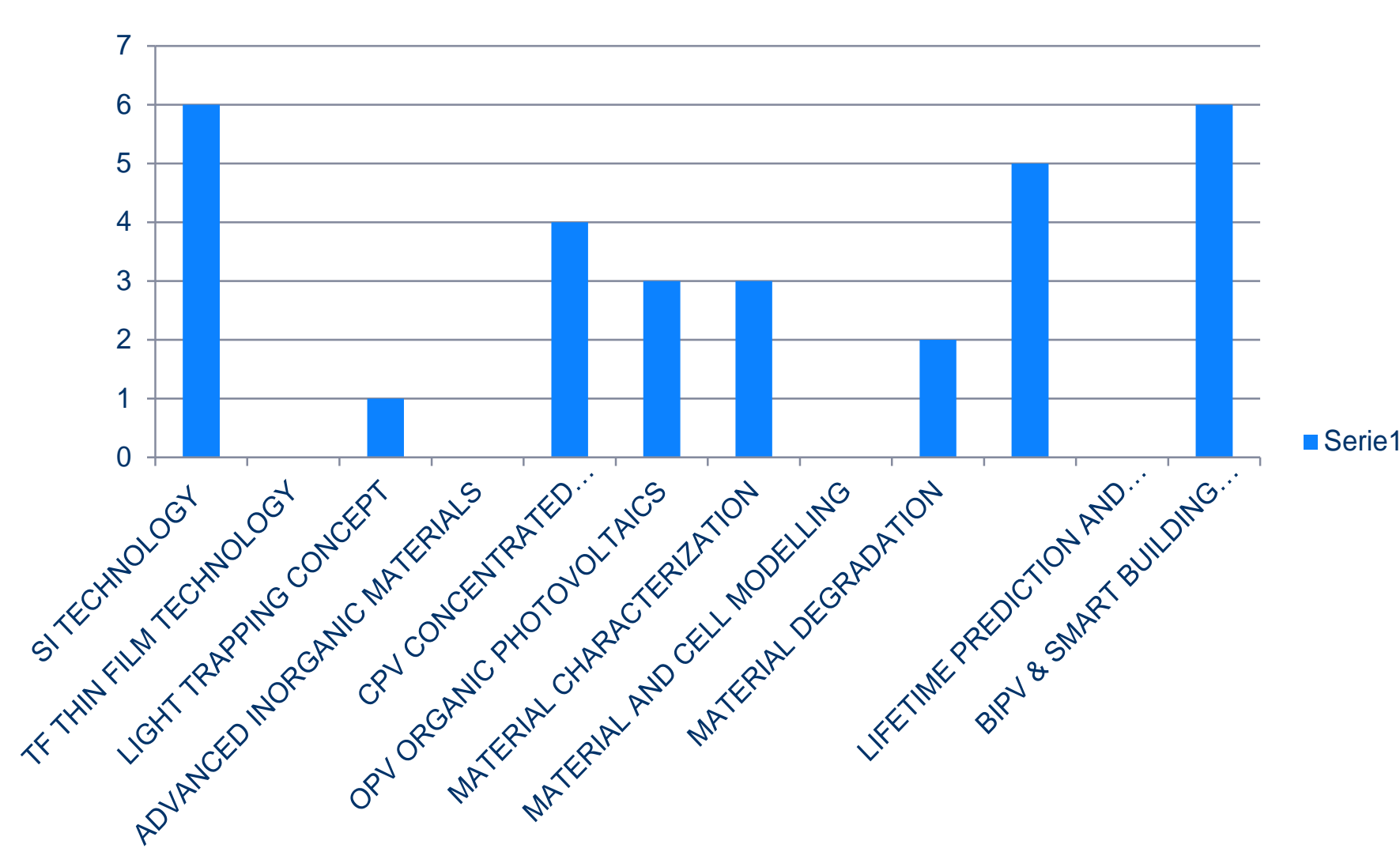
Focused Involvement

Participants can focus on the topic issues of direct interest, saving time from topics in which they are not involved or interested.

Storage and streaming of produced output

The acquired material (i.e. slides and video presentations) can be easily proposed by webcasting them even after the event

SOPHi@Webinars: Achieved results



- ☐ **More than 40 speakers involved** in 16 different events
- ☐ **30 webinars organised** since March 2013
 - around 2-4 events/month organised
- ☐ **830 registrations** of participants (+ >150 in live streaming)
 - more than 560 different scientists/researchers/professionals participated
 - widely represented by students and younger researchers
 - Majority of non-SOPHIA members.
- ☐ **A balanced participation** in comparison to events usually held physically
 - in respect to gender for both speakers and participants has been achieved
 - A very wide participation by country, covering also non-European countries (USA, Asia, South America, Australia, etc.)

SOPHIA Webinars has offered:

- ☐ Comprehensive information on different aspects of the utilization of PV research infrastructure/techniques and research protocols.
- ☐ An overview on advantages/ disadvantages and point of strength/weakness/opportunity/ threat respect other similar infrastructure/characterization techniques.
- ☐ A presentation on several outstanding technical-scientific results highlighting the potential in utilizing the infrastructure/technique/scientific protocol

Further information is available on the following pages: <http://uttp.enea.it/sophiawebinar>

SOPHi@Webinars
Web site



Acknowledgements

We would like to thank all SOPHi@Webinar speakers for their support and contribution. Their excellent presentations have helped to make this initiative possible and successful also for its exploitation in the frame of other initiatives and projects. We also thank all webinar participants that have reacted with enthusiasm and interest to our initiative. We acknowledge the technical staff of ENEA has consistently supported both the development and the use of applications for the realization of the very useful and well structured website. Finally, we would like to thank the European Commission that, with the funding of the FP7-SOPHIA grant agreement n° 262533, has supported the SOPHIA Project and SOPHi@Webinar initiative.



FP7-CHEETAH Project Knowledge Exchange Portal: an advanced tool to efficiently bring information to the European photovoltaic RTD community

Francesco Roca^{1*}, David Casaburi¹, Karsten Bittkau⁶, Martha C. Lux-Steiner⁷ Iver Lauer⁸, Suren Gevorgyan⁴, Philippe Malbranche³, Oriol Nos Aguilà³, Thomas Rachow⁵, Guillermo Sanchez-Plaza⁹, Paul Sommeling², Nigel Taylor⁸, Ioannis-Thomas Theologitis¹¹, Kris Van Nieuwenhuysen⁷, Jan Kroon²

¹ ENEA - Agenzia Nazionale per le Nuove Tecnologie, l'Energia e lo Sviluppo Economico Sostenibile, Italy, ² ECN-Stichting Energieonderzoek Centrum Nederland; ³ CEA-INES Commissariat à l'Energie Atomique Aux Energies Alternatives, France; ⁴ Danmarks Tekniske Universitet, ⁵ FH-ISE Fraunhofer-Institut für Solare Energiesysteme; Germany ⁶ IEK5 - Forschungszentrum Juelich GmbH; Juelich, Germany ⁷ HZB-Helmholtz-Zentrum Berlin für Materialien und Energie GmbH, Germany ⁸ Joint JRC-Research Centre, Ispra, Italy ⁹ Universitat Politècnica de València, Spain ¹⁰ Joint JRC-Research Centre, Ispra, ¹¹ SolarPower Europe, Belgium

FP7-CHEETAH - is a combined collaborative project (CP) and coordination and support action (CSA), funded under the European Commission's 7th Framework programme, and coordinated by ECN, NL with the aims to solve specific R&D issues and to overcome fragmentation of European PV R&D in Europe by intensifying the collaboration between R&D providers and industry to accelerate the industrialization of innovations. The project is also tightly linked to **EERA – the European Energy Research Alliance and its Joint Program on Photovoltaics**.

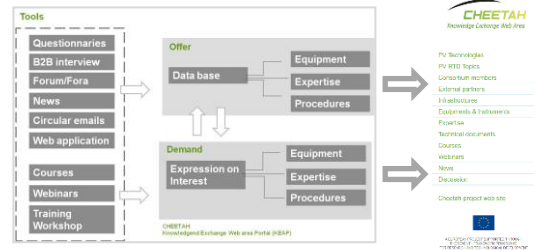
CHEETAH Knowledge Exchange Web Area background:

The **CHEETAH Knowledge Exchange Portal (KEAP)**, in parallel to the project web site and other dissemination activities (newsletter, communication, etc), constitutes the pillar of the project to bring information from different sources on demand and availability of infrastructures, equipment, expertise, technical documents, in a uniform and simple way, to any interested CHEETAH partner and interested external organization.

CHEETAH KEAP represents a *significant step forward in the knowledge exchange* in PV RTD sector among scientists, professionals, students, and companies .

It operates by utilizing user-friendly, dedicated *media tools* based on the typical approach of social, scientific and professional networks, from the collection of availability of expertise/infrastructure (*supply site*), to its elaboration (*management*) and its final offer to project partners (*demand site*)

CHEETAH KEAP Rationale



CHEETAH KEAP web site

The web site is based on utilization of structured cataloguing criteria for PV technologies / PV RTD topics / PV Equipment / PV Expertise and organizations involved in CHEETAH. It facilitates all steps to connect information among the community, to share scientific, educational and technical content, because the portal operates as a *dynamic data base* matrix: any uploaded information is linked to all others by *dynamic links* that allow access to *any individual information* as well as to any information already uploaded (*Available equipment? Expertise? Location? Who could I contact? Etc.*)

<http://www.cheetah-exchange.eu>



PV Technologies web pages



PV RTD Topics web pages



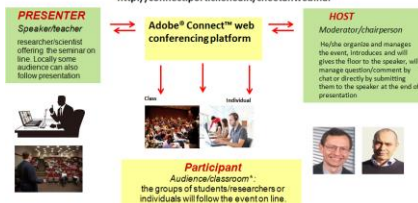
PV RTD Infrastructures and equipment web page



Expertise data base catalogue

CHEETAH KEAP e-learning platform

<http://connect.portici.enea.it/cheetahwebinar>



The CHEETAH Knowledge Exchange Portal, powered and developed by UTPP-ENEA ©2014 , is an integral part of the CHEETAH project web site. It makes contributions coming from all CHEETAH available partners to:

- Identify current CHEETAH partners and the European PV RTD community's technical-scientific needs
- Collect technical & scientific information and efficiently establish and promote channels and procedures to transfer information among each partner in order to enforce potential and effectiveness of each organization in RTD

The CHEETAH KEAP currently collects technical-scientific information by sharing it on line with the entire PV RTD community:

- availability of infrastructures, equipment, expertise, technical documents to widely foster the interaction and collaboration among organizations involved in Photovoltaic RTD.
- Search engines with user-friendly interface
- Public access and reserved area (documents, data, reports, etc.)
- On-line forum/fora for internal/external technical/scientific discussions on specific themes
- On-line questionnaire tool to optimize submission and collection of specific information

In addition, the web area provides by its own e-learning platform dedicated tools to share expertise by organizing also on-line meetings, webinars and on-line tests and experiment can be shared with project members

Acknowledgements

We would like to thank all CHEETAH members for their continuous support and their contribution in helping to enrich the web site of information and technical – scientific content to make the CHEETAH KEAP initiative possible and successful. We also thank all CHEETAH KEAP browsers who have reacted with enthusiasm and interest and who are supporting us with comments and amendments, they are essential for the development portal . We acknowledge the technical staff of ENEA, which has consistently supported both the development and the use of applications and David Casaburi for Web site technical help. Finally, but not least, we would like to thank the European Commission for funding of 7FP7-CHEETAH (grant agreement n ° 609788), supporting the CHEETAH Project and the CHEETAH KEAP initiative.

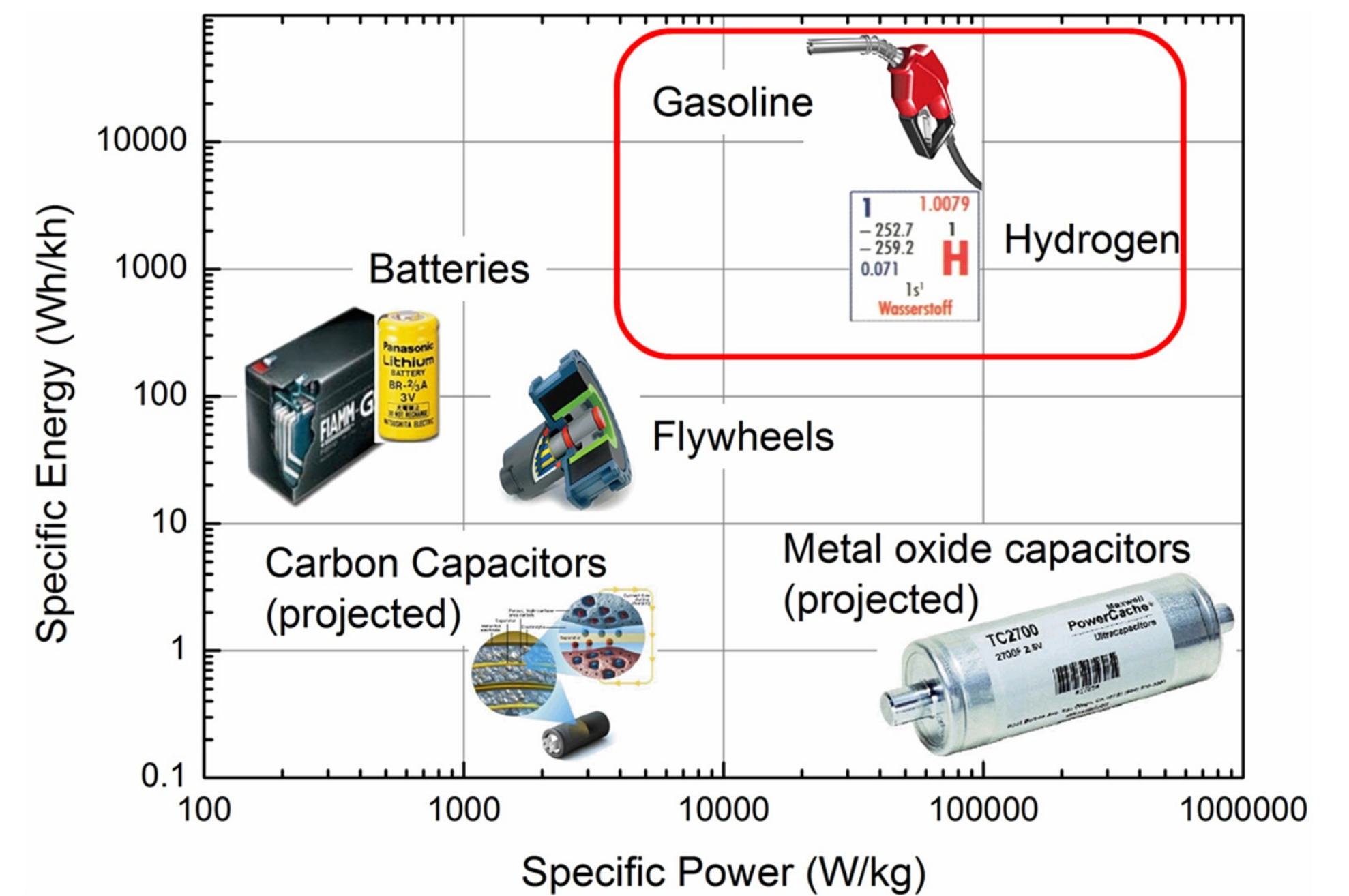
MATERIALS AND DEVICE DEVELOPMENT FOR COST-EFFECTIVE SOLAR HYDROGEN PRODUCTION

Why Solar Fuels?

- Sunlight is by far the most abundant and sustainable source of energy
- We need to store this energy on a Tera-Watt scale
- The energy and power densities of chemical fuels are hard to beat

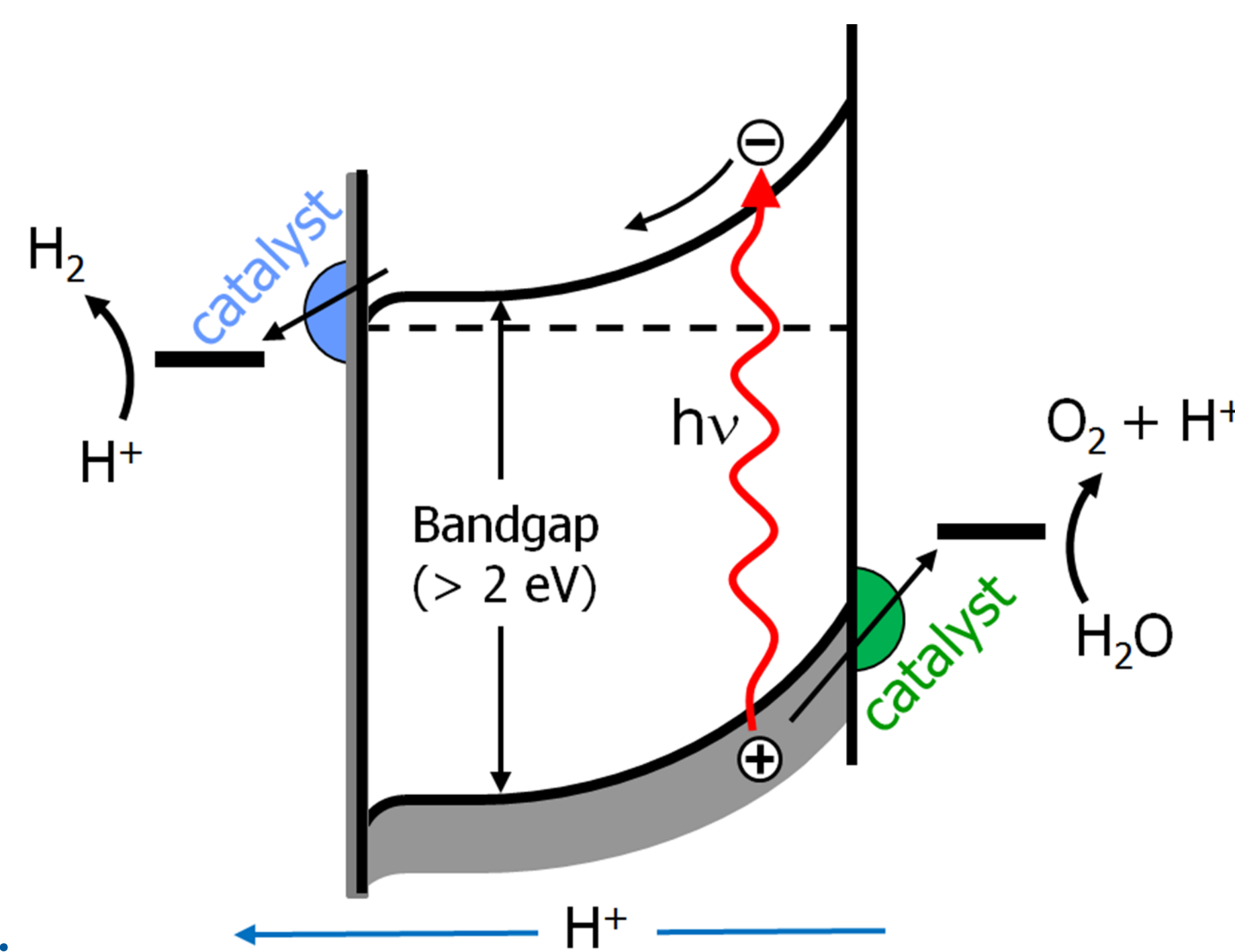
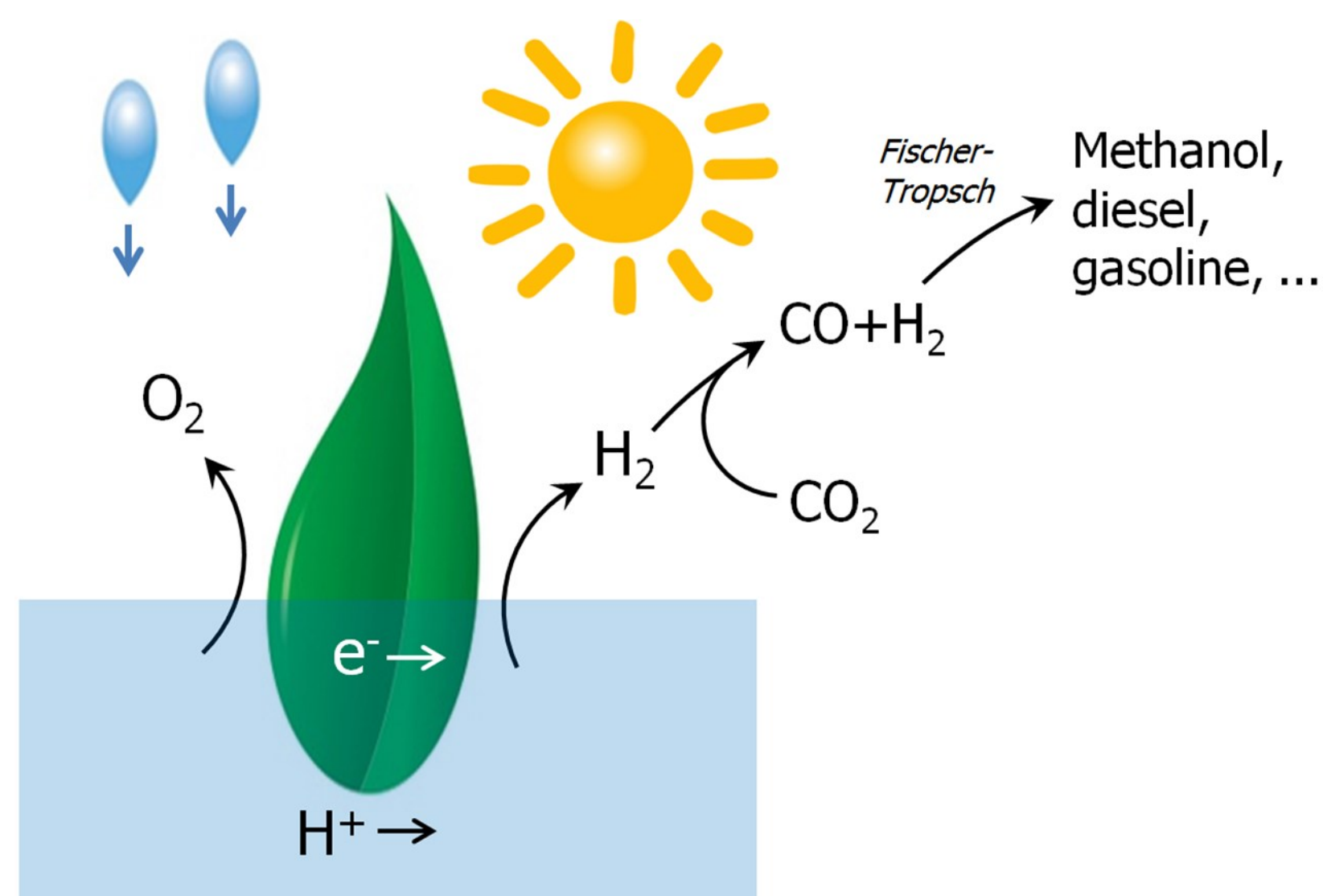
Challenges

- Compete with coupled photovoltaic / electrolysis systems (> \$8 per kg H₂)
- Reduce cost by integrating light absorption and electrolysis functionalities

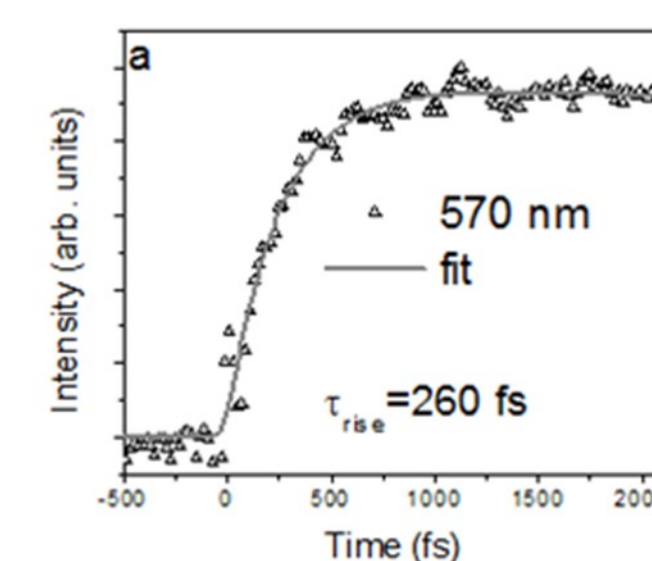


Our Approach

- Explore photo-electrochemical routes
- Focus on water splitting
- Use a semiconductor/ liquid junction
- Explore metal oxides as chemically-stable semiconductors

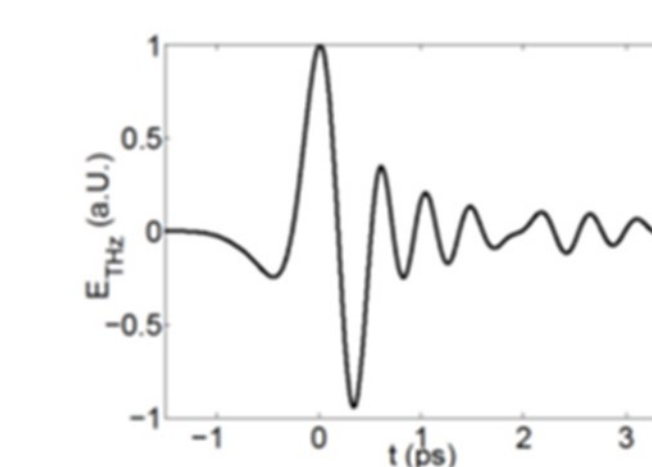


- Study carrier recombination and charge transfer kinetics with time-resolved spectroscopy



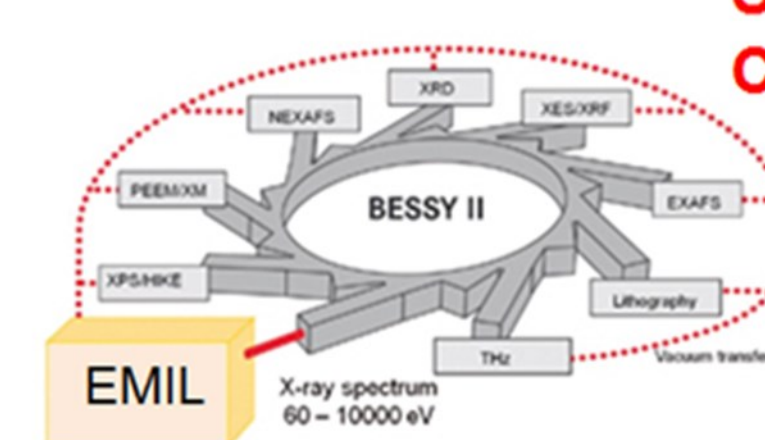
Optical Information

Transient absorption, 2-photon photoemission



Electrical Information

THz and μ -wave conductivity



Structural and Chemical Information

In-situ EXAFS/XANES
Ambient (S)XPS

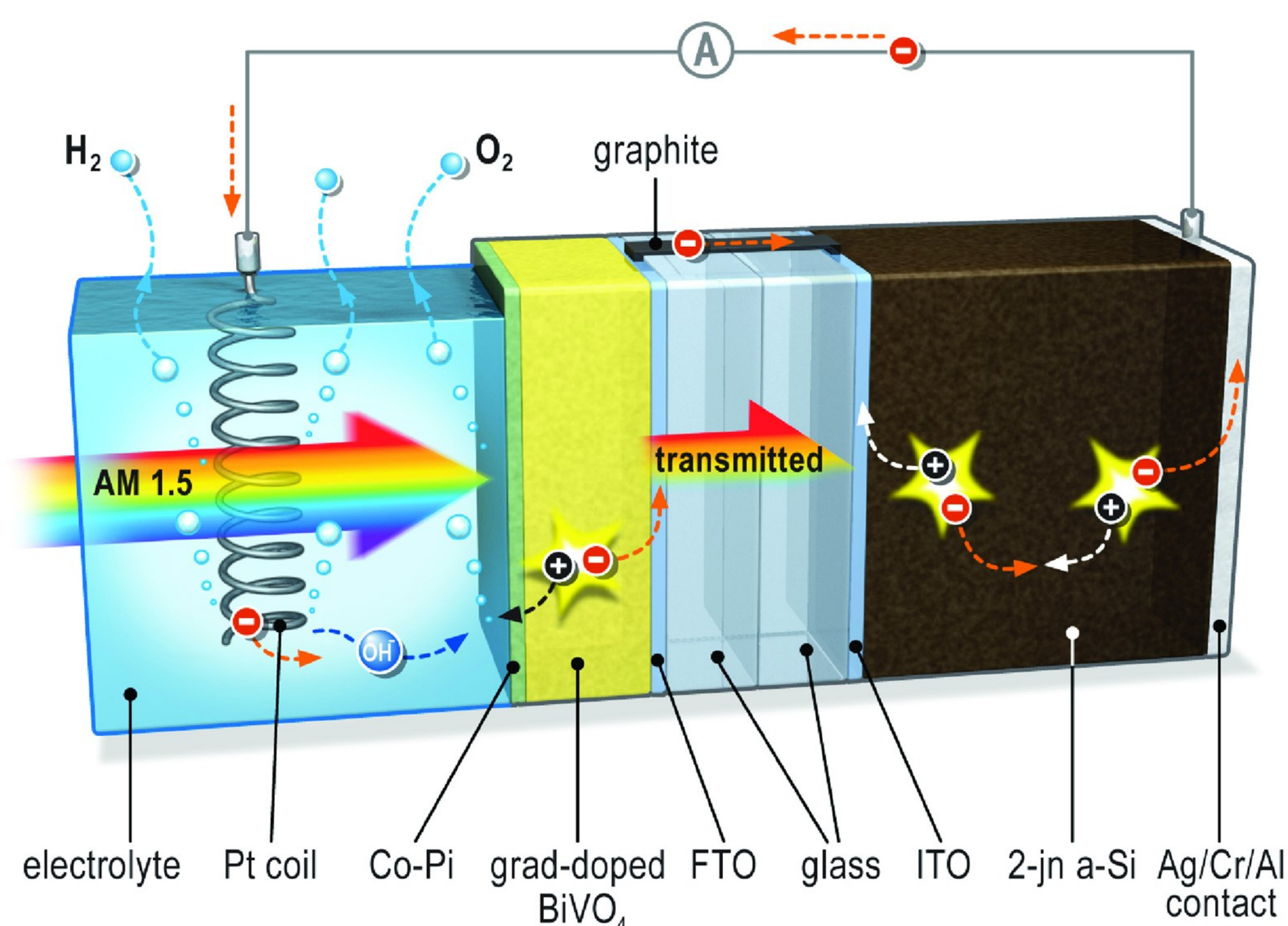
Advantages

- Water splitting is easier than CO₂ reduction
- Separation of H₂ and O₂ is straightforward
- With H₂ (and CO₂) you can make anything!

First Results and Future Objectives

Stand-alone hybrid BiVO₄ / amorphous silicon tandem device showing a solar-to-hydrogen energy conversion efficiency of 4.9% [1]

[1] F.F. Abdi, L. Han, A.H.M. Smets, M. Zeman, B. Dam, and R. van de Krol, Nature Commun. 4:2195, 1-7 (2013)



Objectives

- Explore influence of lattice defects on recombination kinetics
- Study semiconductor catalyst charge transfer kinetics
- Develop novel stable and efficient metal oxide semiconductors
- Scale-up and demonstrate 50 cm² hybrid devices